Soluble LAG-3 binding to cancer cells - Influence of cell types, MHC class II and lipid rafts

By

Kendra Laura Smith

A thesis submitted to the School of Graduate Studies

In partial fulfillment of the requirements for the degree of

Master of Science in Medicine

Immunology and Infectious Diseases, Division of Biomedical Sciences Faculty of Medicine

Memorial University of Newfoundland

May 2024

St. John’s Newfoundland and Labrador

Abstract

Interaction of immunoinhibitory molecules, lymphocyte activating gene-3 (LAG-3) and programmed cell death protein-1 (PD-1) on tumor infiltrating lymphocytes with their respective ligands, contributes to an exhausted immune phenotype. However, soluble LAG-3 (sLAG-3) enhances immunity by inducing dendritic cell maturation by binding MHC-II associated with lipid rafts.

The first part of this thesis assessed the importance of MHC-II/lipid rafts versus peptide/MHC-II complexes (pMHC-II) as sLAG-3 ligands. Analysis of sLAG-3 binding to B-cell lines was done using flow cytometry. Results indicated stable pMHC-II play a larger role in sLAG-3 binding than incorporation of pMHC-II in lipid rafts.

sLAG-3 binding, MHC-II, CD59 and PD-L1 were assessed by flow cytometry on IFN-γ treated melanoma cell line (MDA-MB-435) and different breast cancer cell lines (BCCL). Lipid raft disruptor, methyl-B-cyclodextrin was used to treat cell lines to determine if LAG-3 binding was affected by lipid rafts. Cell lines were MHC-II^{+} and PD-L1^{+}, but only MDA-MB-435 bound sLAG3. Deficient LAG-3 binding to BCCL could not be explained by HLA-DM or lipid raft deficiency. Lipid raft disruption increased sLAG-3 binding, this could not be explained by MHC-II or CD59. This suggests that lipid raft disruption may expose MHC-II and other ligands to promote sLAG-3 binding.

Altogether, results indicate LAG-3 binding is cell-context dependent and more complex than simply binding p/MHC-II complexes, preferentially located in lipid rafts.

General summary

The body's immune system has many molecules that inhibit the immune response. Cancer cells use these molecules to their advantage in order to escape the immune response and continue to grow. One of these molecules is called LAG-3, which interacts with MHC class II, inhibiting downstream immune responses. Research has shown that LAG-3 is found on immune cells that surround tumours. Less is known about how MHC class II on cancer cells interacts with LAG-3.

We have developed a method to detect soluble LAG-3 binding on cancer cell lines. We have found that LAG-3 bound strongly to a melanoma cell line but significantly less to Burkitt's lymphoma and breast cancer cell lines. Factors that influence LAG-3 binding are complex, and differ among cell types.

Immunotherapies blocking interactions between LAG-3 and tumour cells are being well studied. Having a deeper understanding of the mechanisms involved will contribute to the success of these therapies.

Acknowledgements

I would most importantly like to thank my supervisor and mentor Dr. Sheila Drover for her continuous support and patience throughout this journey. She was always there to push me to be my best but academically and personally. Without her guidance and motivation, I would not be where I am today. Through working with her, I was not only inspired to continue with a career in research but learned a number of valuable skills that I will carry with me for years to come.

I would also like to thank my former lab-mates Andrea Rasmussen and Louise Wiede for not only their support through my research but also friendship. Thank you to the Faculty of Medicine flow cytometry unit for their continuous support throughout my experiments and thank you to my committee members Dr. Michael Grant and Dr. Thomas Michalak.

Lastly, I would like to thank the funding agencies Canadian Breast Cancer Foundation (BC-RG-13-1 grant#310985) and the Faculty of Medicine Medical Research Fund as well as Faculty of Medicine Research and Graduate Studies which made this research possible.

Table of Contents

List of Tables

List of Figures

List of Abbreviations

APC	Antigen presenting cell
APS	Ammonium persulfate
ATTC	American Type Culture Collection
BCA	Bicinchoninic acid
BCL	B cell line
BCCL	Breast cancer cell lines
BL	Burkitt's lymphoma
BSA	Bovine serum albumin
CIITA	Class II transactivator
CLIP	Class II-associated Ii peptide
CREB	Cyclic-AMP-responsive element binding protein
DC	Dendritic cell
Ebox	Enhancer box
EBV	Epstein-Barr virus
ER	Endoplasmic reticulum
ER	Estrogen receptor
FACS	Fluorescence-activated cell sorting

FCS	Fetal calf serum
FGL1	Fibrinogen-like protein 1
Gal-3	Galectin-3
GAS	Interferon gamma activator sequence
GC	Germinal centre
HER2	Human epidermal growth factor receptor 2
HLA	Human leukocyte antigen
HLA-I	HLA class I
HLA-II	HLA class II
HRP	Horseradish peroxidase
IFN-γ	Interferon gamma
IFNGR	Interferon gamma receptor
IFNGR1	Interferon gamma receptor 1
IFNGR2	Interferon gamma receptor 2
Ig	Immunoglobulin
Ii	Invariant chain
IMDM	Iscove's Modified Dulbecco's Medium
IRF-E	Inteferon-regulatory factor element

JAK1	Janus kinase 1
JAK2	Janus kinase 2
LAG-3	Lymphocyte activating gene-3
LSECtin	Endothelial cell lectin
MAPK	Mitogen-activated kinase
MFI	Mean fluorescence intensity
MHC	Major histocompatibility complex
MHC-I	MHC class I
MHC-II	MHC Class II
DM	HLA-DM
DO	HLA-DO
MβCD	Methyl-beta-cyclodextrin
NFY	Nuclear factor Y
NK	Natural killer
NKT	Natural killer T
NPI-1	Importin- α 1 nucleoprotein 1
PBS	Phosphate buffered saline

PD-1	Programmed cell death protein 1
PD-L1	Programmed cell death ligand 1
PFA	Paraformaldehyde
pHLA-II	HLA-II/peptide complexes
PI3K	Phosphoinositide-3 kinase
pMHC-II	MHC-II/peptide complex
PR	Progesterone receptor
RIPA	Radioimmunoprecipitation assay
RPMI	Roswell Park Memorial Institute
RXF	Regulatory factor X
sLAG-3	Soluble lymphocyte activating gene-3
STAT1	Signal transducer and activator of transcription
STR	Short tandem repeat
TBS-T	Tris buffered saline-tween 20
TCGA	The Caner Genome Atlas Program
TCR	T cell receptor
Temed	Tetramethylethylenediamine

TNBC	Triple negative breast cancer
TNF- α	Tumour necrosis factor alpha
Treg	Regulatory T cell
USF-1	Upstream stimulatory factor-1
Y440	Tyrosine 440

Chapter 1: Introduction

1.1 Major histocompatibility complex overview

The major histocompatibility complex (MHC) is a polymorphic region of approximately 4000 kb which encodes numerous genes involved in both innate and adaptive immune regulation. In humans, MHC is referred to as the human leukocyte antigen (HLA) system and is located on the short arm of chromosome six (6p.21.3) [1]. HLA is comprised of three regions, class I, class II and class III.

HLA class I (HLA-I) region codes for classical antigens HLA-A, -B and -C. HLA-I is expressed on nearly all nucleated cells, including tumour cells. HLA-I is a heterodimer comprised of HLA encoded α chain which has three domains, α 1, α 2 and α 3, as well as non-HLA encoded β 2 microglobulin. α 1 and α 2 form the peptide binding groove which can display peptides of 8-10 amino acids in length that have been digested within the cell and presents them to $CD8^+$ cytotoxic T cells [2], [3]. Only foreign antigens or altered self-antigens are recognized by $CD8^+$ T cells in a healthy functioning immune system.

HLA class II (HLA-II) molecules are constitutively expressed on professional antigen-presenting cells (APC), including B cells and dendritic cells (DC). APCs also express various co-stimulatory molecules and have efficient class II antigen presentation systems [4]. The HLA-II region encodes for genes of classical HLA-II antigens HLA-DR, -DP and DQ, and non-classical HLA-DM (DM) and HLA-DO (DO). Both classical and non-classical HLA-II are comprised of polymorphic α and β chains, which form heterodimers [4]–[6]. HLA-DR, DP and DQ are surface glycoproteins that present exogenous proteins approximately 12-24 amino acids in length to $CD4^+$ T cells [5], [6].

HLA-II is comprised of four extracellular domains: α chain (α1 and α2) and β chain (β1 and β2). To accommodate long peptides at a high degree of specificity the peptide binding groove is open ended with a variable amino acid sequence (Figure 1.1). Each of the three HLA regions encodes for proteins vital for normal immune function.

Expression of HLA-II can be induced on non-APCs through stimulation with cytokines, including but not limited to IFN-γ [7]–[9]. IFN-γ stimulation can induce HLA-II expression and upregulate HLA-I expression on tumour cells [10]. Studies have shown that high expression of HLA, results in a better outcome for cancer patients [9].

1.2 HLA complex class II presentation pathway

HLA-II α and β chains, as well as multifunctional companion molecule invariant chain (Ii) are made in the rough endoplasmic reticulum (ER) [11]. These three molecules form a nine subunit complex comprised of three αβ dimers and an Ii trimer $(\alpha\beta)_3Ii_3$ [12]–[14]. In this complex Ii is bound to the HLA-II peptide binding groove to deter non-specific peptide binding [13]. Ii also aids by facilitating signals involved in the transport of the complex from the ER to the Golgi apparatus and to the late endosomal-lysosomal antigen processing compartment where antigenic peptides congregate. Foreign and cell surface antigens are internalized by APCs through several specific and non-specific mechanisms including micropinocytosis, phagocytosis, and receptor-mediated endocytosis [15]–[17]. Early endosomes formed during antigen internalization fuse with the antigen processing compartment which has abundant HLA-II molecules [18].

In the MHC class II loading compartments (MIIC), Ii is cleaved leaving behind class II-associated Ii peptide (CLIP) in the peptide binding groove [13], [19]. The protease that facilitates

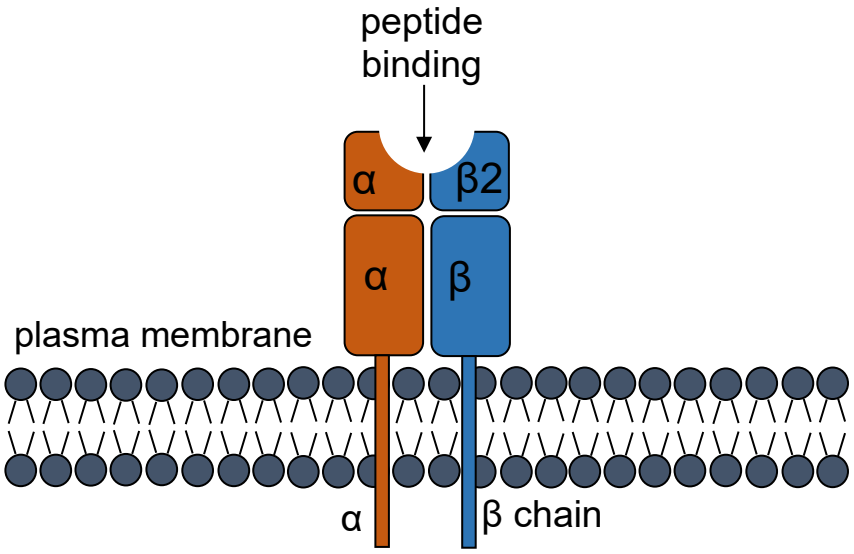
peptide
binding
α
β2
α
β
plasma membrane
α
β chain

Figure 1.1: Human leukocyte antigen class II structure. The HLA-II molecule is comprised of two non-covalently linked domains. The α chain and the β chain are anchored to the plasma membrane by the transmembrane domain and the cytoplasmic tail. Reproduced with permission from [20], Copyright Massachusetts Medical Society.

Ii cleavage is cell dependent, in many professional APCs cathepsin S completes the final step of Ii cleavage [21]–[23]. CLIP is the template for peptide loading. Peptide editor DM is a class II like molecule that exchanges CLIP in favour of high affinity peptides [24]–[27]. DM binding to HLA-II leads to the destabilization of hydrogen bonds ultimately leading to the release of CLIP from the peptide binding groove [28], [29]. DM keeps the open class II complex stable to allow for high affinity peptide binding. It chaperones the association and dissociation of peptides from HLA-II until a high affinity peptide is bound [30]. If DM is not present, CLIP remains in the peptide binding groove, therefore, any peptide complexes that do form are unstable [31]. DO partially regulates DM activity. DO associates with DM in the same site as it binds HLA-II, thereby inhibiting its catalytic activity [32]. Following peptide loading, peptide-HLA-II complexes (pHLA-II) travel from the antigen processing compartment to the cell surface, where T cell interaction and subsequent activation can occur (Figure 1.2).

1.3 Regulation of HLA-II expression

HLA-II expression is primarily regulated at the level of transcription by the class II transactivator (CIITA). CIITA is the master regulator of cytokine induced HLA-II expression [33]. It is considered a transcriptional co-activator as it does not directly bind DNA, rather it associates with a binding platform consisting of a group of transcription factors referred to as the class II enhanceosome [34], [35]. The enhanceosome consists of regulatory module SXY, located in the promoter region of genes that code for HLA-II α and β chains. The SXY module is made up of four sequences, S, X, X2 and Y, each of which binds specific transcription factors [33], [36]. Regulatory factor X (RXF) binds X, cyclic-AMP-responsive element binding protein (CREB) binds X2, nuclear factor Y (NFY) binds Y, and an unknown transcription

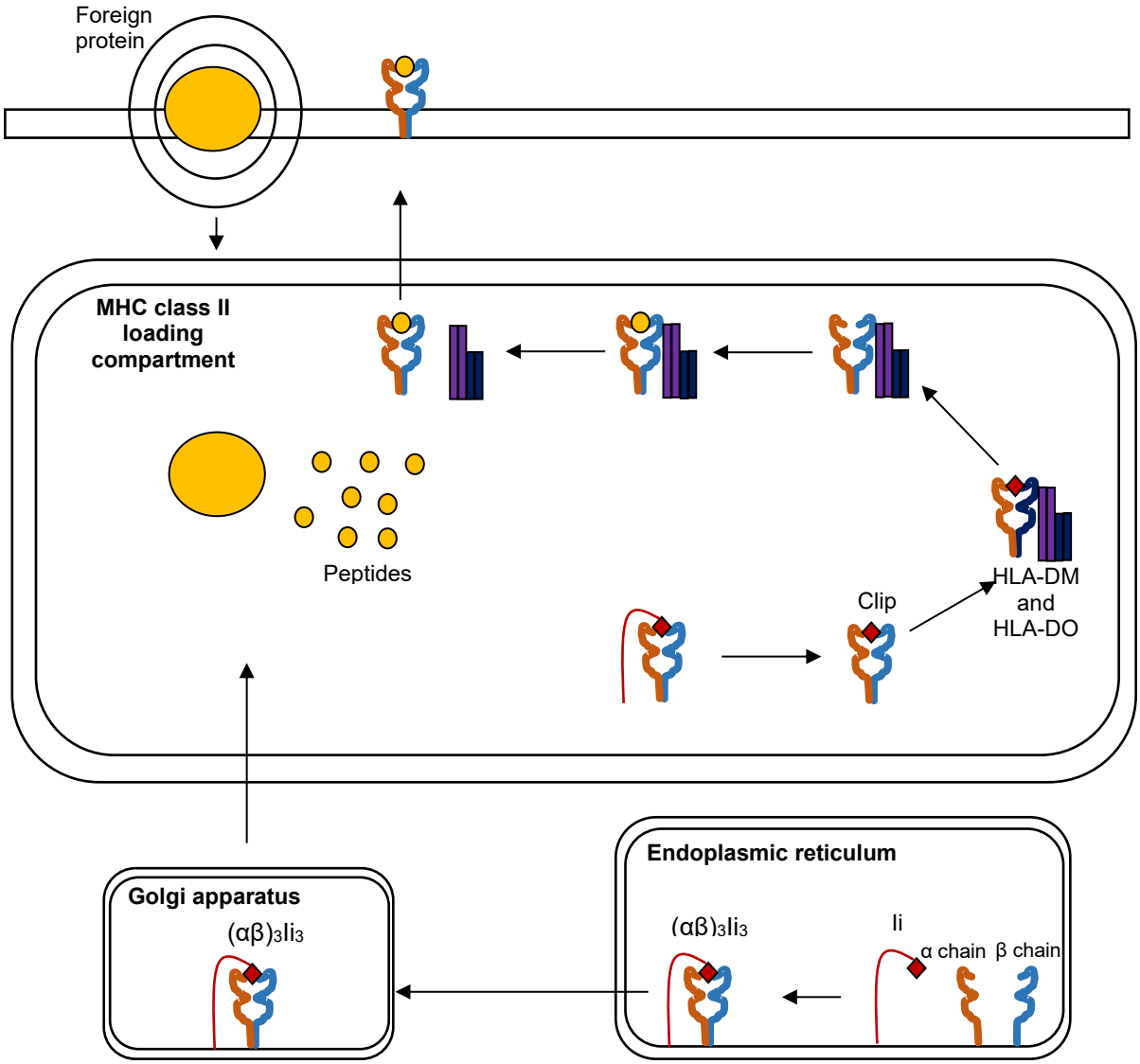
Foreign protein
MHC class II loading compartment
Peptides
HLA-DM and HLA-DO
Clip
Endoplasmic reticulum
(αβ)3Ii3
Ii
α chain
β chain
Golgi apparatus
(αβ)3Ii3

Figure 1.2: Human leukocyte class II presentation pathway. HLA-II α and β chains, as well as invariant chain (Ii) are made in the endoplasmic reticulum and form a nine-unit complex ($(\alpha\beta)_3Ii_3$). This complex moves through the Golgi apparatus and into the MHC class II loading compartment. Ii is degraded leaving behind class II associated peptide (clip) in the pHLA-II binding groove. DM associated with DO facilitates the exchange of clip with high affinity stable peptide. Peptide loaded HLA-II molecules are transported to the cell surface for presentation to $CD4^+$ T cells. Adapted with permission from [37].

factor/molecule binds S [38]–[41]. This complex serves as a binding platform for CIITA [34]. CIITA functions as a transcriptional integrator it binds to the enhanceosome to connect essential transcriptional factors to the class II transcriptional machinery, ultimately leading to the initiation of HLA-II gene transcription [33] (Figure 1.3).

1.4 Interferons

Interferons are cytokines that promote immune responses and play various roles in the immune system [42]. They were initially discovered as proteins that interfere with viral replication [43]. Interferons are secreted by first defender cells of the innate immune system including natural killer (NK) cells and natural killer T (NKT) cells, as well as $CD4^+$ and $CD8^+$ T cells [44]. Interferons are divided into three distinct types: type I (IFN-α and IFN-β), type II (IFN-γ) and type III (IFN-λ). The remainder of this introduction will focus on IFN-γ, its signaling pathway and its role in HLA-II expression.

1.5 Interferon gamma signalling pathway

When secreted by activated immune cells (T cells and NK cells), interferon gamma (IFN-γ) binds to the IFN-γ receptor (IFNGR) on the cell surface [44]. IFNGR consists of two subunits, interferon gamma receptor 1 (IFNGR1) and interferon gamma receptor 2 (IFNGR2), which are responsible for ligand binding and signal transduction, respectively [45]. IFNGR1 is constitutively expressed, while IFNGR2 expression is regulated by the needs of the cell [46], [47].

IFN-γ binding induces a conformational change to IFNGR causing subunits IFNGR1 and IFNGR2 to get closer in proximity. Janus kinase 1 (JAK1) and Janus kinase 2 (JAK2) are

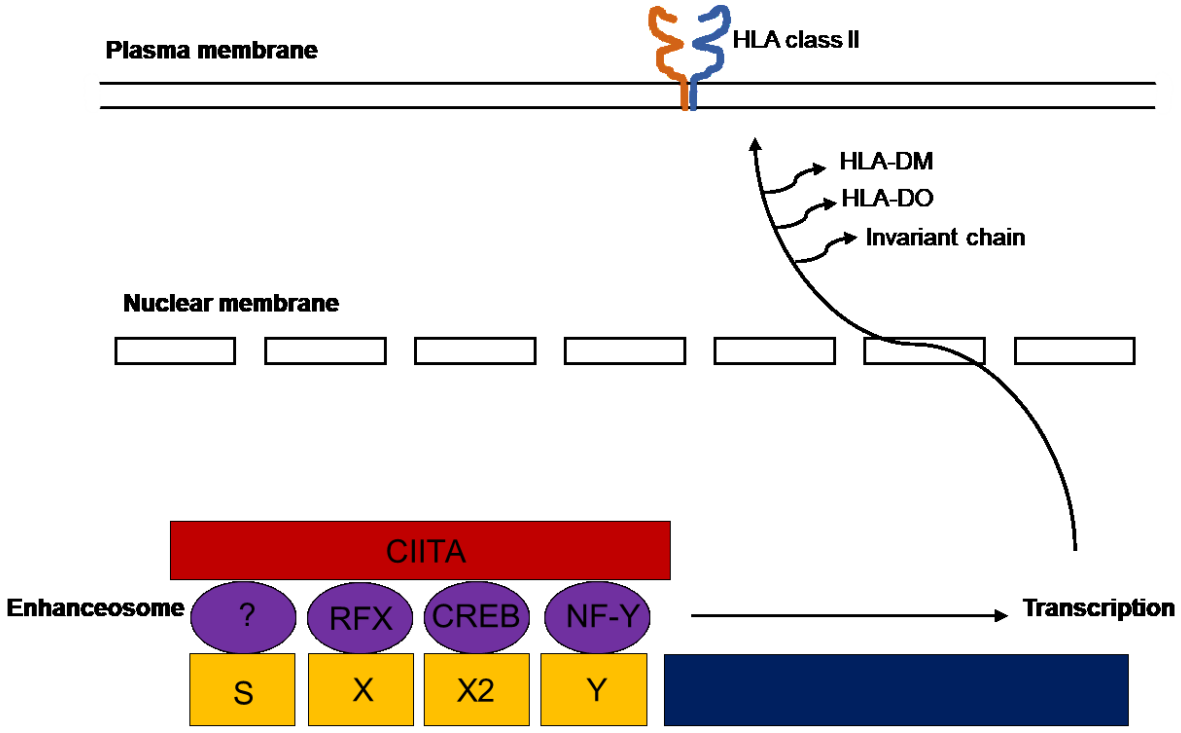
Plasma membrane
HLA class II
HLA-DM
HLA-DO
Invariant chain
Nuclear membrane
CIITA
Enhanceosome
?
RFX
CREB
NF-Y
Transcription
S
X
X2
Y

Figure 1.3: Regulation of HLA-II expression. Expression of HLA-II is regulated at the transcriptional level through the binding of regulatory factor X (RFX), cAMP responsive element binding protein (CREB) and nuclear transcription factor Y (NF-Y) to the S, X, Y module located on the HLA-II promoter. This complex is a binding platform for class II transactivator (CIITA) which regulates transcription machinery. Adapted with permission from [33].

associated with IFNGR1 and IFNGR2 respectively, prior to IFN-γ binding [44]. The conformational change in the IFNGR subunits allows for JAK1 and JAK2 to activate. JAK1 phosphorylates IFNGR1 at tyrosine 440 (Y440), this phosphorylated tyrosine serves as an anchor for signal transducer and activator of transcription 1 (STAT1). STAT1 is then phosphorylated on tyrosine 701 (Y701) by JAK2 [48] and forms a dimer allowing it to translocate to the nucleus facilitated by importin-α-1 nucleoprotein 1 (NPI-1) [49]. In the nucleus, phosphorylated STAT1 dimers bind IFN-γ activator sequence (GAS) in the promoter region of genes responsive to IFN-γ [33], [44] (Figure 1.4).

The classical JAK/STAT signaling pathway described above may be oversimplified. Approximately 30% of genes stimulated by IFN-γ are activated independently of STAT signaling, suggesting that other pathways may be involved [50]. These include the phosphoinositide-3 kinase (PI3K/AKT) pathway and mitogen-activated kinase (MAPK) pathway [50], [51]. IFN-γ can cause the induction and upregulation of important immune surface molecules including HLA-II [10].

1.6 HLA-II inducible expression by IFN-γ

HLA-II expression can be induced on various cancer cells. Similar to constitutive expression, IFN-γ induced expression is regulated by CIITA [52]. In the presence of IFN-γ, activated STAT1 dimers translocate to the nucleus and bind the GAS sequence of CIITA promoter IV [53]. Cooperative binding of upstream stimulatory factor-1 (USF-1) to the enhancer box (Ebox) and IRFI to the IFR element (IRF-E) help stabilize the complex, which helps to activate CIITA [54] (Figure 1.4).

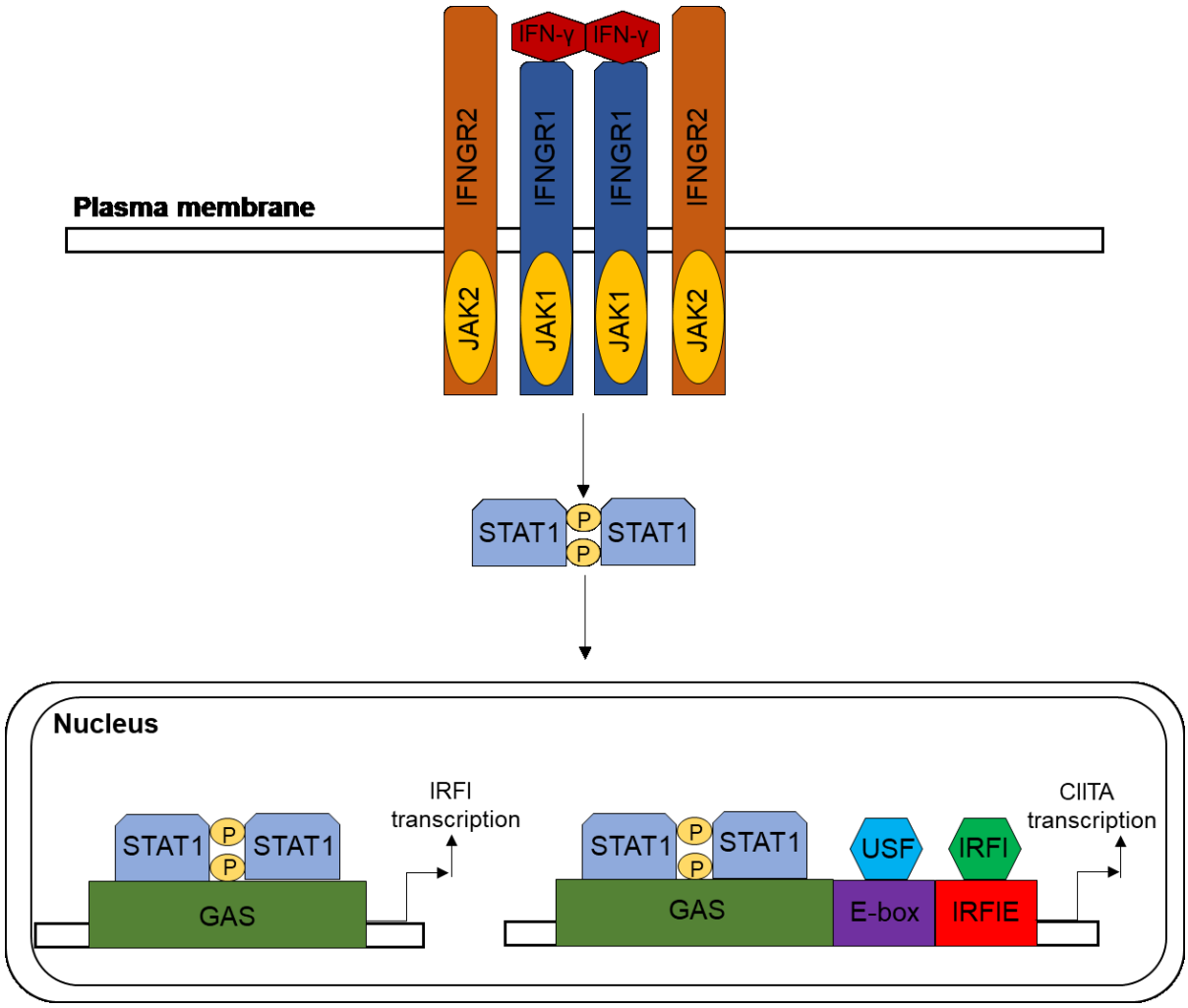
IFN-γ
IFN-γ
IFNGR2
IFNGR1
IFNGR1
IFNGR2
Plasma membrane
JAK2
JAK1
JAK1
JAK2
STAT1
P
P
STAT1
Nucleus
IRFI
transcription
STAT1
P
P
STAT1
GAS
STAT1
P
P
STAT1
USF
IRFI
CIITA
transcription
GAS
E-box
IRFIE

Figure 1.4: HLA-II upregulation by IFN-γ. IFN-γ binds the IFNGR on the cell surface. This initiates the activation of Janus kinase (JAK) and the phosphorylation of signal transducer and activator of transcription 1 (STAT1). Phosphorylated STAT1 dimer translocates to the nucleus where it activates target promoters for transcription of IRF1 and CIITA. Adapted with permission from [33].

1.7 HLA-II function

While HLA-II is often seen as having a valuable role in immune responses, there are certain circumstances where the presence of HLA-II can be inhibitory. As part of the generation of an antigen-specific immune response, HLA-II is involved in antigen presentation. APCs, which constitutively express HLA-II [4], degrade foreign peptides and present them on the surface via HLA-II molecules to CD4+ T helper cells [5]. This leads to a number of downstream effects including, but not limited to apoptosis, B cell activation, etc. [55], [56]. However, the presence of HLA-II is not always positive. As described in further detail in the sections below, HLA-II can dampen the immune response as it is a major ligand of immune inhibitory molecule LAG-3.

1.8 LAG-3 discovery and structure

Lymphocyte activating gene-3 (LAG-3) was first identified in 1990 on activated $CD4^+$ and $CD8^+$ T cell clones and a subset of NK cells [57]. The coding region for the 489 amino acid membrane protein was traced to the distal part of the short arm of chromosome 12. Further structural analysis found LAG-3 to be a member of the immunoglobulin (Ig) superfamily [57]. These early findings suggested that LAG-3 is an evolutionary ancestor to human CD4 as their coding regions are adjacent on chromosome 12 and there are similarities in structure [58]. LAG-3 contains a unique 30 amino acid loop on the first Ig domain and an intracellular KIEELE motif which is required for LAG-3 function (Figure 1.5). The KIEELE motif was believed to be imperative for downstream LAG-3 functions [59]. More recently, it was shown that deleting the KIEELE motif had no effect on T cell function [60]. This group, Meada et al., identified two

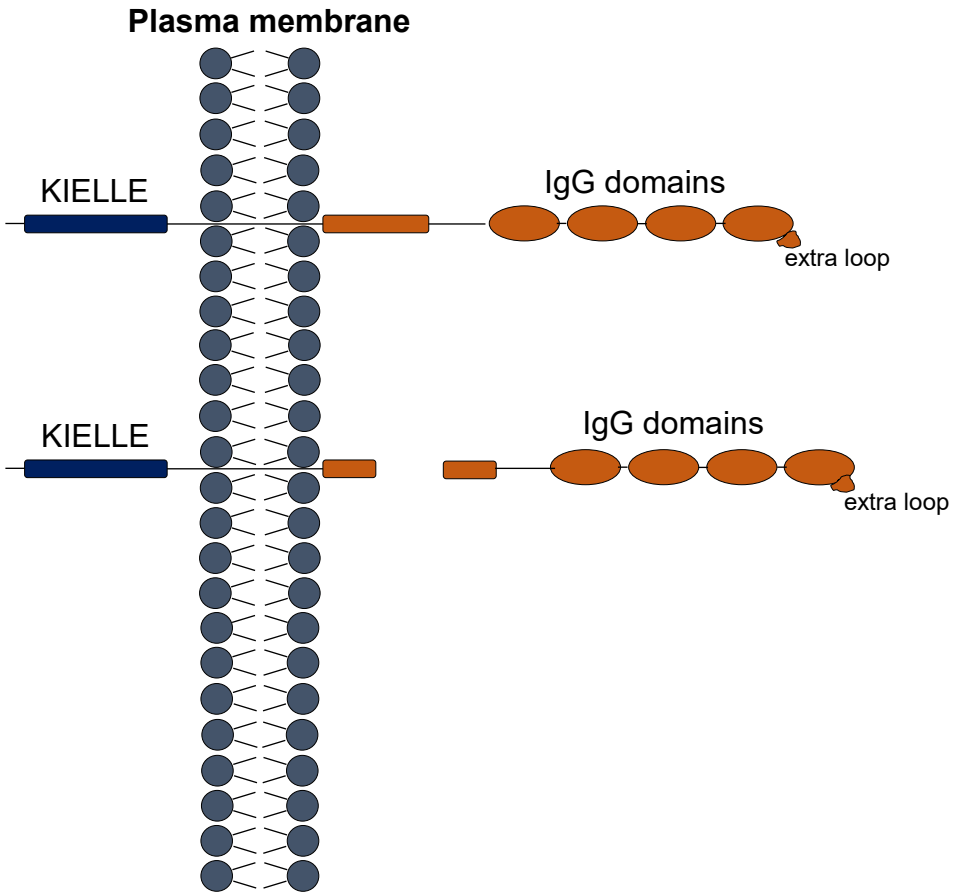
Plasma membrane
KIELLE
IgG domains
extra loop
KIELLE
IgG domains
extra loop

Figure 1.5: Structure of LAG-3. LAG-3 is a transmembrane protein structurally similar to human CD4. It has four extracellular IgG domains with a unique extra loop. Intracellular amino acid sequence KIELLE is required for proper LAG-3 function. LAG-3 can also exist in a soluble form with is functionally different from the membrane bound form. Adapted with permission from [61].

mechanisms through which LAG-3 transduced inhibitory signals, one through the membrane proximal FXXL motif and the other through the C-terminal EX repeat [60]. These features differentiate this molecule from CD4 as well as all other Ig superfamily molecules [62]. While there are substantial differences between human LAG-3 and CD4, they share about 20% amino acid homology, suggesting they are derived from a common evolutionary ancestor [63].

1.9 LAG-3 binding to HLA-II

The early identified structural similarities between CD4 and LAG-3 inspired investigations into functional similarities. LAG-3 transfected cells were able to bind B cells and their interaction could be blocked with antibodies against both LAG-3 and HLA-II [62]. This suggests that LAG-3 and CD4 share a common ligand, HLA-II. Binding of LAG-3 to HLA-II is facilitated through a cluster of amino acids at the base of the unique D1 domain loop of LAG-3 [64]. This is a smaller surface area of amino acids compared to CD4-HLA II binding. Accompanied with differences in binding motifs are variances in HLA-II affinity. Kinetic analysis has shown that LAG-3 binds HLA-II with much higher affinity than CD4 [65].

1.10 Alternate ligands for LAG-3

While the major ligand of LAG-3 is HLA-II, evidence has emerged for alternate LAG-3 binding mechanisms. Galectin-3 (Gal-3) is a galactoside binding soluble lectin that is expressed on a wide variety of cell types, including breast tumour cells [66], [67]. Gal-3 plays a role in many immune inhibitory mechanisms [68]–[70]. Association of LAG-3 and Gal-3 has been shown to be required for Gal-3-mediated suppression of tumour-specific cytotoxic T cells [71].

Interaction of LAG-3 and liver sinusoidal endothelial cell lectin (LSECtin) has immune inhibitory properties. LSECtin is commonly expressed on melanoma cells and upon association with LAG-3 in the tumour microenvironment decreases secretion of IFN-γ by T cells [72]. Binding of LSECtin to LAG-3 can be blocked with antibody C9B7V which targets the D2 domain of LAG-3 indicating that it binds to a different part of LAG-3 than HLA-II [72].

Fibrinogen-like protein 1 (FGL1) has also been associated with LAG-3. FGL1 is most commonly secreted by hepatocytes and has been found on breast cancer cells [73]. In a mouse model, mutation of the D1 domain of LAG-3 did not affect FGL1 binding [74]. This suggests that FGL1 binds to a different region than HLA-II. This would mean that even using antibodies known to block LAG-3 interactions may not inhibit binding of all ligands depending on the target region of the antibody and ligands present. The discovery of these alternate ligands means that LAG-3 has a broader inhibitory effect on the immune system than once thought. Thereby strengthening the potential impact of immunotherapy studies involving LAG-3.

1.11 LAG-3 function

Due to the substantial structural similarities between CD4 and LAG-3, early studies investigated whether these molecules are functional equivalents. The first group to investigate this notion showed a negative regulatory function of LAG-3. LAG-3 binding hindered T cell function and $CD4^+$ T cell proliferation was greater when all LAG-3 interactions were prevented [65], [75]. This is a stark contrast to CD4 which plays a stimulatory role in T cell activation.

The mechanism behind the negative regulatory function of LAG-3 is not entirely understood [76]. LAG-3 binding inhibits T cell receptor (TCR) signaling by interfering with the TCR/CD3 complex, leading to a decrease in calcium influx to the T cell [77], [78]. Upon LAG-3

binding fundamental signals are transmitted; these signals prevent cells from entering the S phase of the cell cycle, thereby inhibiting T cell expansion [59], [79]–[81]. The above-mentioned inhibitory signals were once thought to be transmitted by means of the KIEELE motif, however more recently other potential mechanisms have been identified and is referenced in Section 1.7.

While most of the work concerning LAG-3 function has focused on $CD4^+$ T cells, $CD8^+$ T cells were not overlooked. Just like $CD4^+$ T cells, naïve $CD8^+$ T cells express low levels of LAG-3 but expression increases upon activation [82], [83]. Several studies in both mice and human cells have demonstrated significantly increased $CD8^+$ T cell proliferation in LAG-3 knockout or deficient conditions [59], [81], [84], [85].

LAG-3 is expressed on both natural and induced regulatory T cells (Tregs) [86] and is a characteristic of a regulatory T cell phenotype [86], [87]. Treg differentiation is stimulated by LAG-3 and the blockade of LAG-3 binding steers T cell differentiation away from a regulatory phenotype [75]. LAG-3 has a functional role for Tregs, with findings showing increased suppressive activity of $LAG\text{-}3^+$ Tregs compared to deficient ones [88]. Binding of Treg associated LAG-3 with MHC class II (MHC-II) inhibits DC function [89]. When LAG-3 interactions on Tregs are blocked their suppressive activity is abolished. However, when non-regulatory T cells in the microenvironment were transfected with LAG-3, Treg activity was upregulated [86].

1.12 Soluble LAG-3

In addition to the membrane bound form, LAG-3 has a natural splice variant soluble LAG-3 (sLAG-3). Cell bound LAG-3 is cleaved by metalloproteases ADAM 10 and ADAM 17

between the membrane proximal D4 domain and the transmembrane domain. All activated T cells express LAG-3 and cleavage of LAG-3 can restore normal T cell function [90], [91].

Both forms of LAG-3 have the same major ligand, HLA-II. However, there are some functional variations between soluble and membrane bound LAG-3. Despite multiple reports in various models demonstrating the inhibitory role of LAG-3 on T cell activation, the soluble form of LAG-3 has been shown to enhance immune responses. sLAG-3 enhances the antigen processing capacity of the immune microenvironment through HLA-II binding [92]–[95]. sLAG-3 binds HLA-II associated with lipid rafts on immature DC, inducing the cells maturation. This leads to an increase in production of cytokines by Th1 cells as well as greater antigen presentation and co-stimulatory molecules [84], [93]. High levels of sLAG-3 are associated with resistance to numerous diseases including tuberculosis [96] and certain cancers including breast, lung and gastric [97]–[99]. While high levels of serum LAG-3 are associated with good prognosis, details on what cells are producing the sLAG-3 and what role it has are not fully understood.

For this reason, sLAG-3 has been studied for its adjuvant properties, particularly in vaccination and cancer. Studies show that vaccination plus sLAG-3 generated greater Th1 immune responses [100]. Several clinical trials using sLAG-3 therapies are underway as explained further in Section 1.17.

1.13 Lipid rafts and LAG-3

Lipid rafts play a vital role in various cellular processes, including endocytosis, cell adhesion, signal transduction and T cell activation [101]–[103]. A substantial portion of peptide bound HLA-II resides constitutively in lipid raft microdomains [104]. Lipid rafts aid in the

concentration of HLA-II on the cell membrane to help facilitate efficient T cell activation. During T cell-APC interactions, peptide loaded HLA-II associated in lipid rafts traffic to the immunological synapse. While lipid rafts are helpful for antigen presentation and T cell activation, these processes are also affected by LAG-3 and other inhibitory molecules. Therefore, studies have addressed whether LAG-3 preferentially binds HLA-II incorporated in lipid rafts. Lipid raft disruption through methyl-beta-cyclodextrin (MβCD) treatment has resulted in decreased sLAG-3 binding on immature DCs [93], [94]. These data suggest that LAG-3 is partially restricted to binding to HLA-II in lipid rafts [93], [105]. Since a large amount of HLA-II on APCs is present in lipid rafts and they play a role in antigen clustering, this makes HLA-II easily available for LAG-3 binding.

1.14 LAG-3 and disease

Infection, especially chronic infection, involves prolonged antigen exposure. In an environment where antigen is always in abundance, the surrounding immune cells, while working in attempt to manage the infection will eventually become exhausted. T cells that have developed an exhausted phenotype have high expression of inhibitory molecules, including PD-1, Tim3, CTLA-4 and LAG-3. Therefore, these exhausted T cells have decreased proliferation and function allowing the infection to propagate. Upregulated expression of LAG-3 has been found on T cells of patients with infections such as HIV and tuberculosis [83], [95], [106], [107]. Synergistic cooperation has been found between LAG-3 and PD-1 in preventing autoimmunity and in suppressing T-cell immunity in cancer models [108]–[112].

The basis of any autoimmune disease is a loss of immune self-tolerance. In autoimmune diseases, the immune cells react to the body's own antigens and cells as if they were foreign,

thus destroying cells required for proper function of the system in question. In healthy people, inhibitory receptors like LAG-3 are present in small amounts, nevertheless they play a big role in self-tolerance. Therefore, widespread inhibition of these inhibitory molecules, such as occurs in cancer immunotherapy using immune checkpoint inhibitors, can decrease self-tolerance and increase occurrence of autoimmune diseases [113].

1.15 LAG-3 involvement in cancer

Similar to chronic infections, cancers are associated with prolonged exposure to antigens which can lead to the development of dysfunctional T cells. Because of this tumour infiltrating T cells tend to develop an exhausted phenotype [114]–[117]. This is characterized in part by high expression levels of molecules including LAG-3, Tim3, PD-1 and CTLA-4 [99], [115], [118]–[122]. Through these inhibitory molecules there are consequently multiple potential avenues for tumor immune escape, all using vastly different signaling pathways and ligands.

The action of blocking signaling through exhaustion markers has been extensively studied in various cancer models. Inhibition of interaction through molecules such as LAG-3 with specific antibodies prevents ligand binding and subsequent downstream signaling that would contribute to the downregulation of T cell function and proliferation. Addition of LAG-3 antibodies to hinder HLA-II interaction and partially restore T cell function has been examined in both pre-clinical and clinical studies [60], [123], [124]. Since a single tumour infiltrating lymphocyte often expresses multiple inhibitory molecules on their surface, blocking signaling through just one may only partially restore immune cell function. Therefore, many potential antibody therapies have been studied both alone and in combination.

LAG-3 represents only half of the signaling equation. Expression of its major ligand HLA-II in the tumour microenvironment must also be considered. HLA-II molecules are constitutively expressed only on antigen-presenting cells. IFN-γ stimulation can induce HLA-II expression on tumour cells including breast cancer cells [10]. Induction of HLA-II expression on cancer cells is important to consider in terms of therapies involving LAG-3. Blocking all HLA-II interactions in hopes of knocking out interaction with LAG-3 would likely do more harm than good. In the context of cancer immunity, the primary function of HLA-II is to present tumour specific antigen to $CD4^+$ T cells. With more of its ligand present, there are more chances of LAG-3 engagement and subsequent T cell dysfunction.

1.16 PD-L1 involvement in cancer

Programmed cell death ligand 1 (PD-L1) is an immune inhibitory molecule. Similar to LAG-3, PD-L1 is being widely studied in cancer immunotherapy. Programmed cell death protein (PD-1) is commonly expressed on tumor infiltrating lymphocytes alongside other immune inhibitory molecules including LAG-3 [100], [119], [120], [125]–[127]. Cancer cell lines have been known to have up-regulated levels of PD-L1 expression [128]. PD-1/PD-L1 interaction inhibits T cell activation, proliferation and cytokine secretion [129], [130]. This combination of PD-L1 expression on cancer cells and PD-1 on tumor infiltrating lymphocytes aids in the evasion of the cancer immune response. Thus, this immune inhibitory interaction is a promising target for cancer immunotherapy.

Therapies that target multiple parts of the PD-L1 and PD-1 interaction are being investigated. PD-L1 interaction is currently being studied and used for treating cancer alone and in combination with other therapies. While antibody therapies targeting the PD-1/PD-L1,

Pembrolizumab and Nivolumab, interaction offer encouraging results, there are differences in results depending on factors like cancer type [131], [132]. Analysis of The Cancer Genome Atlas Program (TCGA) breast cancer data has shown that LAG-3 expression is strongly correlated with expression of PD-L1 and other immune inhibitory markers [133]. Given this correlation, the goal of combining multiple therapies is to see a synergistic effect on anti-tumor immunity. Combinations of LAG-3 and PD-L1 blockade are further discussed in Section 1.17

1.17 LAG-3 antibody therapies

For LAG-3 to facilitate T cell dysfunction, binding of HLA-II or an alternate ligand is required. Therefore, blocking all LAG-3 interactions with anti-LAG-3 antibodies could inhibit the negative regulation of tumour-specific T cells. Early LAG-3 studies have shown that blocking interactions through LAG-3 on T cells increases rates of growth and cytokine production [65], [75], [134]. Experiments in cancer models have shown similar results. Treatment with anti-LAG-3 can result in greater T cell function, as shown through increased cytokine production and cell proliferation [134].

While results with anti-LAG-3 alone have been positive thus far, it is unlikely that T cell function will be fully restored. Immune cells in an environment with prolonged antigen exposure, as in the tumour microenvironment, often express multiple inhibitory markers. Therefore, there are certain cases where simply blocking anti-LAG-3 interaction may not be enough to significantly improve T cell function. There may be other inhibitory receptors that overpower the effects of LAG-3 inhibition. Alternatively, even if there are immediate benefits, they may not stand the test of time as the other inhibitory molecules present may evolve to be stronger as an immune evasion mechanism. For these reasons, anti-LAG-3 has been studied in

combination with chemotherapies and other antibody therapies. The main antibody combination therapy studies have involved anti-LAG-3 and anti-PD-1 [135], [136]. Multiple models have shown synergistic increases in T cell function when both antibodies are used in combination compared to either alone [73], [108]–[110], [112], [114].

1.18 sLAG-3 role in cancer treatment

As mentioned in Section 1.12, LAG-3 exists in a soluble form that functions differently from membrane bound LAG-3. The immune adjuvant properties of sLAG-3 make it a promising candidate for cancer therapy. Various clinical studies have been completed and there are even more underway[137]. Motivation behind these studies is strengthened by reports suggesting sLAG-3 may be a good cancer prognosis marker. In a cohort of breast cancer patients, high serum levels of sLAG-3 at the time of diagnosis before the start of treatment were associated with increased overall survival in estrogen and progesterone positive subtypes [97].

IMP321 is a chimeric molecule that comprises the extracellular portion of LAG-3 fused to human IgG1 and has been used in numerous clinical trials, both completed and ongoing. It has been shown to act as a vaccine adjuvant through induction of DC maturation and increased production of stimulatory cytokines [93], [138]–[140]. Given that T cells, including tumour-specific T cells, can be activated indirectly by IMP-321 [141]–[143], it could enhance the success of tumour vaccine treatments [100]. IMP321 was found to bind nearly all DCs in human blood samples of metastatic cancer patients [95] and subsequently could induce antigen-specific T cells to produce Th1 cytokines including IFN- γ and TNF-α [144].

The first sLAG-3 clinical trial was in metastatic renal carcinoma. A subset of these patients who received IMP321 had significantly higher levels of CD8 activation and stable disease at three months [145]. Combination of IMP321 with chemotherapeutic agent gemcitabine

in pancreatic cancer patients, while safe, treatment did not result in immune system activation [146]. In a phase II trial involving metastatic breast cancer IMP321 was found to work as a chemo-immunotherapeutic when combined with chemotherapy drug paclitaxel. At the end of six months 10% of patients had progressive disease compared to over 50% progressive disease in the historical control group receiving just paclitaxel. Patients also had significantly higher levels of natural killer cells, DCs and effector memory T cells compared to baseline [147]–[149]. Clinical studies in melanoma have shown that treatment with IMP321 contributes to a greater anti-tumour immune response with increased activation of APCs and DCs [148], [149].

1.19 Rationale and Objectives

High levels of sLAG-3 in sera of patients with hormone positive breast cancer was reported to associate with a better prognosis; however, the underlying mechanisms for this association were not elucidated. Among the suggested explanations by the authors were: 1) the possibility sLAG-3 stimulates anti-tumor immune responses by binding and activating pAPCs. This same group had previously shown sLAG-3 activates and matures DC by preferentially binding MHC-II localized to lipid rafts and has adjuvant properties. 2) sLAG-3 acted as an inhibitory molecule for LAG3+ regulatory T-cells, thus preventing them from interacting with MHC-II positive cells. This intriguing idea suggested sLAG-3 may bind cancer cells that upregulate their MHC-II during an anti-tumour immune response. Indeed, the Drover group and others have previously shown a significant proportion of breast carcinomas contain MHC-II positive tumour cells, whereby the prognosis is dramatically improved if the tumor cells also express the MHC-II peptide editor, DM. DM was also shown to play an important role in LAG-3 binding due to its stabilizing effects on MHC-II/peptide conformation. To our knowledge no

studies have addressed whether LAG-3 (cell bound or soluble) directly interacts with MHC-II positive cancer cells, or whether lipid rafts on these cells or the presence of DM or other chaperones modulate sLAG-3 binding. Thus, the thesis work described here was performed to address these unknowns. An additional goal, relevant to the potential of LAG-3 and another immune checkpoint molecule, PD-1 as co-targets for immunotherapy, was to determine the expression of both ligands, MHC-II and PD-L1, respectively, on breast cancer cells treated or not with the T_H1 cytokine, IFN-γ.

Objectives:

1) Using human B-cell lines:
    a. Validate the assay to detect sLAG-3 binding.
    b. Explore the role of DM and peptide stability in LAG-3 binding to B-cell lines.
    c. Investigate sLAG-3 binding to Burkitt lymphoma cells.
2) Using a melanoma cell line and a panel of breast cancer cell lines (BCCL), treated or not with IFN-γ, to:
    a. Determine sLAG-3 binding, MHC-II and PD-L1 expression.
    b. Analyze the effect of lipid raft disruption on sLAG-3 binding, MHC-II and PD-L1 expression.

Chapter 2: Materials and Methods

2.1 Cell culture

2.1.1 Adherent cell lines

A cell line panel comprising a wide variety of BCCL as well as a melanoma line were used for this study (Table 2.1). All adherent cancer cell lines were initially obtained from the American Type Culture Collection (ATCC), and stocks are maintained in the Drover laboratory. Cell lines were tested for mycoplasma and authenticated by short tandem repeat (STR) analysis.

Cells were grown in Iscove's Modified Dulbecco's Medium (IMDM) (Invitrogen) supplemented with 10% heat-inactivated fetal calf serum (FCS) (Invitrogen), 2mM L-glutamine (Invitrogen) and 2 mM antibiotic antimycotic (Invitrogen). Cells were maintained in a 5% CO_2 atmosphere at a temperature of 37 °C on 10 cm^2 tissue culture dishes (Falcon, Becton Dickenson Bioscience). An adherent monolayer of cells was refreshed with complete medium every 3-4 days and harvested at 80-90% confluency. Once cells reached desired confluency all medium was removed and the plate was washed with phosphate buffered saline (PBS), then incubated with 0.25% Trypsin EDTA (Invitrogen) at 37 °C for a few minutes to facilitate cell detaching. After separation from the plate, media was added to deactivate the trypsin. In order to maximize cell recovery, media was pipetted back and forth in the plate. The cell suspension was then transferred to a 15 mL tube and centrifuged at 500 x g for 7 minutes at 8-12 °C. After the supernatant was decanted, the cell pellet was washed with medium and centrifuged under the same conditions. Cell pellet was resuspended in medium, and cells were counted using a

hemocytometer and phase contrast microscopy. Cells were plated at a density of 5.0 x 10^5 in a 10 cm^2 tissue culture dish with 10 mL complete medium.

Table 2.1 Human cell lines used in this study

Cell line	**Identification**	**Cell type**	**Cancer classification**	**Receptor expression**
SAVC	10^{th} International Histocompatibility Workshop	EBV transformed B cell line		N/A
Daudi	ATCC CCL-213	B cell	Burkitt lymphoma	N/A
8.1.6		B cell		N/A
8.1.6 0401		DRB1 transfected B cell		N/A
9.5.3		B cell		N/A
9.5.3 0401		DRB1 transfected B cell		N/A
9.5.3 DM		DM transfected B cell		N/A
5.2.4 0401		DRB1 transfected B cell		N/A
5.2.4 0401 DM		DRB1 and DM transfected B cell		N/A
Bjab		B cell	Burkitt lymphoma	N/A
Bjab 0401		DRB1 transfected B cell	Burkitt lymphoma	N/A
Bjab DO		DO transfected B cell	Burkitt lymphoma	N/A
Bjab DO 0401		DO and DRB1 transfected B cell	Burkitt lymphoma	N/A
Bjab V2		Vector control B cell	Burkitt lymphoma	N/A

MDA-MB-435	ATCC HTB-129	Melanoma[1]	Ductal carcinoma	N/A[2]
MDA-MB-231	ATCC HTB-26	TNBC	Adenocarcinoma basal B	ER^{-}[3], PR^{-}[4], $HER2^{-}$[5]
BT-20	ATCC HTB-19	TNBC	Carcinoma basal A	ER^{-}, PR^{-}, $HER2^{-}$
T47D	ATCC HTB-133	Luminal A BCCL	Ductal carcinoma	ER^{+}, PR^{+}, $HER2^{-}$
SKBR3	ATCC HTB-30	HER2 BCCL	Adenocarcinoma	ER^{-}, PR^{-}, $HER2^{+}$
MCF-7	ATCC HTB-22	Luminal A BCCL	Adenocarcinoma	ER^{+}, PR^{+}, $HER2^{-}$

[1] MDA-MB-435 was originally classified as a triple negative breast cancer cell, but is now accepted as a melanoma cell line [150]

[2] Not applicable for this section

[3] Estrogen receptor

[4] Progesterone receptor

[5] Human epidermal growth factor receptor 2

2.1.2 Non-adherent cell lines

Human B cell line (BCL) SAVC originated from the 10th international histocompatibility workshop, while cell lines and transfectants 8.1.6, 8.1.6 0401, 9.5.3, 9.5.3 0401, 9.5.3 DM, 5.2.4 0401 and 5.2.4 0401 DM were kindly provided by Dr. E.D Mellins (Stanford University). Human Burkitt lymphoma (BL) cell line Bjab was provided by Dr. J. Thibodeau (University of Montreal). Bjab transfectants (BjabDO and BjabV2) were provided by Dr. P. Roche (National Institute of Health). These Bjab cells were transfected with DRB1*04:01 in the Drover laboratory by Chris Corkum (Bjab 0401and Bjab DO 0401) [151]. Daudi, another BL cell line originated from ATCC.

All non-adherent cell lines were grown in 25 cm^2 cell culture flasks (Corning) in Roswell Park Memorial Institute (RPMI) (Invitrogen) with 10% inactivated FCS (Invitrogen), 2 mM L-glutamine (Invitrogen), 2 mM antibiotic antimycotic (Invitrogen) and 1 mM sodium pyruvate (Invitrogen). Cells were maintained at a maximum of 5.0 x 10^5 cells/mL in 37 °C conditions at an atmosphere of 5% CO_2.

2.2 IFN-γ treatment of adherent cancer cell lines

Constitutively, many breast cancer cell lines, including those used in this study, express little to no HLA-II on their surface. IFN-γ has the ability to upregulate HLA-II expression [10]. Since HLA-II is the major ligand of LAG-3, it was important to analyze sLAG-3 binding on IFN-γ treated and untreated cells.

Twenty-four hours after cells were plated, 100 units of human recombinant IFN-γ (BD Biosciences) was added to each appropriate culture and incubated at 37°C for 72 hours. The concentration and incubation time was found to be optimal for stimulating HLA-II cell surface

expression on breast cancer cell lines through previous experiments in the Drover laboratory [152].

2.3 Flow Cytometry

2.3.1 Cell surface assay

Adherent cultures were harvested as described in Section 2.1.1 and washed with 5 mL Fluorescence Activated Cell Sorting (FACS) buffer, which consists of 0.02% heat-inactivated FCS and 0.01% sodium azide in PBS. After decanting the supernatant, cells were resuspended at 1.5-2.0 x 10^6 and 100 µL of cells was added to 5 mL polystyrene round bottom tubes (Corning).

For non-adherent cells, cell suspension containing the desired number of cells was removed from the culture flask, washed twice, once with medium and once with FACS buffer and 100 µL of cell suspension in FACS buffer was added to 5 mL round bottom tubes as detailed above.

Primary antibodies were diluted at optimally determined concentrations (Table 2.2) in FACS buffer. After the addition of 25 µL of antibody dilution per tube, tubes were incubated at 4°C for 30 minutes, washed twice with 2 mL FACS buffer at 1550 RPM for 5 minutes at 8-12 °C. Twenty-five µl of optimally diluted secondary antibody (Table 2.3) was added to each tube and incubated for 30 minutes at 4 °C in the dark. Cells were then washed twice with FACS buffer and fixed by adding 150 µL paraformaldehyde (PFA) (Sigma) diluted in PBS. Cells were stored at 4 °C in the dark until time of analysis. Tubes were analyzed at 10,000 events per tube using FACS Calibur flow cytometer (Becton-Dickinson) and Kaluza Software (Beckman Coutler).

Table 2.2 Primary antibodies used for flow cytometry

Antibody	**Isotype**	**Specificity**	**Working concentration**	**Source**
IgG1	Human IgG_1	control	10 μg/mL	AdipoGen Life Sciences
P3.6.2.8	Mouse IgG_1	control	5 μg/mL	eBioscience
NSG_{2a}	Mouse IgG_{2a}	control	5 μg/mL	Local source
P18627	Human IgG_1	Human LAG3 F_c chimera protein	10 μg/mL	R&D Systems
Tu39	Mouse IgG_{2a}	HLA-DR, DP, DQ		Biolegend
MEM-43	Mouse IgG_{2a}	CD59		Abcam
MaP.DM1	Mouse IgG_1	HLA-DM	10 μg/mL	BD Bioscienes
MIH2	Mouse IgG_1	PD-L1	5 μg/mL	Abcam

Table 2.3 Secondary antibodies used for flow cytometry

Antibody	Isotype	Specificity	Working concentration	Source
R-Phycoerythrin Affini Pure (Fab')2 Fragment goat anti-mouse IgG Fcγ fragment specific	IgG	Mouse	1/40	Jackson Immunoresearch
Fluorescein Affini Pure Fragment goat anti-mouse IgG Fcγ fragment specific	IgG	Mouse	1/40	Jackson Immunoresearch
R-Phycoerythrin Affini Pure Fragment goat anti-human IgG Fcγ fragment specific	IgG	Human	1/100	Jackson Immunoresearch
Fluorescein Affini Pure Fragment goat anti-human IgG Fcγ fragment specific	IgG	Human	1/100	Jackson Immunoresearch

2.3.2 Intracellular assay

For analysis of intracellular proteins, cells were fixed with 2% PFA on ice for 15 minutes and washed twice, once with medium and once with PBS. Cells were then permeabilized with permeabilization buffer consisting of 0.2% Tween-20 (Sigma) in PBS on ice for 15 minutes. Following a wash in perm-wash buffer (0.5% FCS and 0.2% Tween-20 in PBS), cells were resuspended in buffer and added to 5 mL round bottom tubes. Primary and secondary antibody incubations are described above (Section 2.1), however all washes were done using perm-wash buffer as opposed to FACS buffer. All tubes were analyzed for 10,000 events using FACS Calibur flow cytometer (Becton-Dickinson) and Kaluza software (Beckman Coutler).

2.4 LAG-3 binding assays

2.4.1 sLAG-3 binding detection assay

Flow cytometric analysis was used to access the ability of sLAG-3 to bind HLA-II. Recombinant human LAG-3 F_c chimera protein (R&D Systems), which consists of the four extracellular domains of LAG-3 fused to the F_c portion of human IgG1, can be detected by fluorescence goat anti-human IgG Fcγ fragment specific.

Cells were prepared according to Section 2.2.1, but prior to distribution in round bottom tubes, cells were incubated for 1 hour with 10% heat-inactivated human AB serum to prevent non-specific binding. Following blocking, two extracellular flow cytometry procedures (Section 2.1) were performed 1) using human LAG-3 F_c chimera protein and human IgG1 control and 2) anti-HLA-II and mouse IgG_{2a} isotype control. Binding was detected using appropriate secondary antibodies (Table 2.2 and 2.3).

2.4.2 Interpretation of sLAG-3 binding results

Kaluza software was used to quantify mean fluorescence intensity (MFI) and percentage of positive cells (%+) for 10,000 events. Test results were considered positive if MFI was at least double the isotype control. The extent of LAG-3 binding was determined by dividing the expression of sLAG-3 by the expression of HLA-II using the two following formulas: [(MFI sLAG-3 - MFI human IgG1) / (MFI class II – MFI mouse IgG_{2a})] x 100 and [(%+ sLAG-3 - %+ human IgG1) / (%+ class II - %+ mouse IgG_{2a}))] x 100. Statistics were evaluated using Microsoft excel. ANOVA was used to compare cell lines and treatments. A p value of equal to or less than 0.05 was determined to be significant.

2.5 Lipid raft disruption

MβCD disrupts cholesterol in the plasma membrane thereby altering protein association in lipid rafts. Lipid raft disruption was facilitated by 37°C incubation with 10 mM MβCD (Sigma) dissolved in serum free media for 30 minutes. Cells were washed once with serum free media before and after MβCD incubation. FCS was omitted from media to limit cholesterol incorporation into the cell membranes. In order to prevent lipid raft reassembly, cells were fixed with 2% PFA in PBS on ice for 15 minutes. Fixation was halted by washing with 100 mM glycine in PBS followed by a PBS wash.

sLAG-3 binding along with expression of HLA-II and CD59 was analyzed by flow cytometry. Optimal MβCD treatment concentration was achieved through previous experiments in the Drover laboratory [151].

2.5.1 Interpretation of lipid raft disruption results

MFI and %+ of cells were quantified using FACS calibur flow cytometer and Kaluza software. Antibody or sLAG-3 binding was determined to be positive if MFI was double that of the negative control antibody. Ratio of MβCD treated/untreated was obtained by dividing (MFI test antibody - isotype control for MβCD treated cells) / (MFI test antibody – isotype control for untreated cells) or (% positive test antibody – isotype control for MβCD treated cells) / (% positive test antibody – isotype control antibody for untreated cells). Interpretation was as follows; ratio of 1, MβCD treatment had "no effect"; ratio >1, MβCD treatment increased binding; ratio <1, MβCD treatment inhibited binding. The percentage of sLAG-3 binding was determined using the same formulas as described in Section 2.3.1. Statistics were evaluated using Microsoft excel. ANOVA was used to compare cell lines and treatments. A p value of equal to or less than 0.05 was determined to be significant.

Chapter 3: Results

3.1 Proof of principle using BCL

LAG-3 Fc chimera protein was used to detect LAG-3 binding on human cell lines by flow cytometry. The protein is comprised of the four extracellular domains of human LAG-3 fused to the Fc portion of IgG1. Through interaction of LAG-3 Fc chimera protein with HLA-II positive cells, the extent of LAG-3-HLA-II binding can be quantified using a fluorescent-labeled anti-human IgG1 antibody that binds the Fc region of the LAG-3 chimera protein.

Published reports indicate LAG-3 binds strongly to HLA-II molecules on mature DCs [105] and Epstein-Barr virus (EBV) transformed BCL [62]. Its binding strength to HLA-II appears dependent on localization of HLA-II in lipid rafts [93], [95], [105] as well as stability of pHLA-II [153]. To evaluate sLAG-3 chimera protein binding efficiency, we first did a single flow cytometry assay using three different HLA homozygous EBV-transformed B cell lines and the BL cell line, Daudi. As shown in Table 3.1, sLAG-3 binding to SAVC was strongest followed by that to Jesthom and Sweig, while binding to Daudi cells was almost nil. This was true when sLAG3 binding was normalized to the amount of HLA-II expressed by each cell line. A potential explanation for negligible sLAG-3 binding to Daudi is absence of lipid rafts.

To further validate sLAG-3 binding and explore whether lipid rafts affected binding, three independent assays were performed on SAVC and Daudi. In addition to sLAG-3 binding, cells were analyzed for HLA-II expression and CD59, a lipid raft marker (Figure 3.1). We found significantly increased sLAG-3 binding to SAVC as compared to Daudi (Figure 3.1A, B and 3.1E). Both cell lines express high amounts of HLA-II (Figure 3.1A and 3.1C), but Daudi was clearly negative for CD59 (Figure 3.1A and 3.1D), indicating lipid raft deficiency. This finding,

Table 3.1: sLAG-3 binding to EBV transformed and Burkitts cell lines

B-Cell Line	HLA-II DRB Alleles	HLA II expression		sLAG-3 Binding		sLAG-3/Class II (%) [3]	
		MFI[1]	%+[2]	MFI	%+	MFI[1]	%+
SAVC	DRB1*0401	12.6	72.3	2.2	47.5	17.6	65.7
Jesthom	DRB1*01:01	11.9	66.3	1.4	20.0	11.3	30.2
Sweig 007	DRB1*11:01	19.7	76.5	1.6	17.1	7.9	22.4
Daudi	DRB1*13:01, 13:02	19.1	80.1	0.7	4.6	3.6	5.7

[1] Mean fluorescence intensity calculated using formula: MFI test antibody - MFI isotype control.

[2] Percentage of positive cells, calculated using formula: %+ test antibody - %+isotype control.

[3] Relative binding of sLAG-3 to HLA class II using the formula: MFI - control sLAG-3 / MFI-control Class II (%) and % positive-control sLAG-3 / % positive-control Class II (%).

A

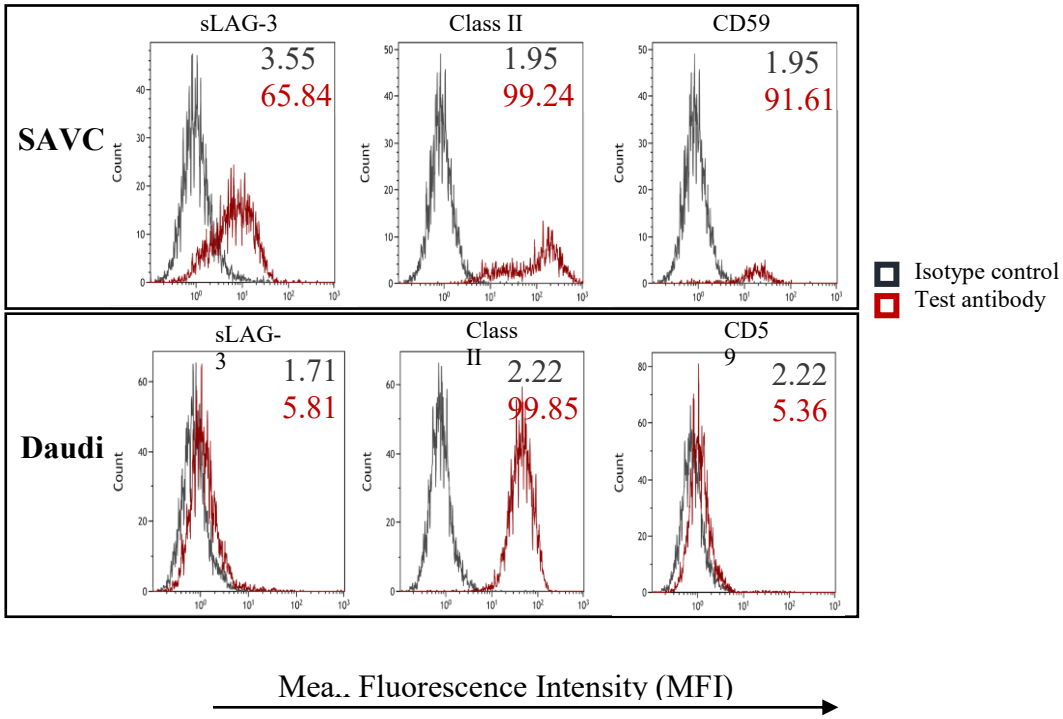
sLAG-3
Class II
CD59
SAVC
3.55
65.84
1.95
99.24
1.95
91.61
Count
Daudi
sLAG-3
Class II
CD59
1.71
5.81
2.22
99.85
2.22
5.36
Isotype control
Test antibody
Mea.. Fluorescence Intensity (MFI)

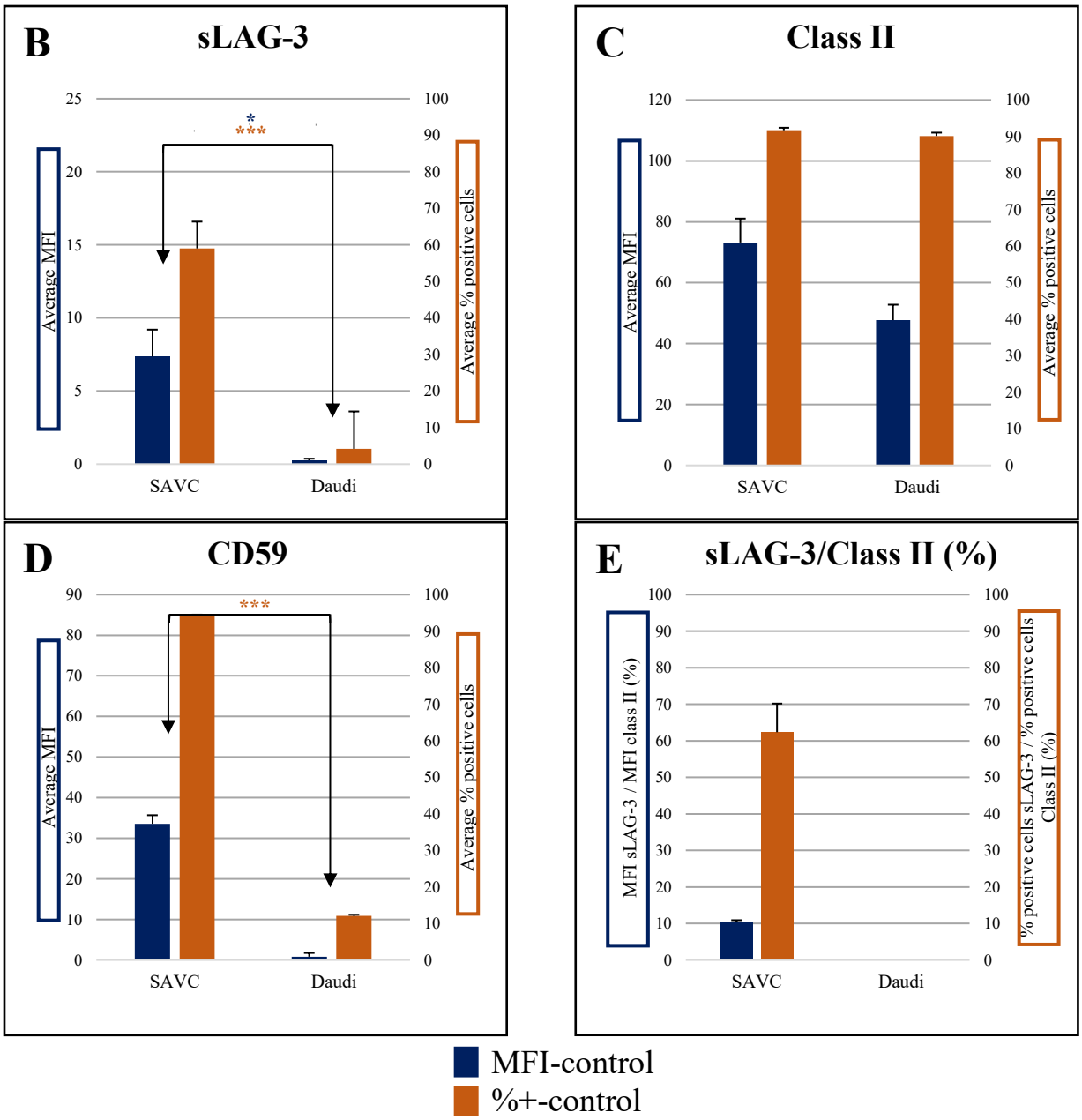
B
sLAG-3
Average MFI
Average % positive cells
SAVC
Daudi
C
Class II
Average MFI
Average % positive cells
SAVC
Daudi
D
CD59
Average MFI
Average % positive cells
SAVC
Daudi
E
sLAG-3/Class II (%)
MFI sLAG-3 / MFI class II (%)
% positive cells sLAG-3 / % positive cells Class II (%)
SAVC
Daudi
MFI-control
%+-control

Figure 3.1: Differential sLAG-3 binding to human B-cell lines expressing different levels of lipid raft marker, CD59 **A)** sLAG-3 binding, HLA class II and CD59 expression on BCL SAVC and BL cell line Daudi. Grey histogram represents isotype control, red histogram represents test antibody. Histograms are representative of one of three independent experiments. Values on histograms represent the percentage of positive cells. **B-D)** Bar diagrams depicting average MFI and % positive cells using the formula, MFI test antibody – MFI isotype control (left axis, blue bars) and % positive test antibody – % positive isotype control (right axis, orange bars): **B)** sLAG-3 binding, **C)** HLA class II and **D)** CD59 expression. **E)** Depicts the relative binding of sLAG-3 to HLA class II using the formula, MFI - control sLAG-3 / MFI - control Class II (%) (left axis, blue bars) and % positive - control sLAG-3 / % positive - control Class II (%) (right axis, orange bars). Error bars represent mean ± SEM of three independent experiments (*$p<0.05$, **$p<0.01$ and ***$p<0.001$ by ANOVA).

consistent with previous reports that Daudi lacks GPI-anchored proteins CD59 [154], [155], suggested deficient sLAG3 binding to Daudi may be due to its lipid raft deficiency.

Given the above results and the aforementioned dependence of LAG-3-HLA-II interactions on lipid rafts and pHLA-II stability, we next analyzed sLAG-3 binding using a set of B cell mutants. These have been extensively studied by the Mellins group [27] and in our laboratory [151] and are instructive for effects of DM and lipid rafts on pHLA-II stability. They included 8.1.6, which has stable pHLA-II; 9.5.3, a derivative of 8.1.6 that has lost DMβ expression, is lipid raft deficient and expresses mainly unstable HLA-II/CLIP complexes; 9.5.3 DM, a DMβ transfectant; 8.1.6 0401 and 9.5.3 0401, each transfected with DRβ1 0401 cDNA; 5.2.4 0401, also derived from 8.1.6, but is both DM and DO deficient and the double transfectant 5.2.4 0401DM. The DRB1*04:01 transfectants were included to explore whether sLAG-3 binding was stronger than on the parent cells (HLA-DRB1*04:01), since the DRB1*04:01+SAVC line was the strongest sLAG-3 binder (Table 3.1).

8.1.6 and 9.5.3 along with DRB1 and DM transfectants express abundant HLA-II, but the amounts on 9.5.3 cells, including 9.5.3 DM, are significantly reduced compared to 8.1.6 cells (Figure 3.2A and 3.2C). sLAG-3 binding, detected on all 8.1.6 and 9.5.3 parental cells and derivatives, clearly bound more strongly to 8.1.6 and 8.1.6 0401 (Figure 3.2D) than to 9.5.3 or 9.5.3 0401 (Figure 3.2A, 3.2B and 3.2E). We initially postulated that this was due to the lipid raft deficiency in 9.5.3 cells (Figure 3.2D); however, binding to 9.5.3 DM was comparable to 8.1.6 (Figure 3.2B and 3.2E). These results suggest that DM, which stabilizes pHLA-II, may play a more important role in LAG-3 binding than do the presence of HLA-II in lipid rafts.

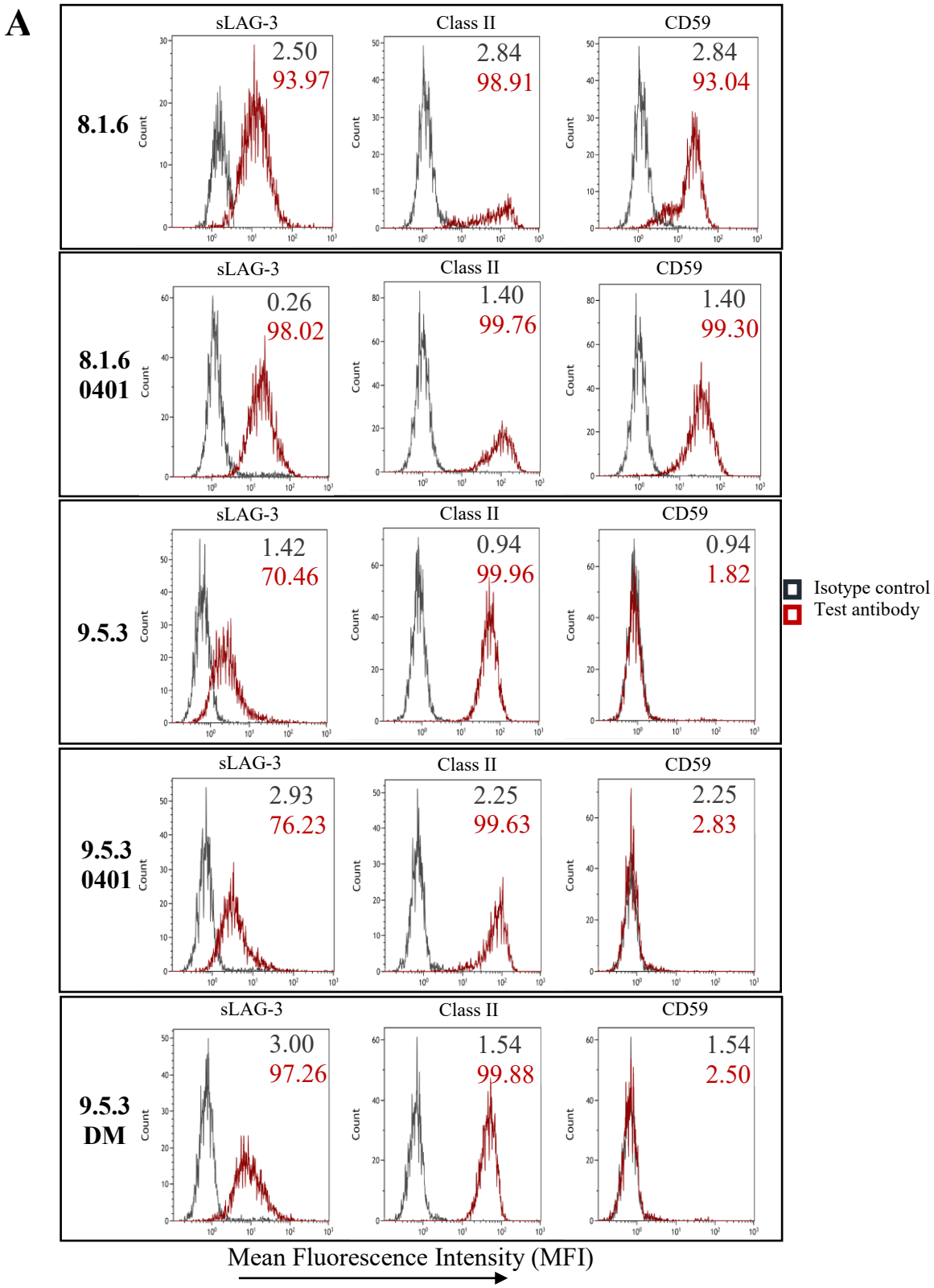
A
sLAG-3
Class II
CD59
8.1.6
2.50
93.97
2.84
98.91
2.84
93.04
8.1.6
0401
0.26
98.02
1.40
99.76
1.40
99.30
9.5.3
1.42
70.46
0.94
99.96
0.94
1.82
9.5.3
0401
2.93
76.23
2.25
99.63
2.25
2.83
9.5.3
DM
3.00
97.26
1.54
99.88
1.54
2.50
Count
Isotype control
Test antibody
Mean Fluorescence Intensity (MFI)

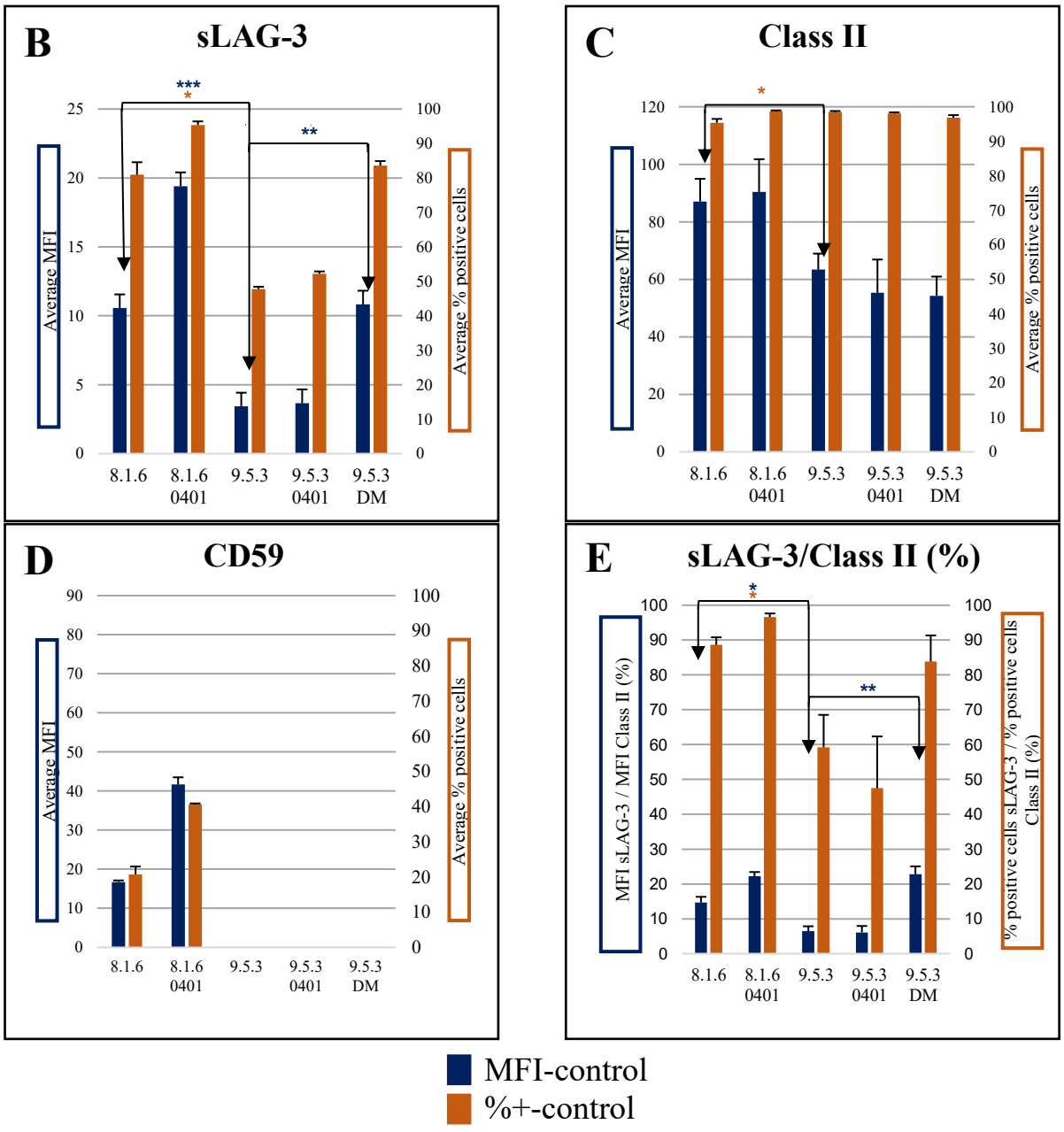
B
sLAG-3
***
*
**
Average MFI
Average % positive cells
25
20
15
10
5
0
100
90
80
70
60
50
40
30
20
10
0
8.1.6
8.1.6 0401
9.5.3
9.5.3 0401
9.5.3 DM
C
Class II
*
Average MFI
Average % positive cells
120
100
80
60
40
20
0
8.1.6
8.1.6 0401
9.5.3
9.5.3 0401
9.5.3 DM
D
CD59
Average MFI
Average % positive cells
90
80
70
60
50
40
30
20
10
0
8.1.6
8.1.6 0401
9.5.3
9.5.3 0401
9.5.3 DM
E
sLAG-3/Class II (%)
*
*
**
MFI sLAG-3 / MFI Class II (%)
% positive cells sLAG-3 / % positive cells Class II (%)
100
90
80
70
60
50
40
30
20
10
0
8.1.6
8.1.6 0401
9.5.3
9.5.3 0401
9.5.3 DM
MFI-control
%+-control

Figure 3.2: sLAG-3 binding to human BCL is modulated by DM expression. **A)** sLAG-3 binding, HLA class II and CD59 expression on human BCL 8.1.6 and 9.5.3, DRB1-transfectants 8.1.6 0401 and 9.5.3 0401 and DM transfectant 9.5.3 DM. Grey histogram represents isotype control, red histogram represents test antibody. Histograms are representative of one of three independent experiments. Values on histograms represent the percentage of positive cells. **B-D)** Bar diagrams depicting average MFI and % positive cells using formula, MFI test antibody – MFI isotype control (left axis, blue bars) and % positive test antibody – % positive isotype control (right axis, orange bars) **B)** sLAG-3 binding, **C)** HLA class II expression and **D)** CD59 expression. **E)** Depicts the relative binding of sLAG-3 to HLA class II using the formula, MFI - control sLAG-3 / MFI - control Class II (%) (left axis, blue bars) and % positive - control sLAG-3 / % positive - control Class II (%) (right axis, orange bars). Error bars represent mean ± SEM of three independent experiments (*$p<0.05$, **$p<0.01$ and ***$p<0.001$ by ANOVA).

To confirm the contribution of DM to LAG-3 binding and to further explore whether the DM regulator, DO, is also implicated in sLAG-3 binding, we utilized 5.2.4 0401 and 5.2.4 0401 DM cells. As previously noted, the 5.2.4 cell line, derived from 8.1.6, lacks DM and DO [151], but is abundant in lipid raft marker CD59 (Figure 3.3 D). Similar to results for 9.5.3 cells, LAG-3 binding to 5.2.4 0401 is greatly reduced; however, unlike fully-restored binding observed with 9.5.3 DM, sLAG-3 binding is only partly restored by DM-transfection in 5.2.4 0401 DM cells (Figure 3.3A and B). A larger ratio of sLAG-3 positive binding relative to HLA- II positive cells is observed in 5.2.4.0401DM (Figure 3.3 E). Since sLAG-3 binding is increased when DM is expressed, regardless of CD59 and HLA-II expression, this further supports the importance of DM in optimizing HLA-II for binding sLAG-3. However, the DO-deficiency in 5.2.4 [142] may potentially explain the less-than-optimal restoration of sLAG-3 binding to 5.2.4 0401DM cells.

3.2 sLAG-3 binding to BL cell lines

The lack of sLAG-3 binding to Daudi, described in Section 3.1 could not be explained by a deficit of lipid rafts. BL cells are known to have antigen presentation deficiencies which possibly could affect pHLA-II stability [27]. We next tested sLAG-3 binding to BL cell line, Bjab, which is DO deficient but DM-positive [151] and therefore, does not have a typical functioning HLA-II presentation system. This cell line and its transfectants had previously been shown to express unstable DRB1:0401 epitopes [151]. Despite having abundant HLA-II and CD59 expression, sLAG-3 binding was poor on Bjab (Figure 3.4A, 3.4B and 3.4C), although stronger on Bjab 0401. Furthermore, sLAG-3 binding was not restored in the Bjab-DO transfectant. Together, these and the preceding results (Figures 3.1, 3.2 and 3.3), indicate the

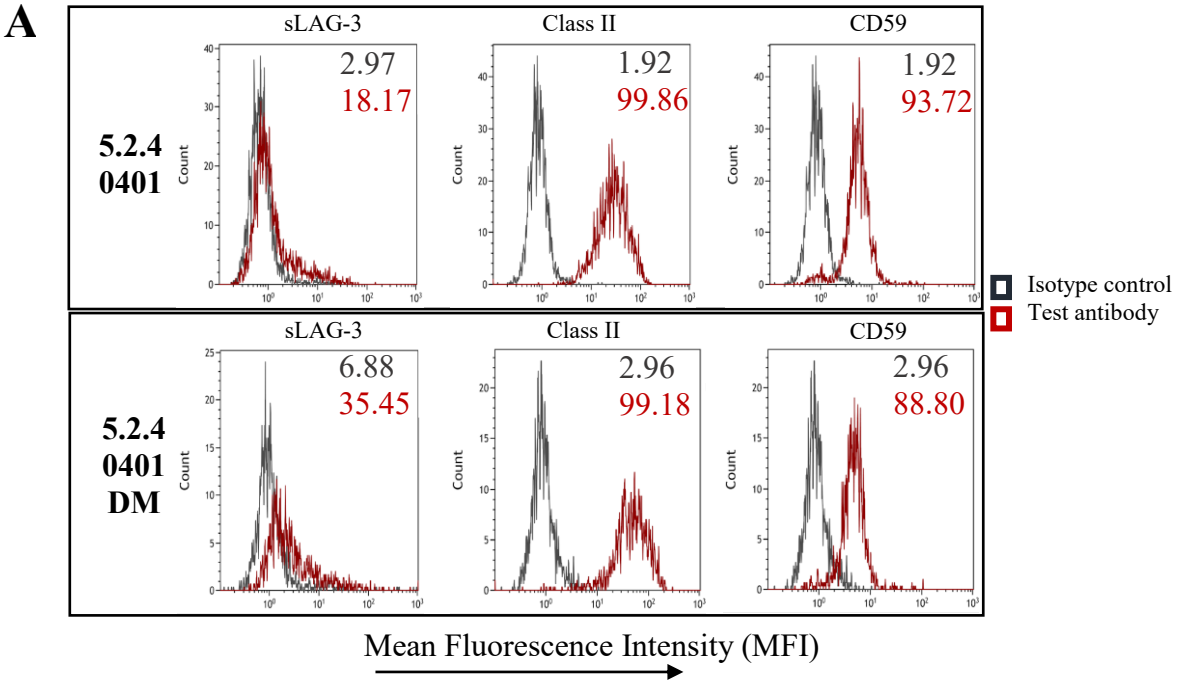
A
sLAG-3
Class II
CD59
5.2.4
0401
2.97
18.17
1.92
99.86
1.92
93.72
Count
5.2.4
0401
DM
6.88
35.45
2.96
99.18
2.96
88.80
Isotype control
Test antibody
Mean Fluorescence Intensity (MFI)

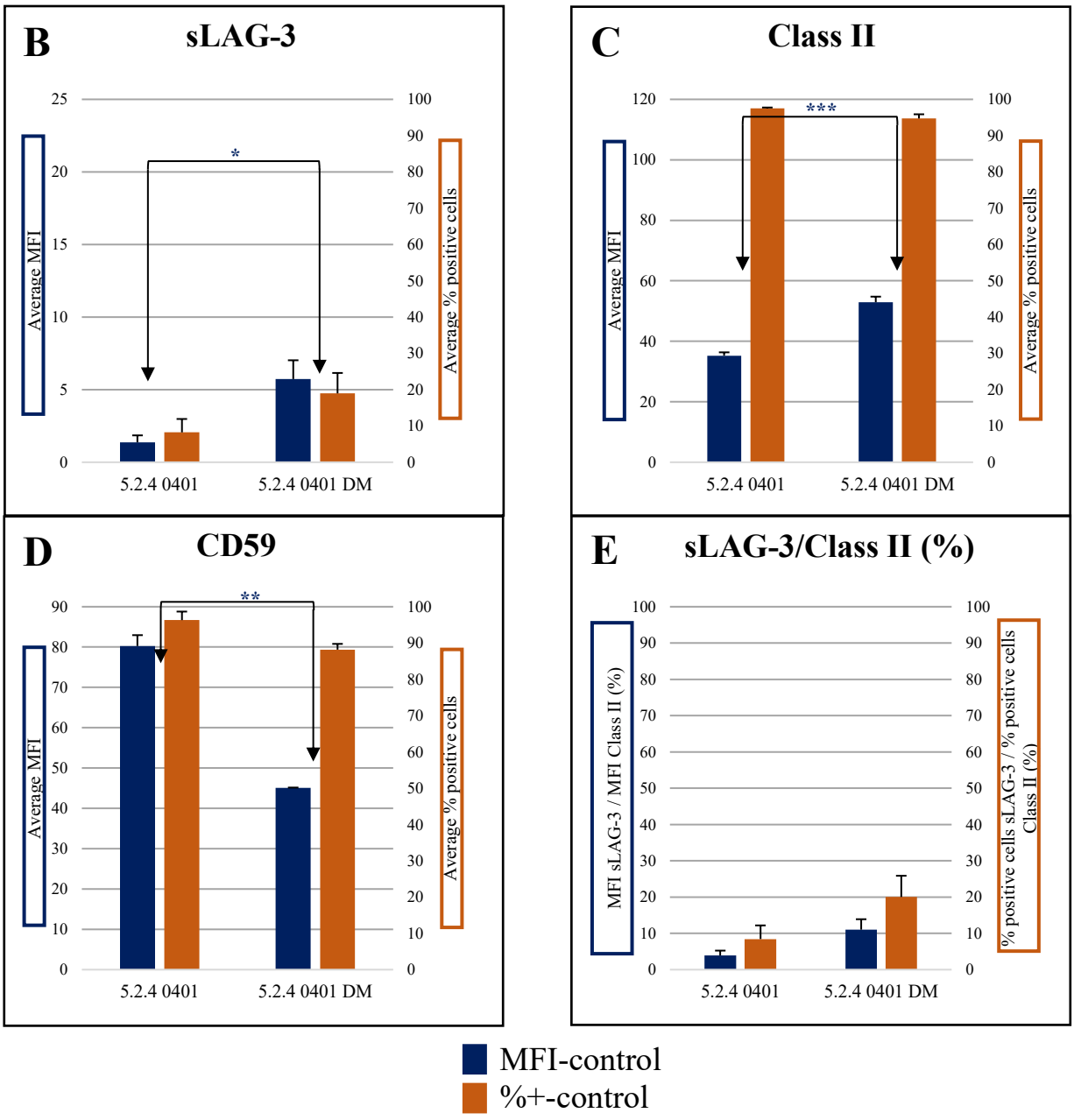
B
sLAG-3
Average MFI
Average % positive cells
*
5.2.4 0401
5.2.4 0401 DM
C
Class II
***
D
CD59
**
E
sLAG-3/Class II (%)
MFI sLAG-3 / MFI Class II (%)
% positive cells sLAG-3 / % positive cells Class II (%)
MFI-control
%+-control

Figure 3.3: sLAG-3 binding to human BCL 5.2.4 0401 transfectant is influenced by DM-expression. **A)** sLAG-3 binding, HLA class II and CD59 expression on human B cell transfectants 5.2.4 0401 and 5.2.4 0401 DM. Grey histogram represents isotype control, red histogram represents test antibody. Histograms are representative of one of three independent experiments. Values on histograms represent the percentage of positive cells. **B-D)** Bar diagrams depicting average MFI and % positive cells using the formula, MFI test antibody – MFI isotype control (left axis, blue bars) and % positive test antibody – % positive isotype control (right axis, orange bars) **B)** sLAG-3 binding, **C)** HLA class II expression and **D)** CD59 expression. **E)** Depicts the relative binding of sLAG-3 to HLA class II using the formula, MFI - control sLAG-3 / MFI - control Class II (%) (left axis, blue bars) and % positive - control sLAG-3 / %positive - control Class II (%) (right axis, orange bars). Error bars represent mean ± SEM of three independent experiments (*$p<0.05$, **$p<0.01$ and ***$p<0.001$ by ANOVA).

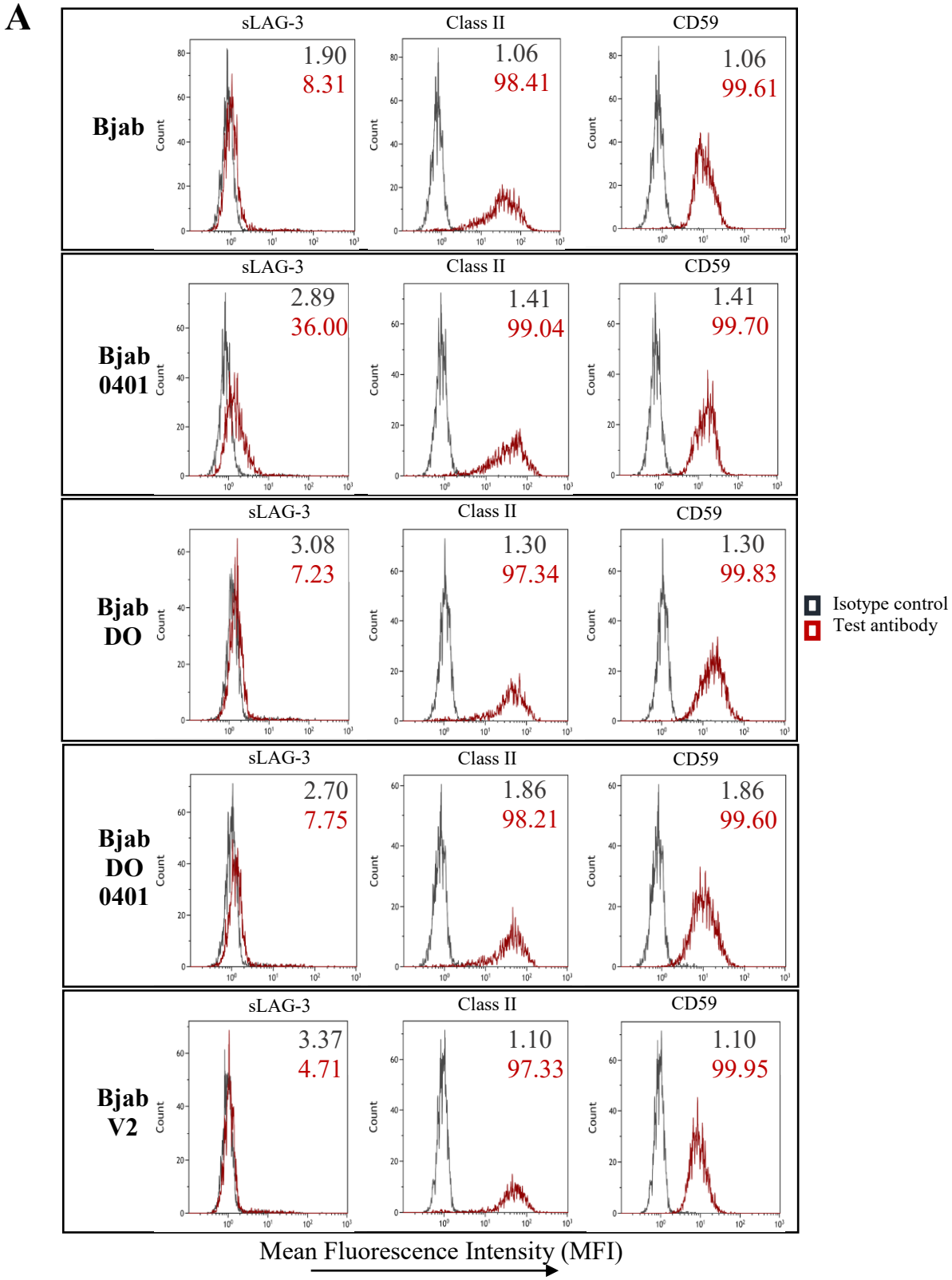
A
sLAG-3
Class II
CD59
Bjab
1.90
8.31
1.06
98.41
1.06
99.61
Bjab 0401
2.89
36.00
1.41
99.04
1.41
99.70
Bjab DO
3.08
7.23
1.30
97.34
1.30
99.83
Bjab DO 0401
2.70
7.75
1.86
98.21
1.86
99.60
Bjab V2
3.37
4.71
1.10
97.33
1.10
99.95
Count
Isotype control
Test antibody
Mean Fluorescence Intensity (MFI)

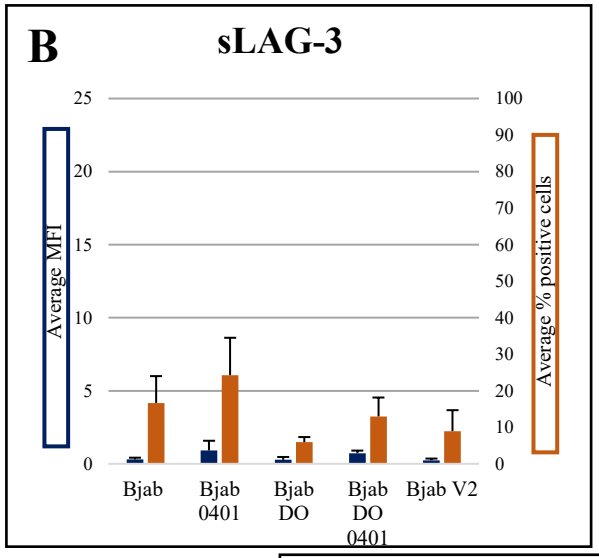
B
sLAG-3
Average MFI
Average % positive cells
25
20
15
10
5
0
100
90
80
70
60
50
40
30
20
10
0
Bjab
Bjab 0401
Bjab DO
Bjab DO 0401
Bjab V2

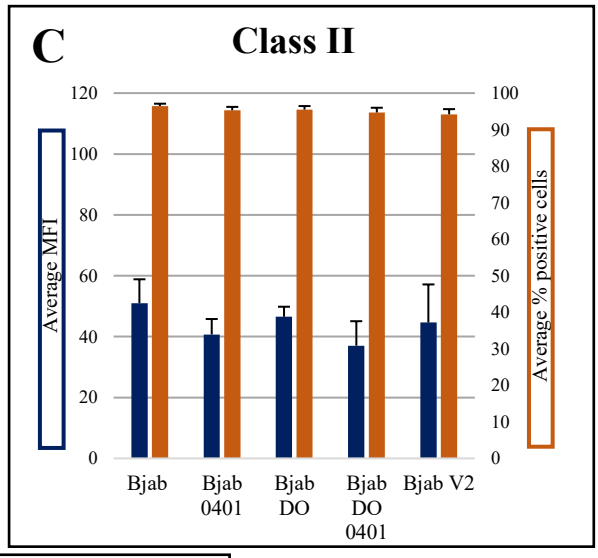
C
Class II
Average MFI
Average % positive cells
120
100
80
60
40
20
0
100
90
80
70
60
50
40
30
20
10
0
Bjab
Bjab 0401
Bjab DO
Bjab DO 0401
Bjab V2

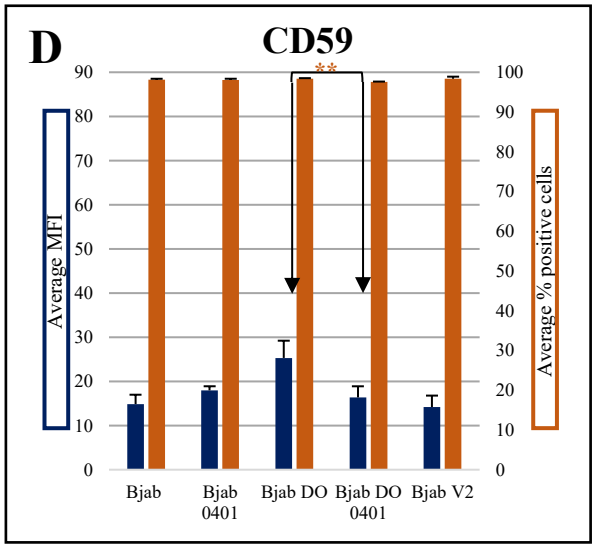
D
CD59
**
Average MFI
Average % positive cells
90
80
70
60
50
40
30
20
10
0
100
90
80
70
60
50
40
30
20
10
0
Bjab
Bjab 0401
Bjab DO
Bjab DO 0401
Bjab V2

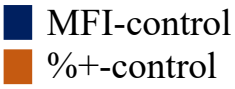
MFI-control
%+-control

Figure 3.4: sLAG-3 binding to BL cell lines is unaffected by DO transfection. **A)** sLAG-3 binding, HLA class II and CD59 expression on human BL cell lines Bjab and BL transfectants Bjab 0401, Bjab DO, Bjab DO 0401 and Bjab V2 (vector control). Grey histogram represents isotype control, red histogram represents test antibody. Histograms are representative of one of three independent experiments. Values on histograms represent the percentage of positive cells. **B-D)** Bar diagrams depicting average MFI and % positive cells using the formula, MFI test antibody – MFI isotype control (left axis, blue bars) and % positive test antibody – % positive isotype control (right axis, orange bars) **B)** sLAG-3 binding, **C)** HLA class II expression and **D)** CD59 expression. Error bars represent mean ± SEM of three independent experiments (*$p<0.05$, **$p<0.01$ and ***$p<0.001$ by ANOVA).

requirement for strong LAG-3-HLA-II interactions is more complex than an APC simply possessing peptide editors and displaying pHLA-II in lipid rafts.

3.3 Investigation of sLAG-3 binding and PD-L1 expression on cancer cell lines

Since the sLAG-3 binding assay demonstrated effective, but cell context dependent sLAG-3 binding to BCL, we next interrogated sLAG-3 binding to non-lymphoid HLA-II positive cancer cell lines. Constitutively, HLA-II is expressed at very low amounts, or not at all, on cancer cell lines. However, expression can be induced by treating the cells with IFN-γ. Likewise PD-L1, the ligand for the checkpoint inhibitor PD-1, is frequently present on cancer cells and is IFN-γ inducible [128]. As LAG-3, PD-1 and PD-L1 are immune checkpoint molecules targeted for cancer immunotherapy, it would be instructive to determine LAG-3 binding, HLA-II and PD-L1 expression simultaneously on cancer cell lines, treated or not with IFN-γ.

To date several studies on breast cancer have shown tumor infiltrating lymphocytes frequently express LAG-3 among other immune inhibitory markers including PD-1 [125]–[127] and tumor cells may be positive for HLA-II and/or PD-L1. High serum sLAG-3 levels in breast cancer patients are associated with a good prognosis [97]. While PD-L1 and HLA-II expression on breast cell lines have also been studied [156]–[158], there is not extensive knowledge on sLAG-3 binding to breast cancer cells that co-express HLA-II and PD-L1.

Here we explored sLAG-3 binding, HLA-II and PD-L1 expression on melanoma cell line MDA-MB-435 and a diverse panel of breast cancer cell lines. These included two triple negative breast cancer (TNBC) cell lines, MDA-MB-231 and BT-20; ER^+ lines, T47D and MCF-7 and

HER$^+$ cell line, SKRB3. Following 72 hour IFN-γ treatment or not treatment, cell lines were analyzed by flow cytometry as described in Section 2.4.

3.3.1 Melanoma cell line MDA-MB-435, binds LAG-3 and expresses PD-L1

MDA-MB-435 was chosen because other HLA-II positive melanoma cell lines were reported to bind membrane bound and sLAG-3 [159]. As shown in Figure 3.5, MDA-MB-435 has low levels of constitutive HLA-II and PD-L1 that are significantly upregulated by treatment with IFN-γ (Figure 3.5A, 3.5C and 4.5D). sLAG-3 binding to untreated MDA-MB-435 cells was negligible, most likely due to weak HLA-II expression. However, sLAG-3 binding was significantly increased in IFN-γ treated cells (Figures 3B and 3E), consistent with reported LAG-3 binding to several HLA-II positive melanoma cell lines [159].

3.3.2 MHC Class II$^+$ BCCL poorly bind sLAG-3

Untreated MDA-MB-231 (TNBC) expressed no-HLA-II and bound no sLAG-3 (Figure 3.6). IFN-γ treatment induced significant HLA-II expression (Figure 3.6C), but sLAG-3 binding remained at levels comparable to untreated cells (Figure 3.6B). PD-L1 was expressed on these cells with and without IFN-γ treatment (Figure 3.6D). A second TNBC, BT-20, expressed little constitutive HLA-II and bound small amounts of sLAG-3 (Figure 3.7A, 3.7B and 3.7C). IFN-γ significantly upregulated HLA-II and PD-L1 (Figure 3.7 C and 3.7D). Only a small portion of IFN-γ treated HLA-II positive cells bound sLAG-3 (Figure 3.7B). While these TNBCs express HLA-II with IFN-γ treatment, the extent of sLAG-3 binding is not much different from sLAG-3 binding to untreated cells.

Luminal A breast cancer cell lines, T47D and MCF-7, also expressed little constitutive HLA-II and bound little sLAG-3 (Figure 3.8 and 3.9). IFN-γ treated T47D upregulated both

HLA-II and PD-L1 (Figure 3.8 C and D); PDL1 expression on MCF-7 cells was not ascertained here, but a previous study [160] showed it was not present or upregulated by IFN-γ. sLAG-3 binding to T47D (Figure 3.8 B) was significantly increased in IFN-γ treated as compared to untreated cells, but levels were very low, under 10% of the cells were positive, and likely physiologically irrelevant (Figure 3.8A and 3.8B). Similarly, sLAG-3 binding was barely detected on IFN-γ treated MCF-7 cells (Figure 3.9 A and B) despite nearly 100% of cells expressing abundant HLA-II (Figure 3.9 C). Thus, deficient sLAG-3 binding to these TNBC and luminal A cells, even with abundant IFN-γ induced HLA-II, suggests pHLA-II conformers may not be optimally displayed for sLAG-3 binding and further suggests a deficit of other available LAG-3 binding ligands.

Approximately 3 % of SKBR3 cells bound any sLAG-3 in the absence of constitutive HLA-II expression (Figure 3.10). While IFN-γ treated SKBR3 cells increased HLA-II, this was not accompanied by increased LAG-3 binding. In fact, sLAG-3 binding decreased post IFN-γ treatment (Figure 3.10B and 3.10C), suggesting low levels of sLAG-3 binding to untreated SKBR3 may be due to an alternative HLA-II ligand, that is not IFN-γ inducible.

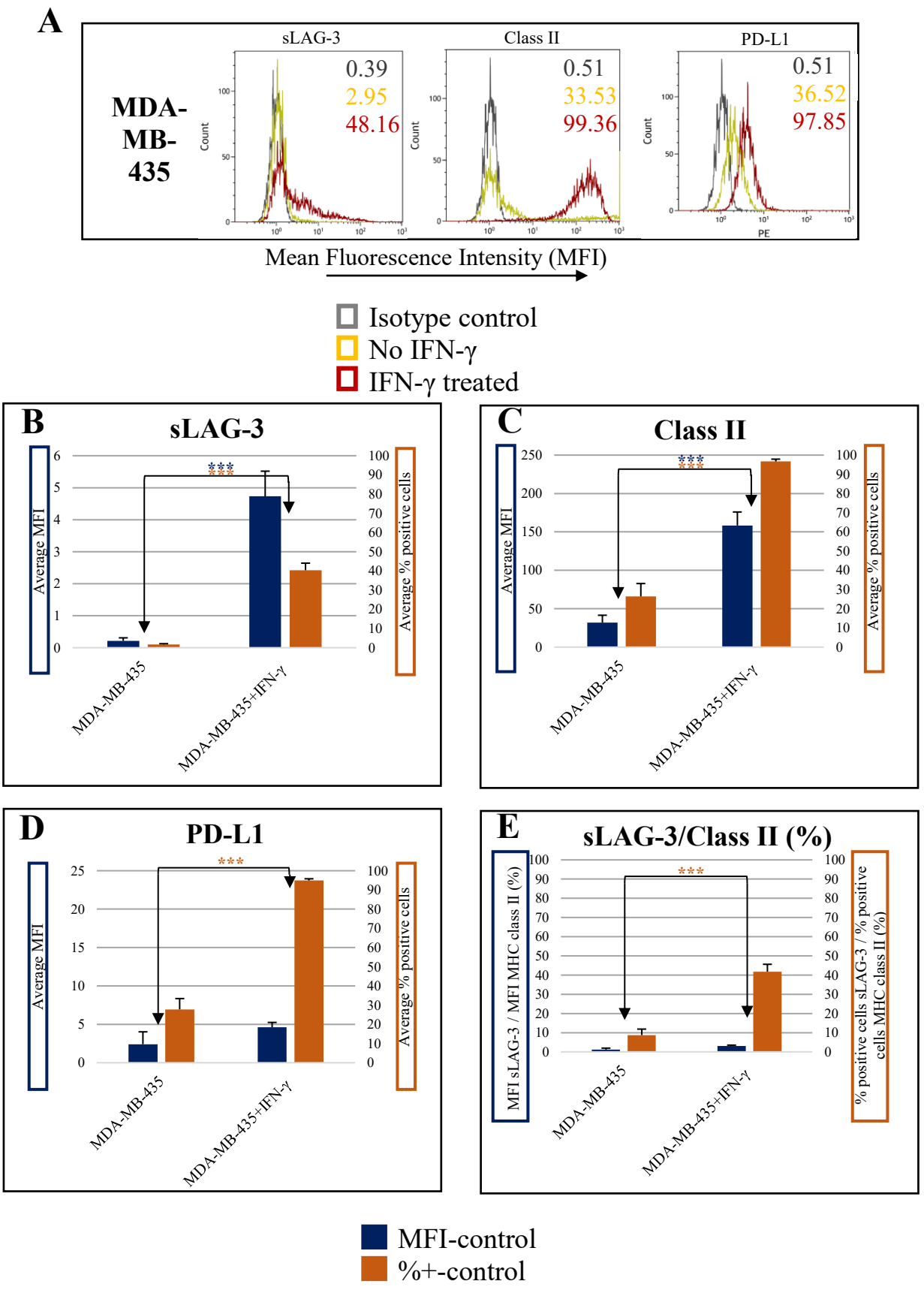
A
MDA-MB-435
sLAG-3
0.39
2.95
48.16
Class II
0.51
33.53
99.36
PD-L1
0.51
36.52
97.85
Count
PE
Mean Fluorescence Intensity (MFI)
Isotype control
No IFN-γ
IFN-γ treated
B
sLAG-3
Average MFI
Average % positive cells
***
MDA-MB-435
MDA-MB-435+IFN-γ
C
Class II
Average MFI
Average % positive cells
***
MDA-MB-435
MDA-MB-435+IFN-γ
D
PD-L1
Average MFI
Average % positive cells
***
MDA-MB-435
MDA-MB-435+IFN-γ
E
sLAG-3/Class II (%)
MFI sLAG-3 / MFI MHC class II (%)
% positive cells sLAG-3 / % positive cells MHC class II (%)
***
MDA-MB-435
MDA-MB-435+IFN-γ
MFI-control
%+-control

Figure 3.5: MDA-MB-435 binds LAG-3, expresses HLA class II and PD-L1. **A)** sLAG-3 binding, HLA class II and PD-L1 expression on constitutive and IFN-γ induced (100 units/mL for 72 hours) MDA-MB-435 cells. Grey histogram represents isotype control, yellow histogram represents no IFN-γ and red histogram represents IFN-γ treated. Histograms are a representative of one of three independent experiments. Values on histogram represent the percentage of positive cells. **B-D)** Bar diagrams depicting average MFI and % positive cells using the formula, MFI test antibody – MFI isotype control (left axis, blue bars) and % positive test antibody – % positive isotype control (right axis, orange bars) **B)** sLAG-3 binding, **C)** HLA class II expression and **D)** PD-L1 expression. **E)** Depicts the relative binding of sLAG-3 to HLA class II using the formula, MFI - control sLAG-3 / MFI - control Class II (%) (left axis, blue bars) and % positive - control sLAG-3 / % positive - control Class II (right axis, orange bars). Error bars represent mean ± SEM of three independent experiments (*$p<0.05$, **$p<0.01$ and ***$p<0.001$ by ANOVA).

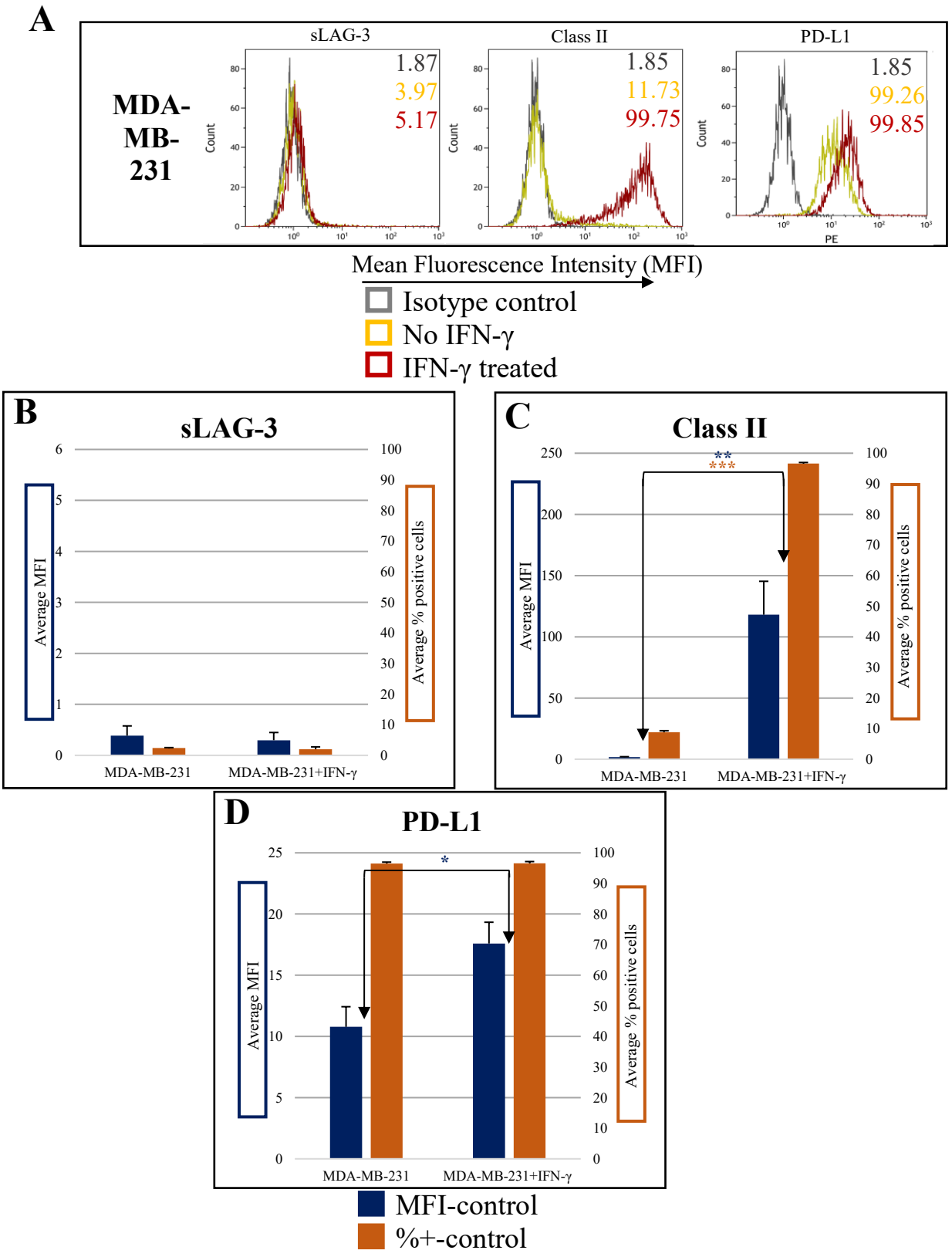
A
MDA-MB-231
sLAG-3
Class II
PD-L1
1.87
3.97
5.17
1.85
11.73
99.75
1.85
99.26
99.85
Count
PE
Mean Fluorescence Intensity (MFI)
Isotype control
No IFN-γ
IFN-γ treated
B
sLAG-3
Average MFI
Average % positive cells
MDA-MB-231
MDA-MB-231+IFN-γ
C
Class II
**
***
D
PD-L1
*
MFI-control
%+-control

Figure 3.6: IFN-γ increases HLA class II and PDL1 expression on MDA-MB-231, but not sLAG-3 binding. **A)** sLAG-3 binding, HLA class II and PD-L1 expression on constitutive and IFN-γ induced (100 units/mL for 72 hours) MDA-MB-231 cells. Grey histogram represents isotype control, yellow histogram represents no IFN-γ and red histogram represents IFN-γ treated. Histograms are representative of one of three independent experiments. Values on histogram represent the percentage of positive cells. **B-D)** Bar diagrams depicting average MFI and % positive cells using the formula, MFI test antibody – MFI isotype control (left axis, blue bars) and % positive test antibody – % positive isotype control (right axis, orange bars) **B)** sLAG-3 binding and **C)** HLA class II expression and **D)** PD-L1 expression. Error bars represent mean ± SEM of three independent experiments (*$p<0.05$, **$p<0.01$ and ***$p<0.001$ by ANOVA).

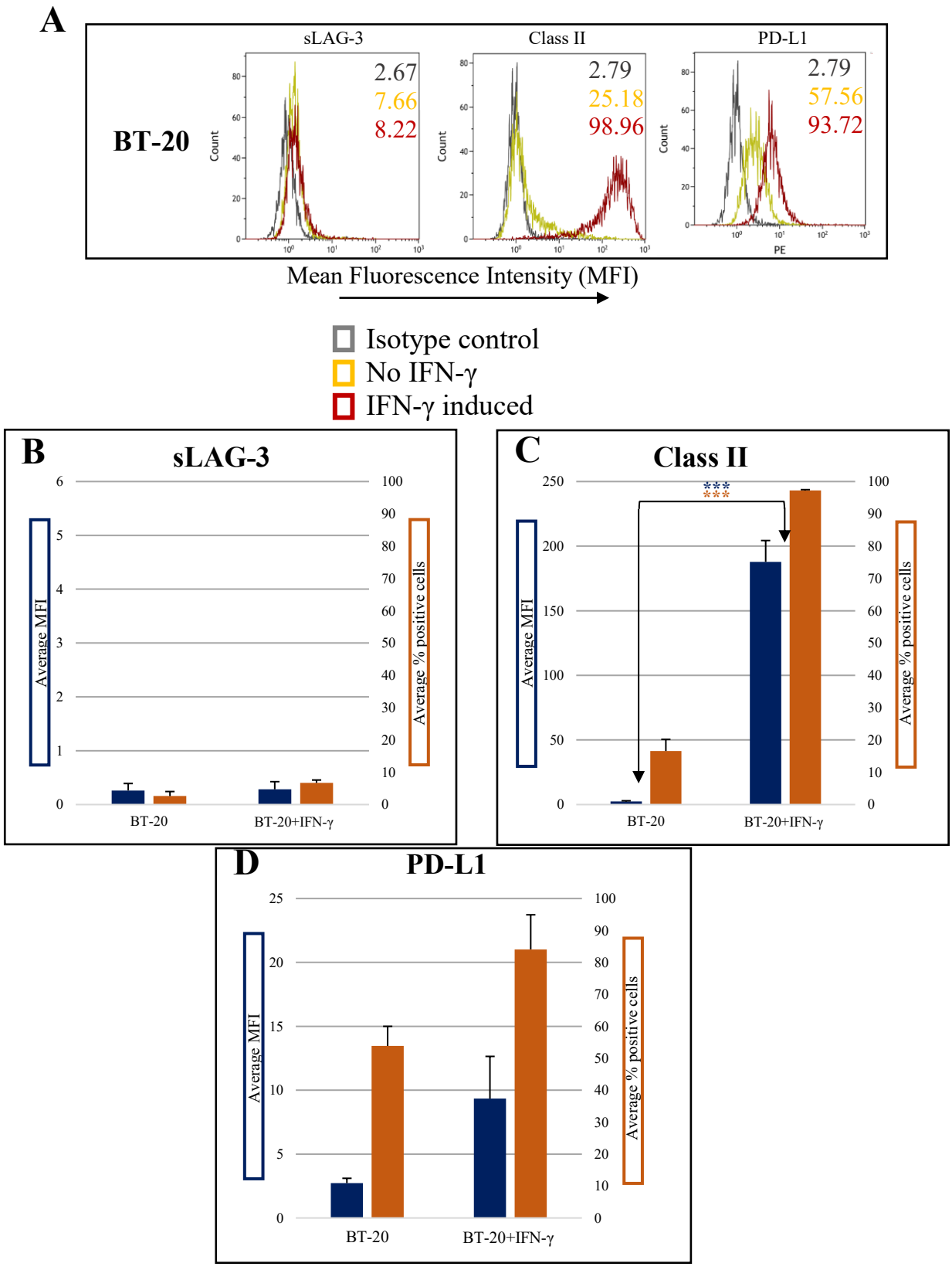
A
sLAG-3
Class II
PD-L1
BT-20
2.67
7.66
8.22
2.79
25.18
98.96
2.79
57.56
93.72
Count
PE
Mean Fluorescence Intensity (MFI)
Isotype control
No IFN-γ
IFN-γ induced
B
sLAG-3
C
Class II
D
PD-L1
Average MFI
Average % positive cells
BT-20
BT-20+IFN-γ
MFI-control
%+-control

Figure 3.7: IFN-γ increases HLA-class II and PD-L1 on BT-20 but not sLAG-3 binding. **A)** sLAG-3 binding, HLA class II and PD-L1 expression on constitutive and IFN-γ induced (100 units/mL for 72 hours) BT-20 cells. Grey histogram represents isotype control, yellow histogram represents no IFN-γ and red histogram represents IFN-γ treated. Histograms are representative of one of three independent experiments. Values on histogram represent the percentage of positive cells. **B-D)** Bar diagrams depicting average MFI and % positive cells using the formula, MFI test antibody – MFI isotype control (left axis, blue bars) and % positive test antibody – % positive isotype control (right axis, orange bars) **B)** sLAG-3 binding and **C)** HLA class II expression and **D)** PD-L1 expression. Error bars represent mean ± SEM of three independent experiments (*$p<0.05$, **$p<0.01$ and ***$p<0.001$ by ANOVA).

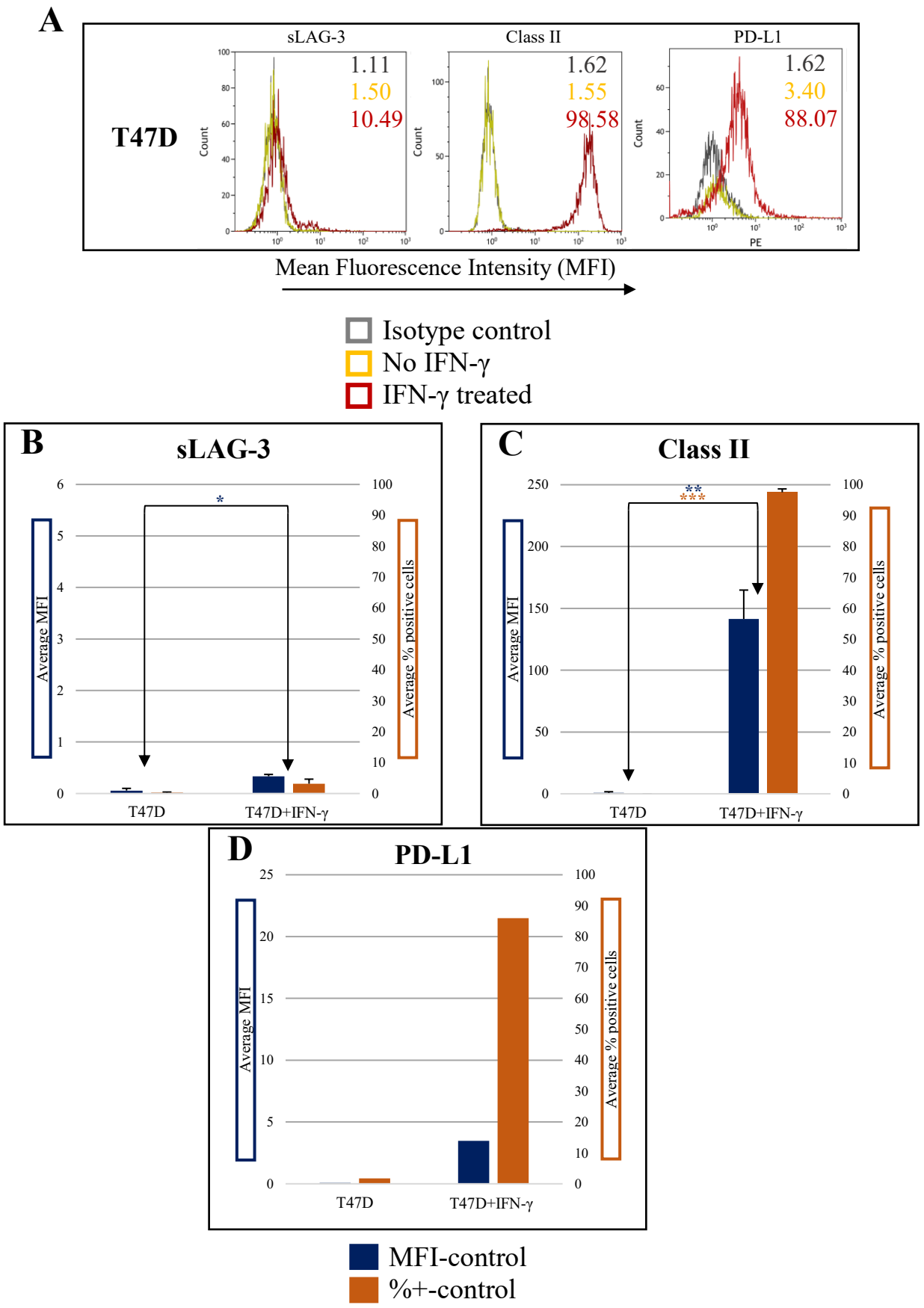
A
T47D
sLAG-3
Class II
PD-L1
1.11
1.50
10.49
1.62
1.55
98.58
1.62
3.40
88.07
Count
PE
Mean Fluorescence Intensity (MFI)
Isotype control
No IFN-γ
IFN-γ treated
B
sLAG-3
Average MFI
Average % positive cells
T47D
T47D+IFN-γ
C
Class II
D
PD-L1
MFI-control
%+-control

Figure 3.8: IFN-γ induces HLA class II and PD-L1 on T47D with a small increase in sLAG3 binding. sLAG-3 binding to T47D. **A)** sLAG-3 binding, HLA class II and PD-L1 expression on constitutive and IFN-γ induced (100 units/mL for 72 hours) T47D cells. Grey histogram represents isotype control, yellow histogram represents no IFN-γ and red histogram represents IFN-γ treated. Histograms are representative of one of three independent experiments. With the exception of PD-L1 which was measured once. Values on histogram represent the percentage of positive cells. **B-D)** Bar diagrams depicting average MFI and % positive cells using the formula, MFI test antibody – MFI isotype control (left axis, blue bars) and % positive test antibody – % positive isotype control (right axis, orange bars) **B)** sLAG-3 binding and **C)** HLA class II expression and **D)** PD-L1 expression Error bars represent mean ± SEM of three independent experiments (*$p<0.05$, **$p<0.01$ and ***$p<0.001$ by ANOVA).

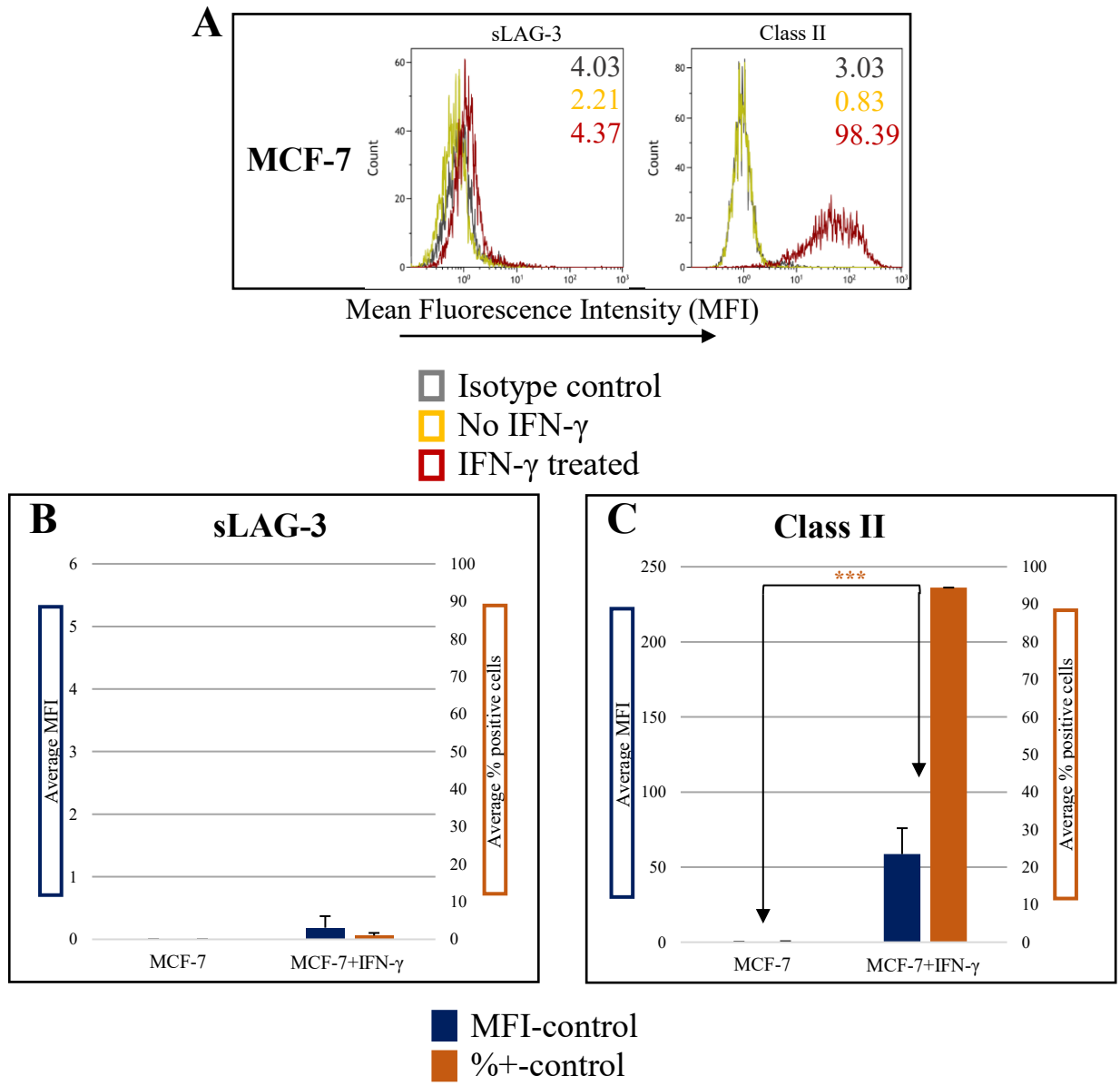
A
sLAG-3
Class II
MCF-7
Count
4.03
2.21
4.37
3.03
0.83
98.39
Mean Fluorescence Intensity (MFI)
Isotype control
No IFN-γ
IFN-γ treated
B
sLAG-3
Average MFI
Average % positive cells
MCF-7
MCF-7+IFN-γ
C
Class II
***
Average MFI
Average % positive cells
MCF-7
MCF-7+IFN-γ
MFI-control
%+-control

Figure 3.9: IFN-y induces HLA class II on MCF-7 but not sLAG-3 binding. **A)** sLAG-3 binding and HLA class II expression on constitutive and IFN-γ induced (100 units/mL for 72 hours) MCF-7 cells. Grey histogram represents isotype control, yellow histogram represents no IFN-γ and red histogram represents IFN-γ treated. Histograms are representative of one of three independent experiments. Values on histogram represent the percentage of positive cells. **B-C)** Bar diagrams depicting average MFI and % positive cells using the formula, MFI test antibody – MFI isotype control (left axis, blue bars) and % positive test antibody – % positive isotype control (right axis, orange bars) **B)** sLAG-3 binding and **C)** HLA class II expression. Error bars represent mean ± SEM of three independent experiments (*$p<0.05$, **$p<0.01$ and ***$p<0.001$ by ANOVA).

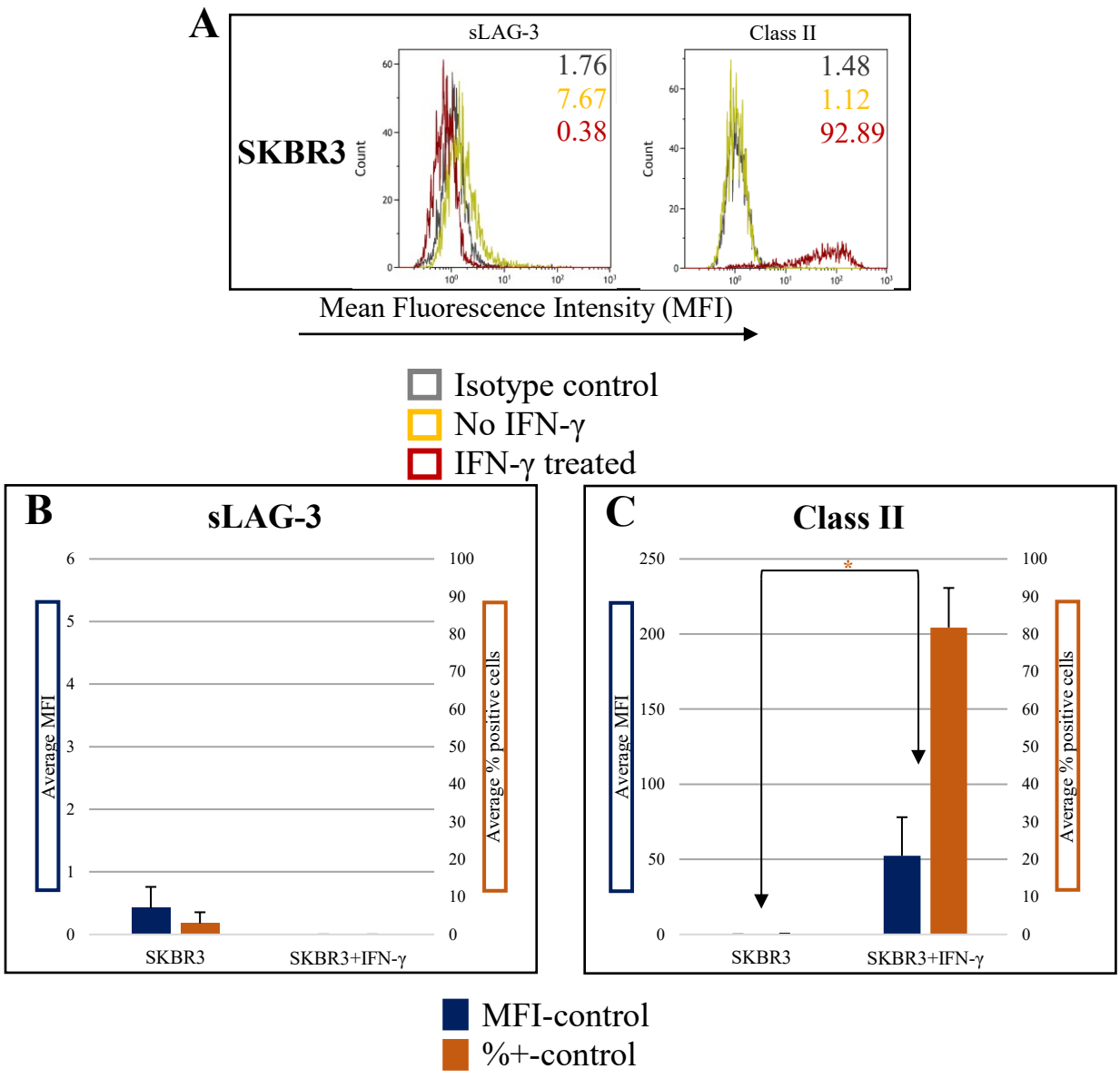
A
sLAG-3
Class II
SKBR3
1.76
7.67
0.38
1.48
1.12
92.89
Count
Mean Fluorescence Intensity (MFI)
Isotype control
No IFN-γ
IFN-γ treated
B
sLAG-3
Average MFI
Average % positive cells
SKBR3
SKBR3+IFN-γ
C
Class II
Average MFI
Average % positive cells
SKBR3
SKBR3+IFN-γ
MFI-control
%+-control

Figure 3.10: IFN-γ induces HLA class II on SKBR3, but reduces sLAG-3 binding. **A)** sLAG-3 binding and HLA class II expression on constitutive and IFN-γ induced (100 units/mL for 72 hours) SKBR3 cells. Grey histogram represents isotype control, yellow histogram represents no IFN-γ and red histogram represents IFN-γ treated. Histograms are representative of one of three independent experiments. Values on histogram represent the percentage of positive cells. **B-C)** Bar diagrams depicting average MFI and % positive cells using the formula, MFI test antibody – MFI isotype control (left axis, blue bars) and % positive test antibody – % positive isotype control (right axis, orange bars) **B)** sLAG-3 binding and **C)** HLA class II expression. Error bars represent mean ± SEM of three independent experiments (*$p<0.05$, **$p<0.01$ and ***$p<0.001$ by ANOVA).

3.4 Poor sLAG-3 binding to BCCL is not due to a deficit of lipid rafts and DM expression

Differences in the sLAG-3 binding capacity between the melanoma cell line, MDA-MB-435 and the panel of BCCL, could potentially be due to differences in lipid raft domains or expression of the pHLA-II editor, DM. Our previously described results using B-cell lines (Section 3.1) suggested DM-stabilization of pHLA-II are more important in LAG-3- binding than localization of HLA-II in lipid raft microdomains. To investigate this further, MDA-MB-435 and BCCLs were treated with IFN-γ, as described in Section 2.2, and analyzed by flow cytometry for the lipid raft marker, CD59, and intracellular DM expression. We found abundant CD59 and high levels of intracellular DM on all cell lines (Figure 3.11). These results suggest sLAG-3 binding differences between MDA-MB-435 (high sLAG-3 binder) and BCCLs: MDA-231, BT-20 and T47D (low sLAG-3 binders) are not due to a deficit of lipid raft-rich microdomains or available DM-assisted peptide loading of HLA-II molecules; however, whether lipid rafts contain stable pHLA-II was not determined.

3.5 Disruption of lipid rafts on HLA-II positive melanoma line enhances LAG-3 binding

Lipid raft microdomains play a role in a number of cellular processes, including antigen presentation, with a substantial portion of pHLA-II on APCs residing in lipid rafts [104]. It was previously shown that lipid raft disruption on DCs decreases LAG-3 binding to HLA-II, suggesting LAG-3 is partially restricted to binding HLA-II located in lipid raft microdomains [93]. Since sLAG-3 binding to IFN-γ induced HLA-II on MDA-MB-435 was similar to that on the normal BCL (Section 3.3), we questioned whether disruption of lipid rafts would alter sLAG-3 binding or expression of HLA-II, PD-L1 and CD59. To address this,

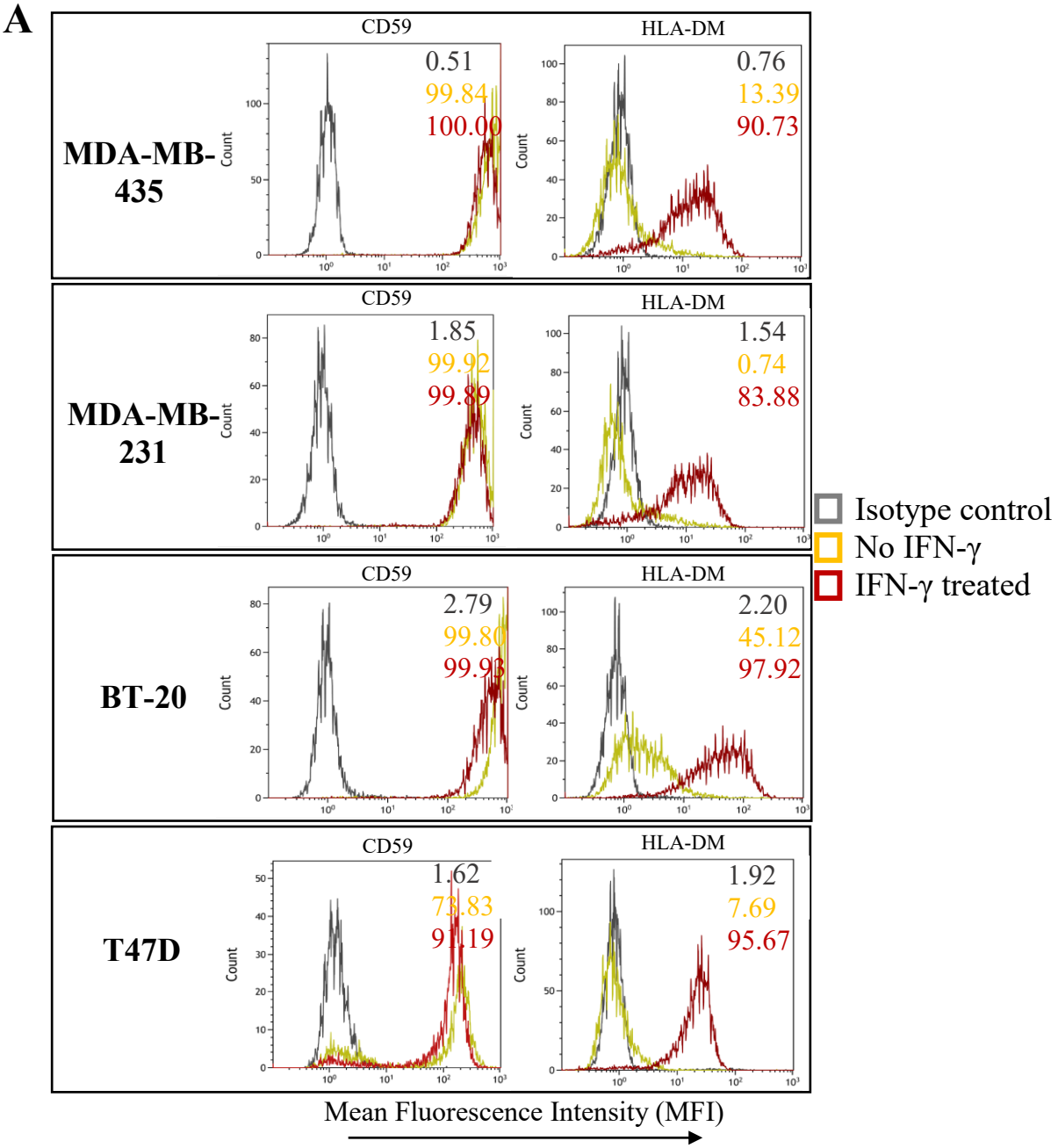
A
CD59
HLA-DM
MDA-MB-435
0.51
99.84
100.00
0.76
13.39
90.73
MDA-MB-231
1.85
99.92
99.89
1.54
0.74
83.88
BT-20
2.79
99.80
99.93
2.20
45.12
97.92
T47D
1.62
73.83
91.19
1.92
7.69
95.67
Count
Isotype control
No IFN-γ
IFN-γ treated
Mean Fluorescence Intensity (MFI)

Figure 3.11: Expression of CD59 and DM on a panel of human cancer cell lines. CD59 and DM expression on constitutive and IFN-γ induced (100 units/mL for 72 hours) MDA-MB-435, MDA-MBA-231, BT-20 and T47D cells. Grey histogram represents isotype control, yellow histogram represents no IFN-γ and red histogram represents IFN-γ treated. Histograms are representative of one of three independent experiments. Values on histogram represent the percentage of positive cells.

MDA-MB-435 cells were treated with IFN-γ for 72 hour, followed by lipid raft disruption using MβCD, which separates membrane cholesterol thereby disrupting cellular lipid rafts [161].

Treatment of MDA-MB-435 cells with MβCD, as compared to control diluent, resulted in markedly reduced CD59 and HLA-II expression (Figure 3.12 A) indicating successful depletion of lipid rafts. Surprisingly, sLAG-3 binding was dramatically increased following MβCD treatment (Figure 3.12). This result was puzzling as reduced HLA-II would be expected to reduce sLAG-3 binding. Notably, PD-L1 expression, like sLAG-3 binding, was also increased by MβCD-treatment.

3.6 Lipid raft disruption of breast cancer cell lines modifies LAG-3 binding

Given the aforementioned results for lipid raft disruption MDA-MB-435, we next investigated whether MβCD treatment of MDA-231, BT-20, T47D and SKBR3 would increase LAG-3 binding. Intriguingly, moderate sLAG-3 binding was observed for all four control treated cells (Figures 3.13 to 3.16), which is incongruent with results in Section 3.3, where very little sLAG3 binding was observed.

Potential explanations for this variance will be addressed in the Discussion (Section 4.4). However, like the preceding results for MDA-MB-435, sLAG-3- binding was enhanced in MβCD-treated MDA-MB-231 (Figure 3.13), BT-20 (Figure 3.14) and T47D (Figure 3.15); the exception was MβCD-treated SKBR3, where sLAG-3 was decreased compared to the control (Figure 3.16). Effects of MβCD treatment on the other immune markers varied according to the cell line: 1) HLA-II was decreased on MDA-MB-231 and BT-20, but not on T47D and SKBR3; 2) CD59 decreased on MDA-MB-231, increased on BT-20 and was unchanged on T47D and SKBR3; 3) PD-L1 decreased on MDA-MB-231 and BT-20, was unchanged on T47D and

increased on SKBR3. Since MβCD had variable effects on CD59, it cannot be concluded that MβCD-mediated changes in sLAG-3 binding resulted from lipid raft depletion. Possibly, MβCD treatment rendered HLA-II more accessible for LAG-3 binding and HLA- II on some cancer cell lines may be restricted by lipid rafts in a way that limits sLAG-3 binding. Alternatively, MβCD may have increased the display of non-HLA ligands for LAG-3.

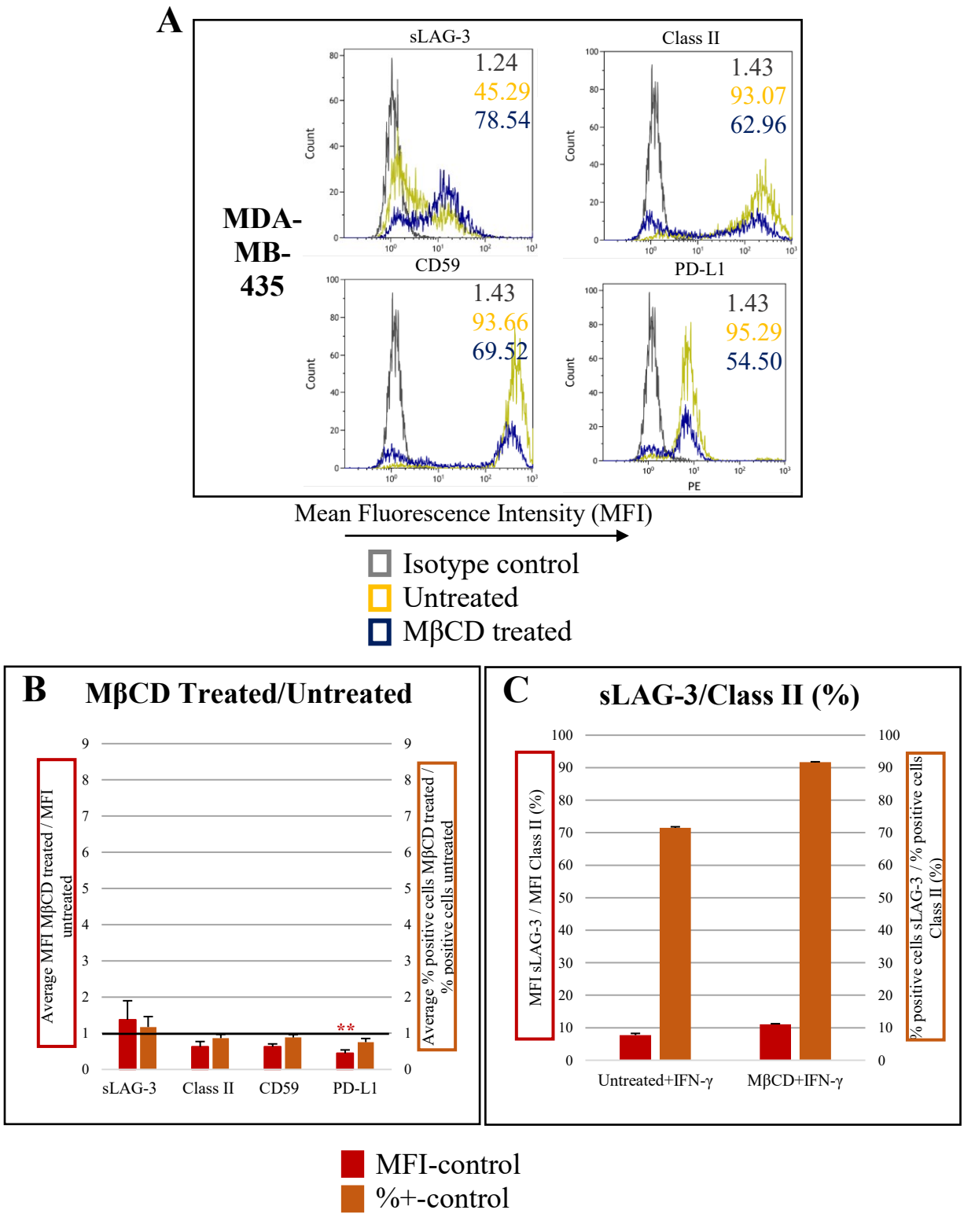
A
MDA-MB-435
sLAG-3
1.24
45.29
78.54
Class II
1.43
93.07
62.96
CD59
1.43
93.66
69.52
PD-L1
1.43
95.29
54.50
Count
PE
Mean Fluorescence Intensity (MFI)
Isotype control
Untreated
MβCD treated
B
MβCD Treated/Untreated
Average MFI MβCD treated / MFI untreated
Average % positive cells MβCD treated / % positive cells untreated
**
sLAG-3
Class II
CD59
PD-L1
C
sLAG-3/Class II (%)
MFI sLAG-3 / MFI Class II (%)
% positive cells sLAG-3 / % positive cells Class II (%)
Untreated+IFN-γ
MβCD+IFN-γ
MFI-control
%+-control

Figure 3.12: Effect of MβCD on LAG-3 binding and expression of immune molecules on MDA-MB-435 cells. **A)** sLAG-3 binding, HLA class II, CD59 and PD-L1 expression on IFN-γ induced MDA-MB-435 cells treated or not with MβCD (10 mM). Grey histogram represents isotype control, yellow histogram represents untreated expression and blue histogram represents MβCD treated expression. Histograms are representative of one of three independent experiments. Values on histograms represent the percentage of positive cells. **B)** Bar graph depicting the ratio of the MFI test antibody – isotype control antibody for MβCD treated cells / MFI test antibody – isotype control antibody for untreated cells (left axis, red bars) and ratio of the % positive test antibody – isotype control for MβCD treated cells / % positive test antibody – isotype control for untreated cells (right axis, orange bars). **C)** Depicts the relative binding of sLAG-3 to HLA class II using the formula, MFI sLAG-3 – isotype control / MFI HLA class II – isotype control (%) (left axis, red bars) and % positive sLAG-3 – isotype control / % positive HLA class II – isotype control (%) (right axis, orange bars) for MβCD treated and untreated cells. Error bars represent mean ± SEM of three independent experiments (*$p<0.05$, **$p<0.01$ and ***$p<0.001$ by ANOVA).

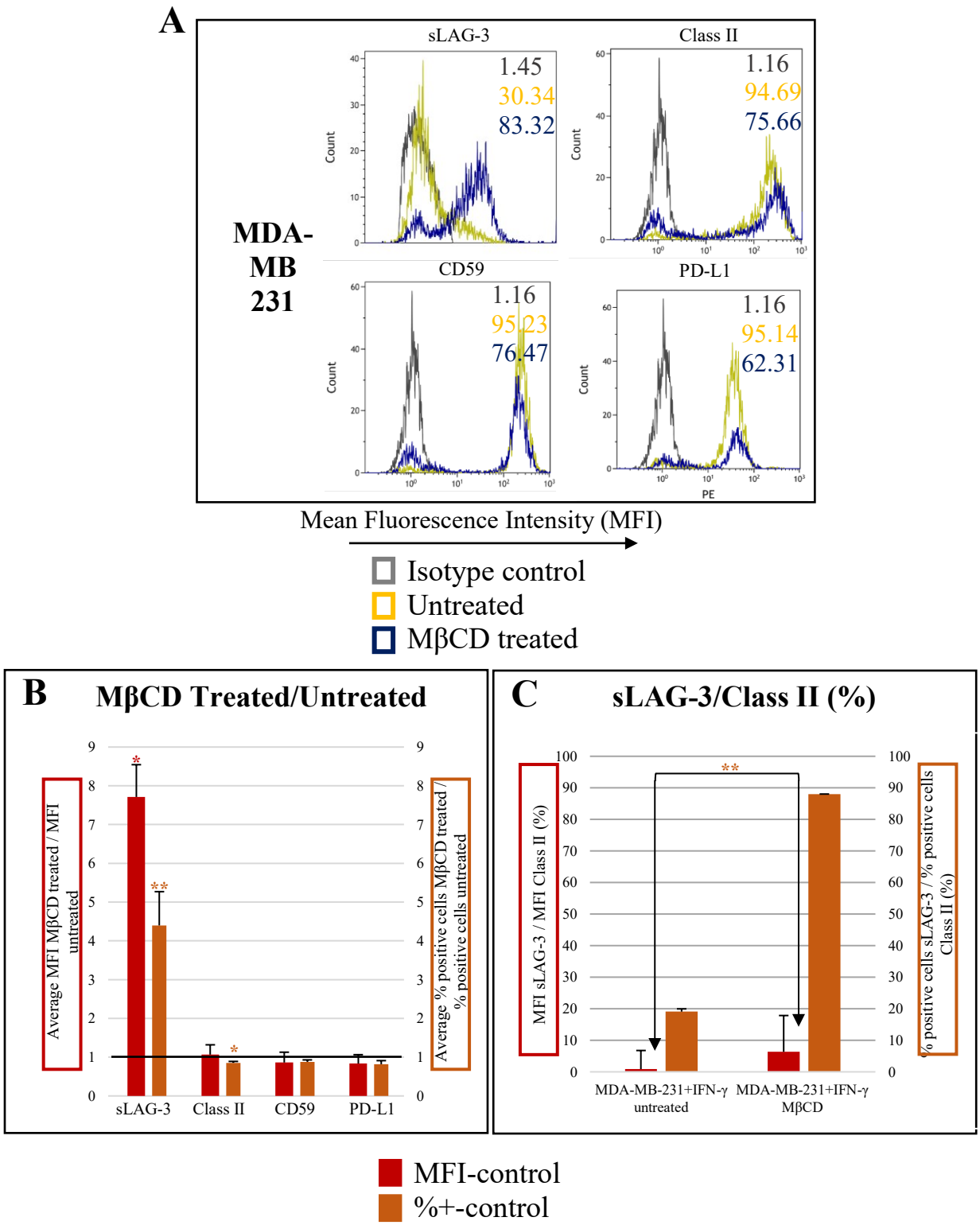
A
MDA-MB 231
sLAG-3
1.45
30.34
83.32
Class II
1.16
94.69
75.66
CD59
1.16
95.23
76.47
PD-L1
1.16
95.14
62.31
Count
PE
Mean Fluorescence Intensity (MFI)
Isotype control
Untreated
MβCD treated
B
MβCD Treated/Untreated
Average MFI MβCD treated / MFI untreated
Average % positive cells MβCD treated / % positive cells untreated
sLAG-3
Class II
CD59
PD-L1
C
sLAG-3/Class II (%)
MFI sLAG-3 / MFI Class II (%)
% positive cells sLAG-3 / % positive cells Class II (%)
MDA-MB-231+IFN-γ untreated
MDA-MB-231+IFN-γ MβCD
MFI-control
%+-control

Figure 3.13: Effects of MβCD on LAG-3 binding and expression of immune molecules on MDA-MB-231 cells. **A)** sLAG-3 binding, HLA class II, CD59 and PD-L1 expression on IFN- γ induced MDA-MB-231 cells treated or not with MβCD (10 mM). Grey histogram represents isotype control, yellow histogram represents untreated expression and blue histogram represents MβCD treated expression. Histograms are representative of one of three independent experiments. Values on histograms represent the percentage of positive cells. **B)** Bar graph depicting the ratio of the MFI test antibody – isotype control antibody for MβCD treated cells / MFI test antibody – isotype control antibody for untreated cells (left axis, red bars) and ratio of the % positive test antibody – isotype control for MβCD treated cells / % positive test antibody – isotype control for untreated cells (right axis, orange bars). **C)** Depicts the relative binding of sLAG-3 to HLA class II using the formula, MFI sLAG-3 – isotype control / MFI HLA class II – isotype control (%) (left axis, red bars) and % positive sLAG-3 – isotype control / % positive HLA class II – isotype control (%) (right axis, orange bars) for MβCD treated and untreated cells. Error bars represent mean ± SEM of three independent experiments (*$p<0.05$, **$p<0.01$ and ***$p<0.001$ by ANOVA).

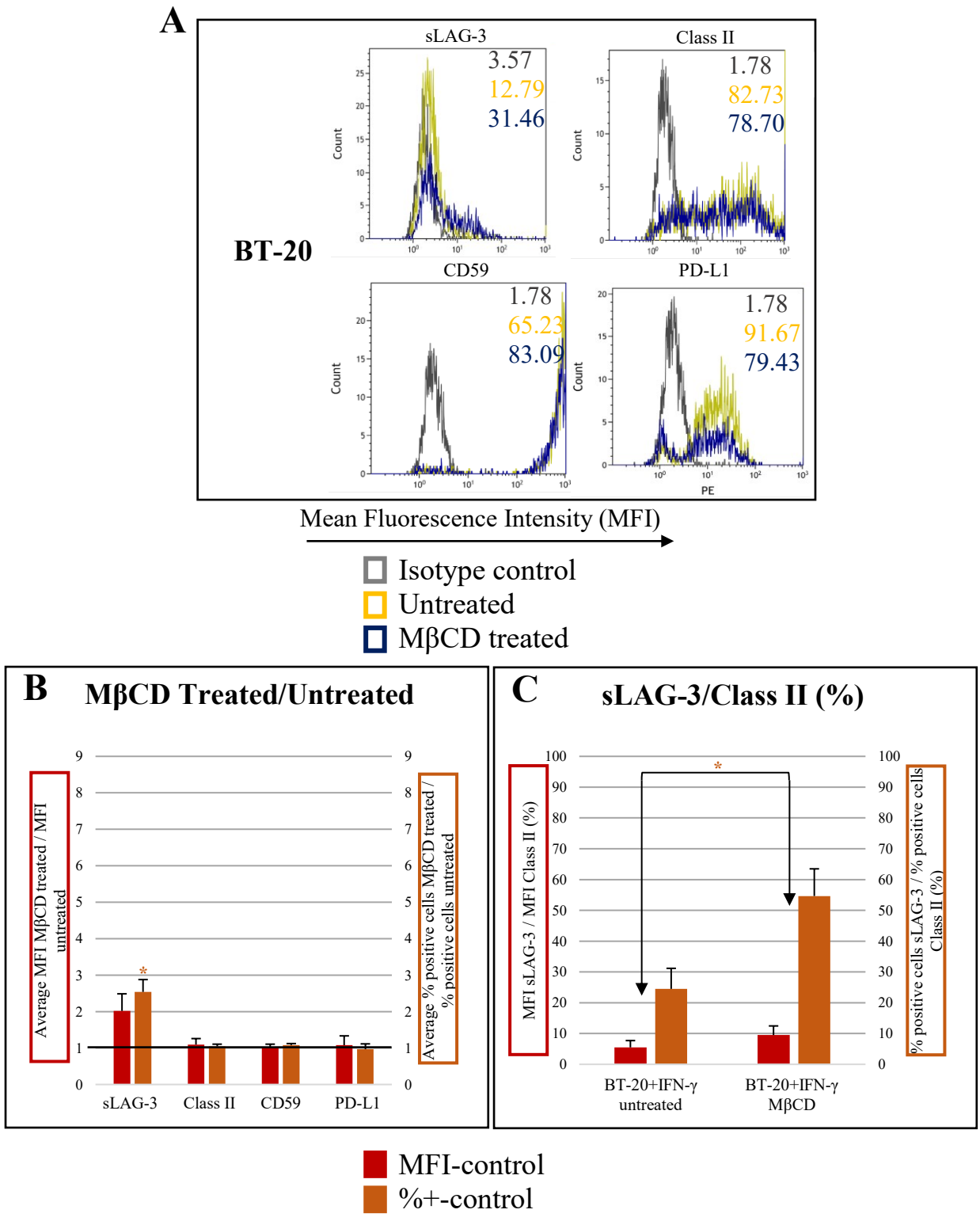
A
BT-20
sLAG-3
3.57
12.79
31.46
Class II
1.78
82.73
78.70
CD59
1.78
65.23
83.09
PD-L1
1.78
91.67
79.43
Count
PE
Mean Fluorescence Intensity (MFI)
Isotype control
Untreated
MβCD treated
B
MβCD Treated/Untreated
Average MFI MβCD treated / MFI untreated
Average % positive cells MβCD treated / % positive cells untreated
sLAG-3
Class II
CD59
PD-L1
C
sLAG-3/Class II (%)
MFI sLAG-3 / MFI Class II (%)
% positive cells sLAG-3 / % positive cells Class II (%)
BT-20+IFN-γ untreated
BT-20+IFN-γ MβCD
MFI-control
%+-control

Figure 3.14: Effects of MβCD on LAG-3 binding and expression of immune molecules on BT-20 cells. **A)** sLAG-3 binding, HLA class II, CD59 and PD-L1 expression on IFN- γ induced BT-20 cells treated or not with MβCD (10 mM). Grey histogram represents isotype control, yellow histogram represents untreated expression and blue histogram represents MβCD treated expression. Histograms are representative of one of three independent experiments. Values on histograms represent the percentage of positive cells. **B)** Bar graph depicting the ratio of the MFI test antibody – isotype control antibody for MβCD treated cells / MFI test antibody – isotype control antibody for untreated cells (left axis, red bars) and ratio of the % positive test antibody – isotype control for MβCD treated cells / % positive test antibody – isotype control for untreated cells (right axis, orange bars). **C)** Depicts the relative binding of sLAG-3 to HLA class II using the formula, MFI sLAG-3 – isotype control / MFI HLA class II – isotype control (%) (left axis, red bars) and % positive sLAG-3 – isotype control / % positive HLA class II – isotype control (%) (right axis, orange bars) for MβCD treated and untreated cells. Error bars represent mean ± SEM of three independent experiments (*$p<0.05$, **$p<0.01$ and ***$p<0.001$ by ANOVA).

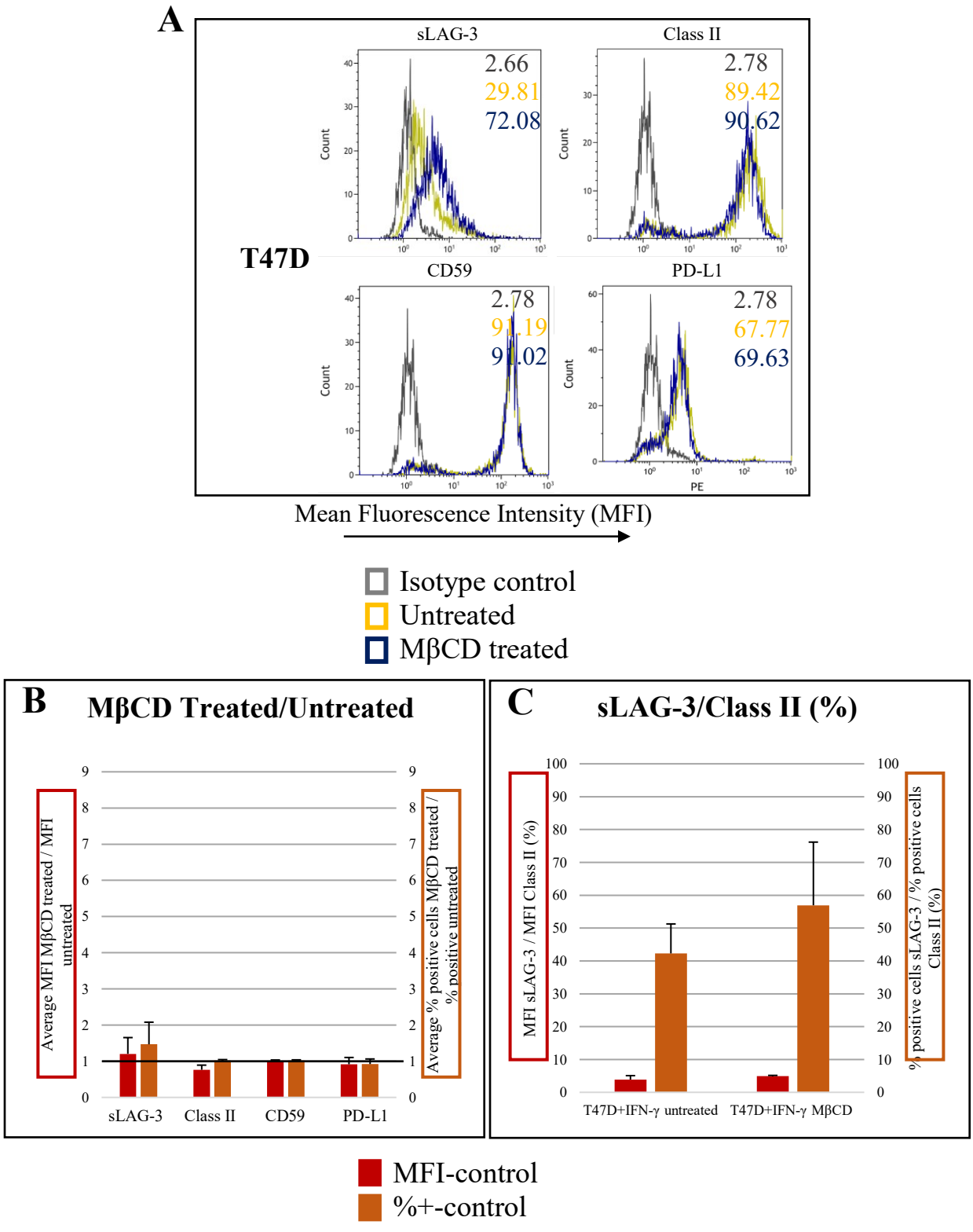
A
T47D
sLAG-3
2.66
29.81
72.08
Class II
2.78
89.42
90.62
CD59
2.78
91.19
91.02
PD-L1
2.78
67.77
69.63
Count
PE
Mean Fluorescence Intensity (MFI)
Isotype control
Untreated
MβCD treated
B
MβCD Treated/Untreated
Average MFI MβCD treated / MFI untreated
Average % positive cells MβCD treated / % positive untreated
sLAG-3
Class II
CD59
PD-L1
C
sLAG-3/Class II (%)
MFI sLAG-3 / MFI Class II (%)
% positive cells sLAG-3 / % positive cells Class II (%)
T47D+IFN-γ untreated
T47D+IFN-γ MβCD
MFI-control
%+-control

Figure 3.15: Effects of MβCD on LAG-3 binding and expression of immune molecules on T47D cells. **A)** sLAG-3 binding, HLA class II, CD59 and PD-L1 expression on IFN- γ induced T47D cells treated or not with MβCD (10 mM). Grey histogram represents isotype control, yellow histogram represents untreated expression and blue histogram represents MβCD treated expression. Histograms are representative of one of three independent experiments. Values on histograms represent the percentage of positive cells. **B)** Bar graph depicting the ratio of the MFI test antibody – isotype control antibody for MβCD treated cells / MFI test antibody – isotype control antibody for untreated cells (left axis, red bars) and ratio of the % positive test antibody – isotype control for MβCD treated cells / % positive test antibody – isotype control for untreated cells (right axis, orange bars). **C)** Depicts the relative binding of sLAG-3 to HLA class II using the formula, MFI sLAG-3 – isotype control / MFI HLA class II – isotype control (%) (left axis, red bars) and % positive sLAG-3 – isotype control / % positive HLA class II – isotype control (%) (right axis, orange bars) for MβCD treated and untreated cells. Error bars represent mean ± SEM of three independent experiments. ANOVA revealed no significant differences.

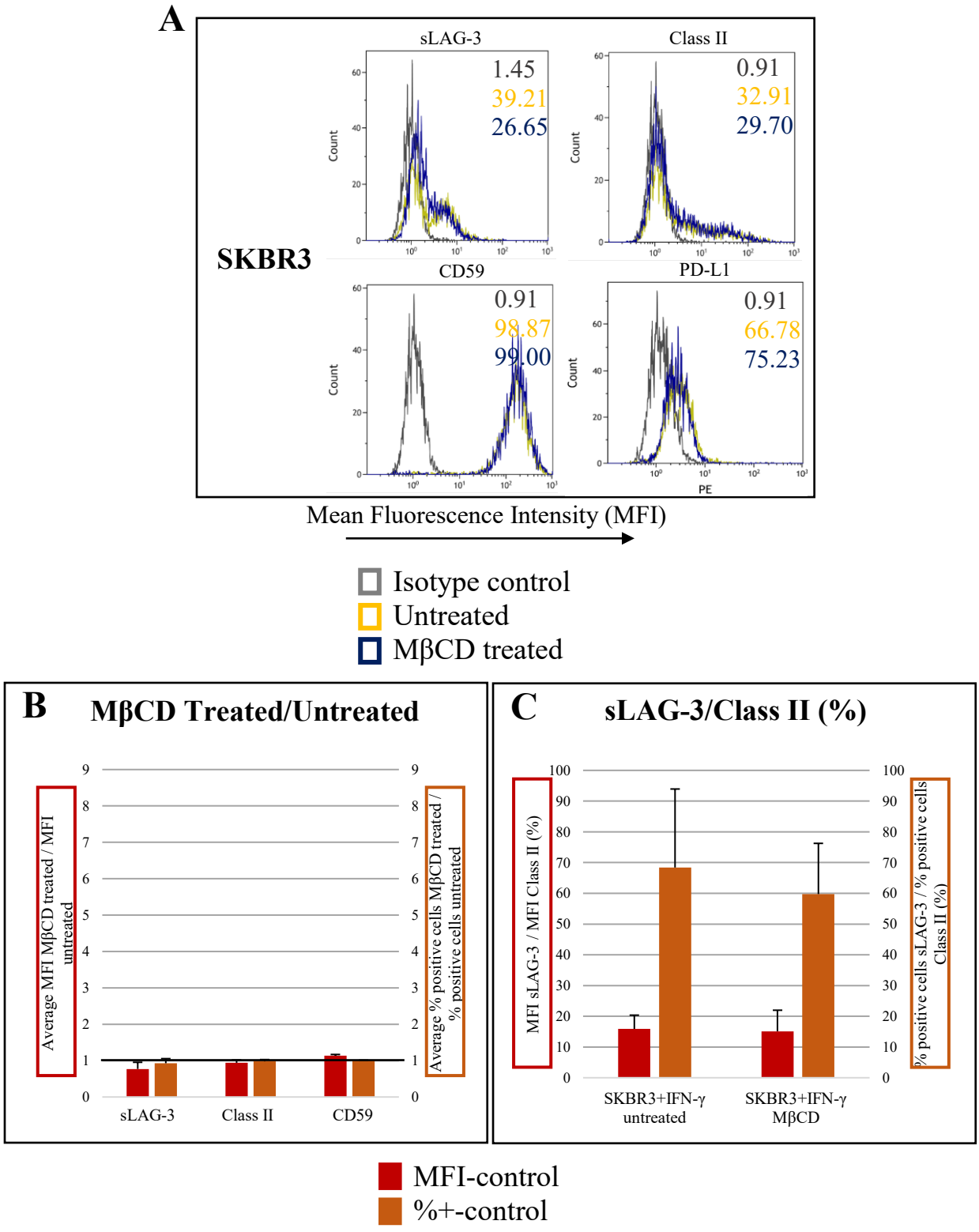
A
SKBR3
sLAG-3
1.45
39.21
26.65
Class II
0.91
32.91
29.70
CD59
0.91
98.87
99.00
PD-L1
0.91
66.78
75.23
Count
PE
Mean Fluorescence Intensity (MFI)
Isotype control
Untreated
MβCD treated
B
MβCD Treated/Untreated
Average MFI MβCD treated / MFI untreated
Average % positive cells MβCD treated / % positive cells untreated
sLAG-3
Class II
CD59
C
sLAG-3/Class II (%)
MFI sLAG-3 / MFI Class II (%)
% positive cells sLAG-3 / % positive cells Class II (%)
SKBR3+IFN-γ untreated
SKBR3+IFN-γ MβCD
MFI-control
%+-control

Figure 3.16: Effects of MβCD on LAG-3 binding and expression of immune molecules on SKBR3 cells. **A)** sLAG-3 binding, HLA class II, CD59 and PD-L1 expression on IFN- γ induced SKBR3 cells treated or not with MβCD (10 mM). Grey histogram represents isotype control, yellow histogram represents untreated expression and blue histogram represents MβCD treated expression. Histograms are representative of one of three independent experiments. Values on histograms represent the percentage of positive cells. **B)** Bar graph depicting the ratio of the MFI test antibody – isotype control antibody for MβCD treated cells / MFI test antibody – isotype control antibody for untreated cells (left axis, red bars) and ratio of the % positive test antibody – isotype control for MβCD treated cells / % positive test antibody – isotype control for untreated cells (right axis, orange bars). **C)** Depicts the relative binding of sLAG-3 to HLA class II using the formula, MFI sLAG-3 – isotype control / MFI HLA class II – isotype control (%) (left axis, red bars) and % positive sLAG-3 – isotype control / % positive HLA class II – isotype control (%) (right axis, orange bars) for MβCD treated and untreated cells. Error bars represent mean ± SEM of three independent experiments. ANOVA reveled no significant differences.

Chapter 4: Discussion

Early studies showed LAG-3 and sLAG-3-Ig fusion proteins bind to B cells [61], [64], [65] and DCs [103], preferentially binding to MHC-II associated with lipid rafts. More recently, using CIITA-deficient or CIITA-proficient MHC-II expressing cells, Maruhashi et al. showed LAG-3 binding requires stable pMHC-II complexes [153]. This was attributed to DM-expression in the CIITA-proficient cells. DM, together with its co-chaperone, DO, plays a critical role in intracellular peptide loading of MHC-II and subsequent expression of pMHC-II complexes on the cell surface. In DM-deficient cells pMHC-II complexes are largely unstable, consisting of CLIP or other self-peptides [31]. Localization of pMHC-II complexes in lipid raft microdomains is well-documented and is required for optimal antigen presentation and T-cell activation [31], [102]. In this study using normal and mutant BCL, BL, melanoma and BCCL, we investigated both the contribution of pMHC-II complexes and lipid rafts to sLAG-3 binding. The results showed DM-modulation of pMHC-II complexes, at least in B-cell lines, is a critical factor for LAG-3 binding, but as discussed in the next sections, LAG-3 binding to cancer cells is more complicated with other factors involved.

4.1 sLag-3 binding to B cells and Burkitt lymphoma cells

Part one of this study investigated differential sLAG-3 binding to a panel of normal and mutant human BCL and BL cells, deficient or not in CD59 (lipid raft marker), DM and/or DO. Key findings include: i) expression of DM-modulated pMHC-II complexes contribute more strongly to sLAG3 binding than does pMHC-II complexes in lipid raft microdomains; ii) co-expression of DO, a DM-negative regulator of peptide binding to MHC-II, may also play a role in the display of some sLAG-3 binding to pMHC-II complexes; iii) negligible sLAG-3 binding

to BL cells could not be consistently attributed to deficient lipid rafts, DM or DO, but our experiments cannot exclude suboptimal DM:DO ratios or other factors specific to BL cells.

The main conclusion is that DM modulation of pMHC-II complexes is more important for sLAG-3 binding to BCL than is pMHC-II clustering in lipid rafts, stems from significantly increased sLAG-3 binding to 9.5.3-DM cells, despite their lipid raft deficit. The lipid raft deficit in these cells, initially identified by a previous student in the Drover Lab using anti-CD59, anti-CD55 and the fluorescent aerolysin assay [151], was confirmed here by negative CD59 staining (Figure 3.2). Indeed, sLAG-3 binding to 9.5.3-DM was greater than to the parental cell line 8.1.6, possibly due to decreased CLIP/MHC-II complexes in 9.5.3-DM compared to 8.1.6 (data not shown). Our data showing lipid rafts are not critical for sLAG-3 binding to BCL differ somewhat from a previous study [93] which showed diminished LAG-3 binding following lipid raft disruption of immature DC. In that study LAG-3 binding to pMHC-II on mature DC was greatly enhanced as compared to binding on immature DC. Most likely this reflects increased display of DM-modulated and stable p/MHC-II, which tend to localize in lipid rafts on mature DC.

While sLAG-3 binding to DM-transfected DO positive 9.5.3 cells was fully restored, only partial restoration was observed for DM transfected DO negative 5.2.4 0401 cells, suggesting co-expressed DO and DM may be required for display of high LAG-3 binding pMHC-II complexes. Nearly all DO protein is bound to DM, but about 50% of DM is free, thus allowing unedited (DM-sensitive) and edited (DM-resistant) pMHC-II complexes to be expressed [27]. DM:DO ratios vary considerably by cell type, activation and differentiation, and as such, influence the pMHC-II repertoire [162]. For example, most circulating mature B-cells

have high DO and DM levels, but after B-cell activation and entry into the lymphoid germinal centers, DO levels are severely reduced, then rise again on transition to memory B-cells. Recently, Nanaware et al, comparing the peptide repertoire from a homozygous DO knockout BCL (HLA-DR1^{+}DM^{+}) to the wildtype cell line, found the DO knockout significantly reduced expression of DM-sensitive peptides, such as CLIP, but not DM resistant peptides [163]. It can be surmised then, if the amount of DO bound to DM and the amount of free DM left to catalyze peptide exchange modulates the abundance and diversity of pMHC-II in APCs, it consequently affects LAG-3 binding.

Factors other than DO and DM contributing to the peptide repertoire could also affect the amount of sLAG-3 binding in 9.5.3 and 5.2.4 cells. Although both cell lines originated from 8.1.6, they differ substantively in their MHC deletions [151]. 9.5.3 cells have the MHC-II region deleted on one chromosome 6, while the other is intact except for a mutation in DMB. Thus, it is DO^{+}DM^{-} and expresses abundant CLIP/MHC-II peptides. By contrast, 5.2.4 cells have both MHC-II and MHC-I regions deleted on one chromosome, nearly all the MHC-II encoding region deleted on the second chromosome, is DM^{-}DO^{-}, and expresses very low levels of HLA-I. The latter could potentially affect the abundance and diversity of the pMHC-II repertoire as most peptides bound to HLA-II molecules in uninfected cells are derived from self-proteins including MHC-I molecules [164] The potential impact of MHC-II diversity on LAG-3 binding is another ill-defined factor with one study showing no allelic effect on LAG-3 binding using HLA-DRB1*01:01 and HLA-DRB1*04:01 [165]; by contrast, a study by Ming et al, showed differential LAG-3 binding to certain mouse and human MHC-II allotypes [166]. Undoubtedly, peptide binding to certain MHC-II alleles, notably HLA-DRB1*04:01, is less DM-dependent, displays reduced CLIP affinity and expresses some stable pMHC-II complexes [167].

Intriguingly, in this study the ratio of sLAG-3/HLA-II binding is higher for the HLA-DRB1*04:01 transfectants than their parent lines (Sections 3.1 and 3.2) while a preliminary screen of four homozygous BCL with different MHC-II allotypes, showed sLAG-3 binding most strongly to DRB1*04:01 SAVC line (Table 3.1).

An explanation for deficient sLAG-3 binding to BL cell lines is complicated by cell-specific differences. Like most BL, Daudi and Bjab express markers consistent with germinal centre (GC) B-cells, suggesting they arose from GC B-cells. Bjab is one of the rare EBV-negative BL lines [168] and while Daudi is EBV-positive, it has retained a very limited number of EBV genes. EBV transformed BCL from healthy individuals such as SAVC are derived from circulating B-cells and express the full complement of EBV genes [169]. Negligible sLAG-3 binding to lipid raft deficient Daudi [154], [155] lend support to sLAG-3 preferentially binding MHC-II located in lipid rafts [93], [94]. However, as previously discussed, strong sLAG-3 binding to lipid raft deficient 9.5.3-DM appears to counter that theory and suggests factors other than lipid raft microdomains are responsible for poor sLAG-3 binding to Daudi cells. For example, Daudi is HLA-I negative due to a deficit of beta-2 microglobulin [170]; as noted above for 5.2.4 cells, this may affect the pMHC-II repertoire since most pMHC-II on BCL contain self-HLA-I derived peptides [171]. Since this thesis study, the Drover lab showed Daudi has an inverse DM:DO ratio with copious amounts of CLIP/MHC-II (data not shown). Altogether, these data suggest deficient sLAG-3 binding may be due to a limited peptide repertoire consisting of abundant unstable pMHC-II complexes with CLIP. Our results for Daudi are inconsistent with those from a previous study which showed positive LAG-3 binding to Daudi [65]. Potential explanations are methodological differences. In the Huard study, LAG-3 expressing transfectants were incubated with Daudi cells and the assay was performed at 37 $^{\circ}$C. Herein, a fluorescent

chimeric sLAG3-IgG construct was used in a standard flow cytometry assay using live cells and performed at ambient temperature. As will be discussed later, the assay differences are also likely to affect LAG-3 binding.

Deficient sLAG-3 binding to Bjab cannot be explained by lipid raft deficiency or decreased MHC-II levels. Previous studies [172] showed Bjab has moderate amounts of DM, essentially no DO, and little to no CLIP/MHC-II complexes, a common phenomenon in DO-negative cells. Based on the aforementioned findings of differential sLAG-3 binding to DO+ 9.5.3DM and DO- 5.2.4 04:01DM+ cells, we hypothesized increased sLAG-3 binding to the Bjab-DO transfected with DO. The transfected cells were previously shown to express both DO and CLIP/MHC-II complexes, with the latter consistent with cells having a functional DO protein [151]. Again, the deficit of sLAG-3 binding could be a suboptimal DM:DO ratio even with DO-transfection, or alternatively due to other defective antigen processing mechanisms that have been described for BL [173].

4.2 sLag-3 binding to melanoma and breast cancer cell lines

Most studies on LAG-3 in cancer have focused on its functional role as a checkpoint inhibitor expressed primarily on tumour infiltrating $CD8^+$ and $CD4^+$ T-cells [75], [83], with promising findings for prognostic and therapeutic implications [137]. Treibel's group reported an association of high serum sLAG-3 levels with a better prognosis in patients with hormone-receptor-positive BC, possibly suggesting sLAG-3 may block LAG-3-positive regulatory T-cells from interacting with HLA-II ligands [97]. HLA-II upregulation on various types of tumor cells is well documented [10] and HLA-II positive melanoma cells were shown to bind sLAG-3 [159]. Herein, we showed, despite IFN-γ induced HLA-II expression on all cell lines, only the

melanoma cells, MDA-MB-435, strongly bound sLAG-3. Of the five BCCL tested, only T47D significantly increased (albeit weak) sLAG-3 binding post IFN-γ treatment. The differences between sLAG-3 binding to melanoma and breast cannot be attributed to DM-deficiency as intracellular DM was present in all IFN-γ treated cell lines. Although DO and CLIP levels, which contribute to pMHC-II repertoire, were not analyzed in these experiments, previous studies in our laboratory found negligible CLIP/MHC-II expression in either MDA-MB-435 or BCCL [152], suggesting DO may not be upregulated. Altogether, the data suggest HLA-II expression is not a good indicator for LAG-3 binding to BCCL.

Observation of noticeable sLAG-3 binding to non-induced (HLA-II negative) BT-20 and SKBR3 cells suggests one of several recently described non-MHC ligands (Section 1.10) may be expressed on these cells. Among potential candidates are FGL-1 [72], found on the surface of cells in various cancer types including breast cancer [71]; Gal-3, expressed on breast cancer cells and considered to be a potential therapeutic marker and LSECtin, expressed on melanoma cells [70] and found in lipid raft fractions [146]. While some of these ligands are associated with lipid rafts [146], [147], there are no reports on whether LAG3 binding to MHC-II or non-MHC ligands depends on their clustering in lipid rafts in cancer cells. Lipid rafts, abundant in most cancer cells [174], were confirmed by CD59 expression on the melanoma and BCCL cells.

4.3 Lipid raft disruption enhances sLAG-3 binding to melanoma and breast cancer cell lines

As previously mentioned, considerable amounts of pMHC-II complexes are localized in lipid raft microdomains [93], [94] and their depletion in MβCD-treated DC diminishes sLAG-3 binding [93], [94]. Thus, our finding of increased sLAG-3 binding to MβCD-treated MDA-MB-435 cells was unexpected (Figure 3.12). Moreover, it occurred despite decreased MHC-II and

CD59 expression, indicators of successful lipid raft disruption. These results were reproducible, as were follow up experiments showing MβCD-treatment dramatically augmented sLAG-3 binding to three of four HLA-II^{+}BCCL. Only MβCD-treated SKBR3 showed reduced sLAG3 binding compared to control-treated cells. The results do not correlate with levels of HLA-II or CD59, which were variably altered by MβCD on BCCL. It is possible MβCD altered the lipid density in the cell membrane in such a way as to more optimally expose MHC-II or non-MHC-II ligands for stronger LAG-3 interactions. Indeed, a recent study reported lipid membrane packing made target cells including MDA-MB-231 resistance to NK cell lysis, which could be overcome by lipid raft disruption, presumably by increasing ligand availability [133].

Intriguingly, control-treated BCCL in the lipid raft depletion experiments also displayed increased binding over that observed in the previous experiments. This inconsistency could be related to methodological differences. Up to this point the sLAG-3 binding assay used live cells, pre-incubated with 10% AB serum to block non-specific F_c receptor binding. For MβCD- and control-treated cells, cells were post-fixed with 2% PFA to prevent lipid raft reassembly and serum was removed from all buffers to prevent cholesterol incorporation into the cell membranes. Given strong sLAG-3 binding to normal B-cells and MDA-MB-435, it seems improbable that free sLAG3 in FCS would interfere with sLAG-3 binding to BCCL. Another possibility is PFA, which cross links proteins during fixation, somehow allowed for more optimal display of LAG-3 binding ligands; the caveat here is increased binding to the control-treated cells only occurred with BCCL and not with MDA-MB-435.

A preliminary experiment, done to explore the effects of incubating sLAG3 with live cells for 24 hours at 37^{o}C, revealed similar levels of sLAG-3 binding to MDA-435 as those in experiments where cells were incubated with sLAG-3 for 30 min (data not shown). However,

sLAG-3 binding to MD-MB-231 and BT-20 were substantially higher than in the previous two experiments. The most likely explanation is either prolonged incubation, change in incubation temperature to 37ºC or both. Notably, prolonged LAG-3 incubation did not significantly affect expression of MHC-II, PD-L1 or DM on these cells as ascertained by flow cytometry.

4.4 PD-L1 expression on cancer cell lines

Although PD-L1 was not the main focus of this work, it was included since like MHC-II, it is upregulated by IFN- γ and together with its ligand, PD-1, and LAG-3 are targets for checkpoint immunotherapy. PD-L1 expression on BL was not included but previous studies show BL cells [175], [176] do not express PD-L1. The results here confirm the presence and/or upregulation of PD-L1 on melanoma and some breast cancer cell lines, work done by a previous student in the Drover lab [156]. Here we additionally tested whether PD-L1 expression was altered by lipid raft disruption. Effect of PD-L1 expression by MβCD treatment varied by cell line. Post MβCD treatment PD-L1 expression increased on MDA-MB-435 and SKBR3, while PD-L1 decreased on MDA-MB-231 and BT-20. The explanation for these finding is currently unclear and requires further experimentation.

4.4 Future directions

It is clear from these results and recent literature that the process of LAG-3 binding has a number of intertwining factors that differ among cell types. LAG-3 is a target for many cancer treatment therapies, with numerous studies and clinical trials investigation the efficacy of LAG-3 immunotherapies, both alone and in combination with other medications. The more we learn about how LAG-3 interacts with cancer cells, the better we can develop and test immunotherapies. Based

on the results from these experiments some additional experiments that would provide valuable knowledge include:

1. Results from LAG-3 binding to lymphoblast experiments suggest that the ratio of DM and DO may play an essential role in the level of LAG-3 binding. Measuring levels of DO expression on both lymphoblast and cancer cell lines could provide helpful information on how the MHC-II processing pathway can affect LAG-3 binding to MHC-II.
2. The flow cytometry protocol for MβCD treatment of cancer cell lines analyzed CD59 as an indicator of lipid raft integrity. However, on cancer cell lines the decrease in CD59 was not as large as expected if lipid rafts have been entirely obliterated. Adding additional methods such as Western blotting to measure lipid raft markers would give more information as to how well the MβCD treatment worked. As well, using a fluorescent marker to label lipid rafts pre- and post-treated MβCD cells would help to effectively interpret results from lipid raft disruption.
3. There were differences in LAG-3 binding to BCCL in initial sLAG-3 binding experiments compared to MβCD untreated cells in lipid raft disruption experiments. There were some differences in the preparation of cells in each of these sets of experiments. Further exploring the differences between these protocols through investigating whether blocking with AB serum or fixing cells significantly affect LAG-3 binding. This would determine if the precautions taken to limit lipid raft reassembly during MβCD experiments can explain the unexpected aLAG-3 binding results in untreated cells.
4. Since commencing this study, much research has been published on alternate ligands for LAG-3. During the course of these experiments the only ligand quantified was the primary ligand of LAG-3, MHC-II. It would be interesting to measure levels of expression of LSECtin, Gal-3 and FGL-1. Other important information would be how these proteins are affected by IFN-γ

treatment of cancer cell lines as well as whether expression is increased post lipid raft disruption by MβCD treatment.

Chapter 5: References

[1] R. Horton *et al.*, "Gene map of the extended human MHC.," *Nat. Rev. Genet.*, vol. 5, no. 12, pp. 889–899, Dec. 2004, doi: 10.1038/nrg1489.

[2] W. F. Bodmer, "The HLA system: structure and function.," *J. Clin. Pathol.*, vol. 40, no. 9, pp. 948–958, Sep. 1987, doi: 10.1136/jcp.40.9.948.

[3] B. M. Pratheek *et al.*, "Mammalian non-classical major histocompatibility complex I and its receptors: Important contexts of gene, evolution, and immunity.," *Indian J. Hum. Genet.*, vol. 20, no. 2, pp. 129–141, Apr. 2014, doi: 10.4103/0971-6866.142855.

[4] M. Croce *et al.*, "Different levels of control prevent interferon-gamma-inducible HLA-class II expression in human neuroblastoma cells.," *Oncogene*, vol. 22, no. 49, pp. 7848–7857, Oct. 2003, doi: 10.1038/sj.onc.1207054.

[5] P. A. Roche and K. Furuta, "The ins and outs of MHC class II-mediated antigen processing and presentation.," *Nat. Rev. Immunol.*, vol. 15, no. 4, pp. 203–216, Apr. 2015, doi: 10.1038/nri3818.

[6] "Complete sequence and gene map of a human major histocompatibility complex. The MHC sequencing consortium.," *Nature*, vol. 401, no. 6756, pp. 921–923, Oct. 1999, doi: 10.1038/44853.

[7] T. Y. Basham, B. J. Nickoloff, T. C. Merigan, and V. B. Morhenn, "Recombinant gamma interferon differentially regulates class II antigen expression and biosynthesis on cultured normal human keratinocytes.," *J. Interferon Res.*, vol. 5, no. 1, pp. 23–32, Winter 1985, doi: 10.1089/jir.1985.5.23.

[8] T. D. Geppert and P. E. Lipsky, "Antigen presentation by interferon-gamma-treated endothelial cells and fibroblasts: differential ability to function as antigen-presenting cells despite comparable Ia expression.," *J. Immunol. Baltim. Md 1950*, vol. 135, no. 6, pp. 3750–3762, Dec. 1985.

[9] C. M. Boyer *et al.*, "Differential induction by interferons of major histocompatibility complex-encoded and non-major histocompatibility complex-encoded antigens in human breast and ovarian carcinoma cell lines.," *Cancer Res.*, vol. 49, no. 11, pp. 2928–2934, Jun. 1989.

[10] N. Jabrane-Ferrat, A. Faille, P. Loiseau, O. Poirier, D. Charron, and F. Calvo, "Effect of gamma interferon on HLA class-I and -II transcription and protein expression in human breast adenocarcinoma cell lines.," *Int. J. Cancer*, vol. 45, no. 6, pp. 1169–1176, Jun. 1990, doi: 10.1002/ijc.2910450630.

[11] P. Cresswell, "Assembly, transport, and function of MHC class II molecules.," *Annu. Rev. Immunol.*, vol. 12, pp. 259–293, 1994, doi: 10.1146/annurev.iy.12.040194.001355.

[12] P. A. Roche and P. Cresswell, "Invariant chain association with HLA-DR molecules inhibits immunogenic peptide binding.," *Nature*, vol. 345, no. 6276, pp. 615–618, Jun. 1990, doi: 10.1038/345615a0.

[13] P. A. Roche, M. S. Marks, and P. Cresswell, "Formation of a nine-subunit complex by HLA class II glycoproteins and the invariant chain.," *Nature*, vol. 354, no. 6352, pp. 392–394, Dec. 1991, doi: 10.1038/354392a0.

[14] J. Pieters, "MHC class II restricted antigen presentation.," *Curr. Opin. Immunol.*, vol. 9, no. 1, pp. 89–96, Feb. 1997, doi: 10.1016/s0952-7915(97)80164-1.

[15] F. Sallusto, M. Cella, C. Danieli, and A. Lanzavecchia, "Dendritic cells use macropinocytosis and the mannose receptor to concentrate macromolecules in the major histocompatibility complex class II compartment: downregulation by cytokines and

bacterial products.," *J. Exp. Med.*, vol. 182, no. 2, pp. 389–400, Aug. 1995, doi: 10.1084/jem.182.2.389.
[16] L. M. Stuart and R. A. B. Ezekowitz, "Phagocytosis: elegant complexity.," *Immunity*, vol. 22, no. 5, pp. 539–550, May 2005, doi: 10.1016/j.immuni.2005.05.002.
[17] J. P. Lim and P. A. Gleeson, "Macropinocytosis: an endocytic pathway for internalising large gulps.," *Immunol. Cell Biol.*, vol. 89, no. 8, pp. 836–843, Nov. 2011, doi: 10.1038/icb.2011.20.
[18] P. J. Peters, J. J. Neefjes, V. Oorschot, H. L. Ploegh, and H. J. Geuze, "Segregation of MHC class II molecules from MHC class I molecules in the Golgi complex for transport to lysosomal compartments.," *Nature*, vol. 349, no. 6311, pp. 669–676, Feb. 1991, doi: 10.1038/349669a0.
[19] P. Ghosh, M. Amaya, E. Mellins, and D. C. Wiley, "The structure of an intermediate in class II MHC maturation: CLIP bound to HLA-DR3.," *Nature*, vol. 378, no. 6556, pp. 457–462, Nov. 1995, doi: 10.1038/378457a0.
[20] J. Klein and A. Sato, "The HLA system. First of two parts.," *N. Engl. J. Med.*, vol. 343, no. 10, pp. 702–709, Sep. 2000, doi: 10.1056/NEJM200009073431006.
[21] R. J. Riese *et al.*, "Essential role for cathepsin S in MHC class II-associated invariant chain processing and peptide loading.," *Immunity*, vol. 4, no. 4, pp. 357–366, Apr. 1996, doi: 10.1016/s1074-7613(00)80249-6.
[22] D. Lankar, H. Vincent-Schneider, V. Briken, T. Yokozeki, G. Raposo, and C. Bonnerot, "Dynamics of major histocompatibility complex class II compartments during B cell receptor-mediated cell activation.," *J. Exp. Med.*, vol. 195, no. 4, pp. 461–472, Feb. 2002, doi: 10.1084/jem.20011543.
[23] L. C. Hsing and A. Y. Rudensky, "The lysosomal cysteine proteases in MHC class II antigen presentation.," *Immunol. Rev.*, vol. 207, pp. 229–241, Oct. 2005, doi: 10.1111/j.0105-2896.2005.00310.x.
[24] L. K. Denzin and P. Cresswell, "HLA-DM induces CLIP dissociation from MHC class II alpha beta dimers and facilitates peptide loading.," *Cell*, vol. 82, no. 1, pp. 155–165, Jul. 1995, doi: 10.1016/0092-8674(95)90061-6.
[25] V. S. Sloan *et al.*, "Mediation by HLA-DM of dissociation of peptides from HLA-DR.," *Nature*, vol. 375, no. 6534, pp. 802–806, Jun. 1995, doi: 10.1038/375802a0.
[26] H. Kropshofer, A. B. Vogt, G. Moldenhauer, J. Hammer, J. S. Blum, and G. J. Hämmerling, "Editing of the HLA-DR-peptide repertoire by HLA-DM.," *EMBO J.*, vol. 15, no. 22, pp. 6144–6154, Nov. 1996.
[27] E. D. Mellins and L. J. Stern, "HLA-DM and HLA-DO, key regulators of MHC-II processing and presentation.," *Curr. Opin. Immunol.*, vol. 26, pp. 115–122, Feb. 2014, doi: 10.1016/j.coi.2013.11.005.
[28] A.-K. Anders *et al.*, "HLA-DM captures partially empty HLA-DR molecules for catalyzed removal of peptide.," *Nat. Immunol.*, vol. 12, no. 1, pp. 54–61, Jan. 2011, doi: 10.1038/ni.1967.
[29] C. A. Painter, M. P. Negroni, K. A. Kellersberger, Z. Zavala-Ruiz, J. E. Evans, and L. J. Stern, "Conformational lability in the class II MHC 310 helix and adjacent extended strand dictate HLA-DM susceptibility and peptide exchange.," *Proc. Natl. Acad. Sci. U. S. A.*, vol. 108, no. 48, pp. 19329–19334, Nov. 2011, doi: 10.1073/pnas.1108074108.

[30] R. Busch *et al.*, “Achieving stability through editing and chaperoning: regulation of MHC class II peptide binding and expression.,” *Immunol. Rev.*, vol. 207, pp. 242–260, Oct. 2005, doi: 10.1111/j.0105-2896.2005.00306.x.
[31] J. M. Riberdy, J. R. Newcomb, M. J. Surman, J. A. Barbosa, and P. Cresswell, “HLA-DR molecules from an antigen-processing mutant cell line are associated with invariant chain peptides.,” *Nature*, vol. 360, no. 6403, pp. 474–477, Dec. 1992, doi: 10.1038/360474a0.
[32] A. I. Guce *et al.*, “HLA-DO acts as a substrate mimic to inhibit HLA-DM by a competitive mechanism.,” *Nat. Struct. Mol. Biol.*, vol. 20, no. 1, pp. 90–98, Jan. 2013, doi: 10.1038/nsmb.2460.
[33] W. Reith, S. LeibundGut-Landmann, and J.-M. Waldburger, “Regulation of MHC class II gene expression by the class II transactivator.,” *Nat. Rev. Immunol.*, vol. 5, no. 10, pp. 793–806, Oct. 2005, doi: 10.1038/nri1708.
[34] K. Masternak, A. Muhlethaler-Mottet, J. Villard, M. Zufferey, V. Steimle, and W. Reith, “CIITA is a transcriptional coactivator that is recruited to MHC class II promoters by multiple synergistic interactions with an enhanceosome complex.,” *Genes Dev.*, vol. 14, no. 9, pp. 1156–1166, May 2000.
[35] J. P.-Y. Ting and J. Trowsdale, “Genetic control of MHC class II expression.,” *Cell*, vol. 109 Suppl, pp. S21-33, Apr. 2002, doi: 10.1016/s0092-8674(02)00696-7.
[36] J. M. Boss and P. E. Jensen, “Transcriptional regulation of the MHC class II antigen presentation pathway.,” *Curr. Opin. Immunol.*, vol. 15, no. 1, pp. 105–111, Feb. 2003, doi: 10.1016/s0952-7915(02)00015-8.
[37] B. Seliger, M. J. Maeurer, and S. Ferrone, “Antigen-processing machinery breakdown and tumor growth.,” *Immunol. Today*, vol. 21, no. 9, pp. 455–464, Sep. 2000, doi: 10.1016/s0167-5699(00)01692-3.
[38] N. Jabrane-Ferrat, J. D. Fontes, J. M. Boss, and B. M. Peterlin, “Complex architecture of major histocompatibility complex class II promoters: reiterated motifs and conserved protein-protein interactions.,” *Mol. Cell. Biol.*, vol. 16, no. 9, pp. 4683–4690, Sep. 1996, doi: 10.1128/MCB.16.9.4683.
[39] R. Mantovani, “The molecular biology of the CCAAT-binding factor NF-Y.,” *Gene*, vol. 239, no. 1, pp. 15–27, Oct. 1999, doi: 10.1016/s0378-1119(99)00368-6.
[40] C. S. Moreno, G. W. Beresford, P. Louis-Plence, A. C. Morris, and J. M. Boss, “CREB regulates MHC class II expression in a CIITA-dependent manner.,” *Immunity*, vol. 10, no. 2, pp. 143–151, Feb. 1999, doi: 10.1016/s1074-7613(00)80015-1.
[41] U. M. Nagarajan, P. Louis-Plence, A. DeSandro, R. Nilsen, A. Bushey, and J. M. Boss, “RFX-B is the gene responsible for the most common cause of the bare lymphocyte syndrome, an MHC class II immunodeficiency.,” *Immunity*, vol. 10, no. 2, pp. 153–162, Feb. 1999, doi: 10.1016/s1074-7613(00)80016-3.
[42] H. Ikeda, L. J. Old, and R. D. Schreiber, “The roles of IFN gamma in protection against tumor development and cancer immunoediting.,” *Cytokine Growth Factor Rev.*, vol. 13, no. 2, pp. 95–109, Apr. 2002, doi: 10.1016/s1359-6101(01)00038-7.
[43] A. Isaacs and J. Lindenmann, “Virus interference. I. The interferon. By A. Isaacs and J. Lindenmann, 1957.,” *J. Interferon Res.*, vol. 7, no. 5, pp. 429–438, Oct. 1987, doi: 10.1089/jir.1987.7.429.
[44] K. Schroder, P. J. Hertzog, T. Ravasi, and D. A. Hume, “Interferon-gamma: an overview of signals, mechanisms and functions.,” *J. Leukoc. Biol.*, vol. 75, no. 2, pp. 163–189, Feb. 2004, doi: 10.1189/jlb.0603252.

[45] E. Thoreau, B. Petridou, P. A. Kelly, J. Djiane, and J. P. Mornon, “Structural symmetry of the extracellular domain of the cytokine/growth hormone/prolactin receptor family and interferon receptors revealed by hydrophobic cluster analysis.,” *FEBS Lett.*, vol. 282, no. 1, pp. 26–31, Apr. 1991, doi: 10.1016/0014-5793(91)80437-8.
[46] P. Bernabei *et al.*, “Interferon-gamma receptor 2 expression as the deciding factor in human T, B, and myeloid cell proliferation or death.,” *J. Leukoc. Biol.*, vol. 70, no. 6, pp. 950–960, Dec. 2001.
[47] U. Vinkemeier, S. L. Cohen, I. Moarefi, B. T. Chait, J. Kuriyan, and J. E. J. Darnell, “DNA binding of in vitro activated Stat1 alpha, Stat1 beta and truncated Stat1: interaction between NH2-terminal domains stabilizes binding of two dimers to tandem DNA sites.,” *EMBO J.*, vol. 15, no. 20, pp. 5616–5626, Oct. 1996.
[48] M. H. Heim, “The Jak-STAT pathway: cytokine signalling from the receptor to the nucleus.,” *J. Recept. Signal Transduct. Res.*, vol. 19, no. 1–4, pp. 75–120, Jul. 1999, doi: 10.3109/10799899909036638.
[49] T. Sekimoto, N. Imamoto, K. Nakajima, T. Hirano, and Y. Yoneda, “Extracellular signal-dependent nuclear import of Stat1 is mediated by nuclear pore-targeting complex formation with NPI-1, but not Rch1.,” *EMBO J.*, vol. 16, no. 23, pp. 7067–7077, Dec. 1997, doi: 10.1093/emboj/16.23.7067.
[50] C. V. Ramana, M. P. Gil, R. D. Schreiber, and G. R. Stark, “Stat1-dependent and -independent pathways in IFN-gamma-dependent signaling.,” *Trends Immunol.*, vol. 23, no. 2, pp. 96–101, Feb. 2002, doi: 10.1016/s1471-4906(01)02118-4.
[51] H. M. Johnson, E. N. Noon-Song, K. Kemppainen, and C. M. Ahmed, “Steroid-like signalling by interferons: making sense of specific gene activation by cytokines.,” *Biochem. J.*, vol. 443, no. 2, pp. 329–338, Apr. 2012, doi: 10.1042/BJ20112187.
[52] V. Steimle, C. A. Siegrist, A. Mottet, B. Lisowska-Grospierre, and B. Mach, “Regulation of MHC class II expression by interferon-gamma mediated by the transactivator gene CIITA.,” *Science*, vol. 265, no. 5168, pp. 106–109, Jul. 1994, doi: 10.1126/science.8016643.
[53] A. Muhlethaler-Mottet, W. Di Berardino, L. A. Otten, and B. Mach, “Activation of the MHC class II transactivator CIITA by interferon-gamma requires cooperative interaction between Stat1 and USF-1.,” *Immunity*, vol. 8, no. 2, pp. 157–166, Feb. 1998, doi: 10.1016/s1074-7613(00)80468-9.
[54] A. Muhlethaler-Mottet, L. A. Otten, V. Steimle, and B. Mach, “Expression of MHC class II molecules in different cellular and functional compartments is controlled by differential usage of multiple promoters of the transactivator CIITA.,” *EMBO J.*, vol. 16, no. 10, pp. 2851–2860, May 1997, doi: 10.1093/emboj/16.10.2851.
[55] M. Leverkus *et al.*, “MHC class II-mediated apoptosis in dendritic cells: a role for membrane-associated and mitochondrial signaling pathways.,” *Int. Immunol.*, vol. 15, no. 8, pp. 993–1006, Aug. 2003, doi: 10.1093/intimm/dxg099.
[56] D. S. Katikaneni and L. Jin, “B cell MHC class II signaling: A story of life and death.,” *Hum. Immunol.*, vol. 80, no. 1, pp. 37–43, Jan. 2019, doi: 10.1016/j.humimm.2018.04.013.
[57] F. Triebel *et al.*, “LAG-3, a novel lymphocyte activation gene closely related to CD4.,” *J. Exp. Med.*, vol. 171, no. 5, pp. 1393–1405, May 1990, doi: 10.1084/jem.171.5.1393.
[58] M. Isobe, K. Huebner, P. J. Maddon, D. R. Littman, R. Axel, and C. M. Croce, “The gene encoding the T-cell surface protein T4 is located on human chromosome 12.,” *Proc. Natl.*

Acad. Sci. U. S. A., vol. 83, no. 12, pp. 4399–4402, Jun. 1986, doi: 10.1073/pnas.83.12.4399.
[59] C. J. Workman, L. S. Cauley, I.-J. Kim, M. A. Blackman, D. L. Woodland, and D. A. A. Vignali, "Lymphocyte activation gene-3 (CD223) regulates the size of the expanding T cell population following antigen activation in vivo.," *J. Immunol. Baltim. Md 1950*, vol. 172, no. 9, pp. 5450–5455, May 2004, doi: 10.4049/jimmunol.172.9.5450.
[60] T. K. Maeda, D. Sugiura, I.-M. Okazaki, T. Maruhashi, and T. Okazaki, "Atypical motifs in the cytoplasmic region of the inhibitory immune co-receptor LAG-3 inhibit T cell activation.," *J. Biol. Chem.*, vol. 294, no. 15, pp. 6017–6026, Apr. 2019, doi: 10.1074/jbc.RA119.007455.
[61] M. V. Goldberg and C. G. Drake, "LAG-3 in Cancer Immunotherapy.," *Curr. Top. Microbiol. Immunol.*, vol. 344, pp. 269–278, 2011, doi: 10.1007/82_2010_114.
[62] E. Baixeras *et al.*, "Characterization of the lymphocyte activation gene 3-encoded protein. A new ligand for human leukocyte antigen class II antigens.," *J. Exp. Med.*, vol. 176, no. 2, pp. 327–337, Aug. 1992, doi: 10.1084/jem.176.2.327.
[63] J. M. Dijkstra, T. Somamoto, L. Moore, I. Hordvik, M. Ototake, and U. Fischer, "Identification and characterization of a second CD4-like gene in teleost fish.," *Mol. Immunol.*, vol. 43, no. 5, pp. 410–419, Feb. 2006, doi: 10.1016/j.molimm.2005.03.005.
[64] B. Huard *et al.*, "Characterization of the major histocompatibility complex class II binding site on LAG-3 protein.," *Proc. Natl. Acad. Sci. U. S. A.*, vol. 94, no. 11, pp. 5744–5749, May 1997, doi: 10.1073/pnas.94.11.5744.
[65] B. Huard, P. Prigent, M. Tournier, D. Bruniquel, and F. Triebel, "CD4/major histocompatibility complex class II interaction analyzed with CD4- and lymphocyte activation gene-3 (LAG-3)-Ig fusion proteins.," *Eur. J. Immunol.*, vol. 25, no. 9, pp. 2718–2721, Sep. 1995, doi: 10.1002/eji.1830250949.
[66] V. Castronovo *et al.*, "Decreased expression of galectin-3 is associated with progression of human breast cancer.," *J. Pathol.*, vol. 179, no. 1, pp. 43–48, May 1996, doi: 10.1002/(SICI)1096-9896(199605)179:1<43::AID-PATH541>3.0.CO;2-N.
[67] R. Zhang, T. Sun, L. Song, D. Zuo, and W. Xiao, "Increased levels of serum galectin-3 in patients with primary Sjögren's syndrome: associated with interstitial lung disease.," *Cytokine*, vol. 69, no. 2, pp. 289–293, Oct. 2014, doi: 10.1016/j.cyto.2014.06.008.
[68] T. Fukumori *et al.*, "CD29 and CD7 mediate galectin-3-induced type II T-cell apoptosis.," *Cancer Res.*, vol. 63, no. 23, pp. 8302–8311, Dec. 2003.
[69] L. Breuilh *et al.*, "Galectin-3 modulates immune and inflammatory responses during helminthic infection: impact of galectin-3 deficiency on the functions of dendritic cells.," *Infect. Immun.*, vol. 75, no. 11, pp. 5148–5157, Nov. 2007, doi: 10.1128/IAI.02006-06.
[70] H.-Y. Chen *et al.*, "Galectin-3 negatively regulates TCR-mediated CD4+ T-cell activation at the immunological synapse.," *Proc. Natl. Acad. Sci. U. S. A.*, vol. 106, no. 34, pp. 14496–14501, Aug. 2009, doi: 10.1073/pnas.0903497106.
[71] T. Kouo *et al.*, "Galectin-3 Shapes Antitumor Immune Responses by Suppressing CD8+ T Cells via LAG-3 and Inhibiting Expansion of Plasmacytoid Dendritic Cells.," *Cancer Immunol. Res.*, vol. 3, no. 4, pp. 412–423, Apr. 2015, doi: 10.1158/2326-6066.CIR-14-0150.
[72] F. Xu *et al.*, "LSECtin expressed on melanoma cells promotes tumor progression by inhibiting antitumor T-cell responses.," *Cancer Res.*, vol. 74, no. 13, pp. 3418–3428, Jul. 2014, doi: 10.1158/0008-5472.CAN-13-2690.

[73] H. Du, Z. Yi, L. Wang, Z. Li, B. Niu, and G. Ren, "The co-expression characteristics of LAG3 and PD-1 on the T cells of patients with breast cancer reveal a new therapeutic strategy.," *Int. Immunopharmacol.*, vol. 78, p. 106113, Jan. 2020, doi: 10.1016/j.intimp.2019.106113.
[74] J. Wang *et al.*, "Fibrinogen-like Protein 1 Is a Major Immune Inhibitory Ligand of LAG-3.," *Cell*, vol. 176, no. 1–2, pp. 334-347.e12, Jan. 2019, doi: 10.1016/j.cell.2018.11.010.
[75] N. M. Durham *et al.*, "Lymphocyte Activation Gene 3 (LAG-3) modulates the ability of CD4 T-cells to be suppressed in vivo.," *PloS One*, vol. 9, no. 11, p. e109080, 2014, doi: 10.1371/journal.pone.0109080.
[76] C. G. Graydon, S. Mohideen, and K. R. Fowke, "LAG3's Enigmatic Mechanism of Action.," *Front. Immunol.*, vol. 11, p. 615317, 2020, doi: 10.3389/fimmu.2020.615317.
[77] S. Hannier, M. Tournier, G. Bismuth, and F. Triebel, "CD3/TCR complex-associated lymphocyte activation gene-3 molecules inhibit CD3/TCR signaling.," *J. Immunol. Baltim. Md 1950*, vol. 161, no. 8, pp. 4058–4065, Oct. 1998.
[78] S. Hannier and F. Triebel, "The MHC class II ligand lymphocyte activation gene-3 is co-distributed with CD8 and CD3-TCR molecules after their engagement by mAb or peptide-MHC class I complexes.," *Int. Immunol.*, vol. 11, no. 11, pp. 1745–1752, Nov. 1999, doi: 10.1093/intimm/11.11.1745.
[79] C. J. Workman, K. J. Dugger, and D. A. A. Vignali, "Cutting edge: molecular analysis of the negative regulatory function of lymphocyte activation gene-3.," *J. Immunol. Baltim. Md 1950*, vol. 169, no. 10, pp. 5392–5395, Nov. 2002, doi: 10.4049/jimmunol.169.10.5392.
[80] C. J. Workman, D. S. Rice, K. J. Dugger, C. Kurschner, and D. A. A. Vignali, "Phenotypic analysis of the murine CD4-related glycoprotein, CD223 (LAG-3).," *Eur. J. Immunol.*, vol. 32, no. 8, pp. 2255–2263, Aug. 2002, doi: 10.1002/1521-4141(200208)32:8<2255::AID-IMMU2255>3.0.CO;2-A.
[81] L. Maçon-Lemaître and F. Triebel, "The negative regulatory function of the lymphocyte-activation gene-3 co-receptor (CD223) on human T cells.," *Immunology*, vol. 115, no. 2, pp. 170–178, Jun. 2005, doi: 10.1111/j.1365-2567.2005.02145.x.
[82] E. Scala *et al.*, "Lymphocyte activation gene-3 (LAG-3) expression and IFN-gamma production are variably coregulated in different human T lymphocyte subpopulations.," *J. Immunol. Baltim. Md 1950*, vol. 161, no. 1, pp. 489–493, Jul. 1998.
[83] J. Peña, N. G. Jones, S. Bousheri, D. R. Bangsberg, and H. Cao, "Lymphocyte activation gene-3 expression defines a discrete subset of HIV-specific CD8+ T cells that is associated with lower viral load.," *AIDS Res. Hum. Retroviruses*, vol. 30, no. 6, pp. 535–541, Jun. 2014, doi: 10.1089/aid.2012.0195.
[84] C. J. Workman *et al.*, "LAG-3 regulates plasmacytoid dendritic cell homeostasis.," *J. Immunol. Baltim. Md 1950*, vol. 182, no. 4, pp. 1885–1891, Feb. 2009, doi: 10.4049/jimmunol.0800185.
[85] J. F. Grosso *et al.*, "LAG-3 regulates CD8+ T cell accumulation and effector function in murine self- and tumor-tolerance systems.," *J. Clin. Invest.*, vol. 117, no. 11, pp. 3383–3392, Nov. 2007, doi: 10.1172/JCI31184.
[86] C.-T. Huang *et al.*, "Role of LAG-3 in regulatory T cells.," *Immunity*, vol. 21, no. 4, pp. 503–513, Oct. 2004, doi: 10.1016/j.immuni.2004.08.010.

[87] T. Okamura, K. Fujio, S. Sumitomo, and K. Yamamoto, “Roles of LAG3 and EGR2 in regulatory T cells.,” *Ann. Rheum. Dis.*, vol. 71 Suppl 2, pp. i96-100, Apr. 2012, doi: 10.1136/annrheumdis-2011-200588.
[88] C. Camisaschi *et al.*, “LAG-3 expression defines a subset of CD4(+)CD25(high)Foxp3(+) regulatory T cells that are expanded at tumor sites.,” *J. Immunol. Baltim. Md 1950*, vol. 184, no. 11, pp. 6545–6551, Jun. 2010, doi: 10.4049/jimmunol.0903879.
[89] B. Liang *et al.*, “Regulatory T cells inhibit dendritic cells by lymphocyte activation gene-3 engagement of MHC class II.,” *J. Immunol. Baltim. Md 1950*, vol. 180, no. 9, pp. 5916–5926, May 2008, doi: 10.4049/jimmunol.180.9.5916.
[90] N. Li, C. J. Workman, S. M. Martin, and D. A. A. Vignali, “Biochemical analysis of the regulatory T cell protein lymphocyte activation gene-3 (LAG-3; CD223).,” *J. Immunol. Baltim. Md 1950*, vol. 173, no. 11, pp. 6806–6812, Dec. 2004, doi: 10.4049/jimmunol.173.11.6806.
[91] N. Li *et al.*, “Metalloproteases regulate T-cell proliferation and effector function via LAG-3.,” *EMBO J.*, vol. 26, no. 2, pp. 494–504, Jan. 2007, doi: 10.1038/sj.emboj.7601520.
[92] M. N. Avice, M. Sarfati, F. Triebel, G. Delespesse, and C. E. Demeure, “Lymphocyte activation gene-3, a MHC class II ligand expressed on activated T cells, stimulates TNF-alpha and IL-12 production by monocytes and dendritic cells.,” *J. Immunol. Baltim. Md 1950*, vol. 162, no. 5, pp. 2748–2753, Mar. 1999.
[93] S. Andreae, F. Piras, N. Burdin, and F. Triebel, “Maturation and activation of dendritic cells induced by lymphocyte activation gene-3 (CD223).,” *J. Immunol. Baltim. Md 1950*, vol. 168, no. 8, pp. 3874–3880, Apr. 2002, doi: 10.4049/jimmunol.168.8.3874.
[94] S. Andreae, S. Buisson, and F. Triebel, “MHC class II signal transduction in human dendritic cells induced by a natural ligand, the LAG-3 protein (CD223).,” *Blood*, vol. 102, no. 6, pp. 2130–2137, Sep. 2003, doi: 10.1182/blood-2003-01-0273.
[95] C. Brignone, C. Grygar, M. Marcu, K. Schäkel, and F. Triebel, “A soluble form of lymphocyte activation gene-3 (IMP321) induces activation of a large range of human effector cytotoxic cells.,” *J. Immunol. Baltim. Md 1950*, vol. 179, no. 6, pp. 4202–4211, Sep. 2007, doi: 10.4049/jimmunol.179.6.4202.
[96] B. L. Phillips, S. Mehra, M. H. Ahsan, M. Selman, S. A. Khader, and D. Kaushal, “LAG3 expression in active Mycobacterium tuberculosis infections.,” *Am. J. Pathol.*, vol. 185, no. 3, pp. 820–833, Mar. 2015, doi: 10.1016/j.ajpath.2014.11.003.
[97] F. Triebel, K. Hacene, and M.-F. Pichon, “A soluble lymphocyte activation gene-3 (sLAG-3) protein as a prognostic factor in human breast cancer expressing estrogen or progesterone receptors.,” *Cancer Lett.*, vol. 235, no. 1, pp. 147–153, Apr. 2006, doi: 10.1016/j.canlet.2005.04.015.
[98] X. Li *et al.*, “Emerging immune checkpoints for cancer therapy.,” *Acta Oncol. Stockh. Swed.*, vol. 54, no. 10, pp. 1706–1713, Nov. 2015, doi: 10.3109/0284186X.2015.1071918.
[99] Y. He *et al.*, “LAG-3 Protein Expression in Non-Small Cell Lung Cancer and Its Relationship with PD-1/PD-L1 and Tumor-Infiltrating Lymphocytes.,” *J. Thorac. Oncol. Off. Publ. Int. Assoc. Study Lung Cancer*, vol. 12, no. 5, pp. 814–823, May 2017, doi: 10.1016/j.jtho.2017.01.019.
[100] P. Cappello *et al.*, “LAG-3 enables DNA vaccination to persistently prevent mammary carcinogenesis in HER-2/neu transgenic BALB/c mice.,” *Cancer Res.*, vol. 63, no. 10, pp. 2518–2525, May 2003.

[101] M. F. Hanzal-Bayer and J. F. Hancock, “Lipid rafts and membrane traffic.,” *FEBS Lett.*, vol. 581, no. 11, pp. 2098–2104, May 2007, doi: 10.1016/j.febslet.2007.03.019.
[102] E. C. Jury, F. Flores-Borja, and P. S. Kabouridis, “Lipid rafts in T cell signalling and disease.,” *Semin. Cell Dev. Biol.*, vol. 18, no. 5, pp. 608–615, Oct. 2007, doi: 10.1016/j.semcdb.2007.08.002.
[103] V. Horejsi and M. Hrdinka, “Membrane microdomains in immunoreceptor signaling.,” *FEBS Lett.*, vol. 588, no. 15, pp. 2392–2397, Aug. 2014, doi: 10.1016/j.febslet.2014.05.047.
[104] H. A. Anderson, E. M. Hiltbold, and P. A. Roche, “Concentration of MHC class II molecules in lipid rafts facilitates antigen presentation.,” *Nat. Immunol.*, vol. 1, no. 2, pp. 156–162, Aug. 2000, doi: 10.1038/77842.
[105] N. Iouzalen, S. Andreae, S. Hannier, and F. Triebel, “LAP, a lymphocyte activation gene-3 (LAG-3)-associated protein that binds to a repeated EP motif in the intracellular region of LAG-3, may participate in the down-regulation of the CD3/TCR activation pathway.,” *Eur. J. Immunol.*, vol. 31, no. 10, pp. 2885–2891, Oct. 2001, doi: 10.1002/1521-4141(2001010)31:10<2885::aid-immu2885>3.0.co;2-2.
[106] C. G. Graydon, A. L. Balasko, and K. R. Fowke, “Roles, function and relevance of LAG3 in HIV infection.,” *PLoS Pathog.*, vol. 15, no. 1, p. e1007429, Jan. 2019, doi: 10.1371/journal.ppat.1007429.
[107] X. Tian *et al.*, “The upregulation of LAG-3 on T cells defines a subpopulation with functional exhaustion and correlates with disease progression in HIV-infected subjects.,” *J. Immunol. Baltim. Md 1950*, vol. 194, no. 8, pp. 3873–3882, Apr. 2015, doi: 10.4049/jimmunol.1402176.
[108] T. Okazaki *et al.*, “PD-1 and LAG-3 inhibitory co-receptors act synergistically to prevent autoimmunity in mice.,” *J. Exp. Med.*, vol. 208, no. 2, pp. 395–407, Feb. 2011, doi: 10.1084/jem.20100466.
[109] S.-R. Woo *et al.*, “Immune inhibitory molecules LAG-3 and PD-1 synergistically regulate T-cell function to promote tumoral immune escape.,” *Cancer Res.*, vol. 72, no. 4, pp. 917–927, Feb. 2012, doi: 10.1158/0008-5472.CAN-11-1620.
[110] T. Okagawa *et al.*, “Cooperation of PD-1 and LAG-3 Contributes to T-Cell Exhaustion in Anaplasma marginale-Infected Cattle.,” *Infect. Immun.*, vol. 84, no. 10, pp. 2779–2790, Oct. 2016, doi: 10.1128/IAI.00278-16.
[111] Q. Zhang *et al.*, “LAG3 limits regulatory T cell proliferation and function in autoimmune diabetes.,” *Sci. Immunol.*, vol. 2, no. 9, Mar. 2017, doi: 10.1126/sciimmunol.aah4569.
[112] M. Wierz *et al.*, “Dual PD1/LAG3 immune checkpoint blockade limits tumor development in a murine model of chronic lymphocytic leukemia.,” *Blood*, vol. 131, no. 14, pp. 1617–1621, Apr. 2018, doi: 10.1182/blood-2017-06-792267.
[113] M. Bettini *et al.*, “Cutting edge: accelerated autoimmune diabetes in the absence of LAG-3.,” *J. Immunol. Baltim. Md 1950*, vol. 187, no. 7, pp. 3493–3498, Oct. 2011, doi: 10.4049/jimmunol.1100714.
[114] J. Matsuzaki *et al.*, “Tumor-infiltrating NY-ESO-1-specific CD8+ T cells are negatively regulated by LAG-3 and PD-1 in human ovarian cancer.,” *Proc. Natl. Acad. Sci. U. S. A.*, vol. 107, no. 17, pp. 7875–7880, Apr. 2010, doi: 10.1073/pnas.1003345107.
[115] D. M. Pardoll, “The blockade of immune checkpoints in cancer immunotherapy.,” *Nat. Rev. Cancer*, vol. 12, no. 4, pp. 252–264, Mar. 2012, doi: 10.1038/nrc3239.

[116] S. R. Goding *et al.*, “Restoring immune function of tumor-specific CD4+ T cells during recurrence of melanoma.,” *J. Immunol. Baltim. Md 1950*, vol. 190, no. 9, pp. 4899–4909, May 2013, doi: 10.4049/jimmunol.1300271.
[117] Q.-Y. Ma, D.-Y. Huang, H.-J. Zhang, S. Wang, and X.-F. Chen, “Function and regulation of LAG3 on CD4(+)CD25(-) T cells in non-small cell lung cancer.,” *Exp. Cell Res.*, vol. 360, no. 2, pp. 358–364, Nov. 2017, doi: 10.1016/j.yexcr.2017.09.026.
[118] Z.-Z. Yang *et al.*, “Expression of LAG-3 defines exhaustion of intratumoral PD-1(+) T cells and correlates with poor outcome in follicular lymphoma.,” *Oncotarget*, vol. 8, no. 37, pp. 61425–61439, Sep. 2017, doi: 10.18632/oncotarget.18251.
[119] S. Takaya, H. Saito, and M. Ikeguchi, “Upregulation of Immune Checkpoint Molecules, PD-1 and LAG-3, on CD4+ and CD8+ T Cells after Gastric Cancer Surgery.,” *Yonago Acta Med.*, vol. 58, no. 1, pp. 39–44, Mar. 2015.
[120] G. Bottai *et al.*, “An immune stratification reveals a subset of PD-1/LAG-3 double-positive triple-negative breast cancers.,” *Breast Cancer Res. BCR*, vol. 18, no. 1, p. 121, Dec. 2016, doi: 10.1186/s13058-016-0783-4.
[121] J.-Y. Kim *et al.*, “Immune signature of metastatic breast cancer: Identifying predictive markers of immunotherapy response.,” *Oncotarget*, vol. 8, no. 29, pp. 47400–47411, Jul. 2017, doi: 10.18632/oncotarget.17653.
[122] X. S. Zhu, M. W. Linhoff, G. Li, K. C. Chin, S. N. Maity, and J. P. Ting, “Transcriptional scaffold: CIITA interacts with NF-Y, RFX, and CREB to cause stereospecific regulation of the class II major histocompatibility complex promoter.,” *Mol. Cell. Biol.*, vol. 20, no. 16, pp. 6051–6061, Aug. 2000, doi: 10.1128/MCB.20.16.6051-6061.2000.
[123] W.-W. Deng *et al.*, “LAG-3 confers poor prognosis and its blockade reshapes antitumor response in head and neck squamous cell carcinoma.,” *Oncoimmunology*, vol. 5, no. 11, p. e1239005, 2016, doi: 10.1080/2162402X.2016.1239005.
[124] Y. Que *et al.*, “LAG-3 expression on tumor-infiltrating T cells in soft tissue sarcoma correlates with poor survival.,” *Cancer Biol. Med.*, vol. 16, no. 2, pp. 331–340, May 2019, doi: 10.20892/j.issn.2095-3941.2018.0306.
[125] X. Ren *et al.*, “PD1 protein expression in tumor infiltrated lymphocytes rather than PDL1 in tumor cells predicts survival in triple-negative breast cancer.,” *Cancer Biol. Ther.*, vol. 19, no. 5, pp. 373–380, May 2018, doi: 10.1080/15384047.2018.1423919.
[126] G. Brockhoff *et al.*, “The presence of PD-1 positive tumor infiltrating lymphocytes in triple negative breast cancers is associated with a favorable outcome of disease.,” *Oncotarget*, vol. 9, no. 5, pp. 6201–6212, Jan. 2018, doi: 10.18632/oncotarget.23717.
[127] A. Kitano *et al.*, “Tumour-infiltrating lymphocytes are correlated with higher expression levels of PD-1 and PD-L1 in early breast cancer.,” *ESMO Open*, vol. 2, no. 2, p. e000150, 2017, doi: 10.1136/esmoopen-2016-000150.
[128] X. Cheng, Z. Zhao, E. Ventura, B. Gran, K. S. Shindler, and A. Rostami, “The PD-1/PD-L pathway is up-regulated during IL-12-induced suppression of EAE mediated by IFN-gamma.,” *J. Neuroimmunol.*, vol. 185, no. 1–2, pp. 75–86, Apr. 2007, doi: 10.1016/j.jneuroim.2007.01.012.
[129] L. Carter *et al.*, “PD-1:PD-L inhibitory pathway affects both CD4(+) and CD8(+) T cells and is overcome by IL-2.,” *Eur. J. Immunol.*, vol. 32, no. 3, pp. 634–643, Mar. 2002, doi: 10.1002/1521-4141(200203)32:3<634::AID-IMMU634>3.0.CO;2-9.

[130] R. Mizuno *et al.*, “PD-1 Primarily Targets TCR Signal in the Inhibition of Functional T Cell Activation.,” *Front. Immunol.*, vol. 10, p. 630, 2019, doi: 10.3389/fimmu.2019.00630.
[131] S. L. Topalian *et al.*, “Safety, activity, and immune correlates of anti-PD-1 antibody in cancer.,” *N. Engl. J. Med.*, vol. 366, no. 26, pp. 2443–2454, Jun. 2012, doi: 10.1056/NEJMoa1200690.
[132] S. Gettinger *et al.*, “Nivolumab Monotherapy for First-Line Treatment of Advanced Non-Small-Cell Lung Cancer.,” *J. Clin. Oncol. Off. J. Am. Soc. Clin. Oncol.*, vol. 34, no. 25, pp. 2980–2987, Sep. 2016, doi: 10.1200/JCO.2016.66.9929.
[133] Q. Liu *et al.*, “Molecular and Clinical Characterization of LAG3 in Breast Cancer Through 2994 Samples.,” *Front. Immunol.*, vol. 12, p. 599207, 2021, doi: 10.3389/fimmu.2021.599207.
[134] H. Zhou, T. Liu, and Z. Wang, “Analysis of non-small cell lung cancer microenvironment indicates preponderance of T cell exhaustion marker expression.,” *Exp. Cell Res.*, vol. 360, no. 2, pp. 205–209, Nov. 2017, doi: 10.1016/j.yexcr.2017.09.008.
[135] A. E. Vilgelm, D. B. Johnson, and A. Richmond, “Combinatorial approach to cancer immunotherapy: strength in numbers.,” *J. Leukoc. Biol.*, vol. 100, no. 2, pp. 275–290, Aug. 2016, doi: 10.1189/jlb.5RI0116-013RR.
[136] R.-Y. Huang, C. Eppolito, S. Lele, P. Shrikant, J. Matsuzaki, and K. Odunsi, “LAG3 and PD1 co-inhibitory molecules collaborate to limit CD8+ T cell signaling and dampen antitumor immunity in a murine ovarian cancer model.,” *Oncotarget*, vol. 6, no. 29, pp. 27359–27377, Sep. 2015, doi: 10.18632/oncotarget.4751.
[137] L. Chocarro *et al.*, “Clinical landscape of LAG-3-targeted therapy.,” *Immuno-Oncol. Technol.*, vol. 14, p. 100079, Jun. 2022, doi: 10.1016/j.iotech.2022.100079.
[138] S. El Mir and F. Triebel, “A soluble lymphocyte activation gene-3 molecule used as a vaccine adjuvant elicits greater humoral and cellular immune responses to both particulate and soluble antigens.,” *J. Immunol. Baltim. Md 1950*, vol. 164, no. 11, pp. 5583–5589, Jun. 2000, doi: 10.4049/jimmunol.164.11.5583.
[139] S. Buisson and F. Triebel, “MHC class II engagement by its ligand LAG-3 (CD223) leads to a distinct pattern of chemokine and chemokine receptor expression by human dendritic cells.,” *Vaccine*, vol. 21, no. 9–10, pp. 862–868, Feb. 2003, doi: 10.1016/s0264-410x(02)00533-9.
[140] S. Buisson and F. Triebel, “LAG-3 (CD223) reduces macrophage and dendritic cell differentiation from monocyte precursors.,” *Immunology*, vol. 114, no. 3, pp. 369–374, Mar. 2005, doi: 10.1111/j.1365-2567.2004.02087.x.
[141] P. Prigent, S. El Mir, M. Dréano, and F. Triebel, “Lymphocyte activation gene-3 induces tumor regression and antitumor immune responses.,” *Eur. J. Immunol.*, vol. 29, no. 12, pp. 3867–3876, Dec. 1999, doi: 10.1002/(SICI)1521-4141(199912)29:12<3867::AID-IMMU3867>3.0.CO;2-E.
[142] C. E. Demeure, J. Wolfers, N. Martin-Garcia, P. Gaulard, and F. Triebel, “T Lymphocytes infiltrating various tumour types express the MHC class II ligand lymphocyte activation gene-3 (LAG-3): role of LAG-3/MHC class II interactions in cell-cell contacts.,” *Eur. J. Cancer Oxf. Engl. 1990*, vol. 37, no. 13, pp. 1709–1718, Sep. 2001, doi: 10.1016/s0959-8049(01)00184-8.

[143] C. Casati *et al.*, “Soluble human LAG-3 molecule amplifies the in vitro generation of type 1 tumor-specific immunity.,” *Cancer Res.*, vol. 66, no. 8, pp. 4450–4460, Apr. 2006, doi: 10.1158/0008-5472.CAN-05-2728.
[144] C. Casati *et al.*, “Human lymphocyte activation gene-3 molecules expressed by activated T cells deliver costimulation signal for dendritic cell activation.,” *J. Immunol. Baltim. Md 1950*, vol. 180, no. 6, pp. 3782–3788, Mar. 2008, doi: 10.4049/jimmunol.180.6.3782.
[145] C. Brignone, B. Escudier, C. Grygar, M. Marcu, and F. Triebel, “A phase I pharmacokinetic and biological correlative study of IMP321, a novel MHC class II agonist, in patients with advanced renal cell carcinoma.,” *Clin. Cancer Res. Off. J. Am. Assoc. Cancer Res.*, vol. 15, no. 19, pp. 6225–6231, Oct. 2009, doi: 10.1158/1078-0432.CCR-09-0068.
[146] A. Wang-Gillam *et al.*, “A phase I study of IMP321 and gemcitabine as the front-line therapy in patients with advanced pancreatic adenocarcinoma.,” *Invest. New Drugs*, vol. 31, no. 3, pp. 707–713, Jun. 2013, doi: 10.1007/s10637-012-9866-y.
[147] C. Brignone *et al.*, “First-line chemoimmunotherapy in metastatic breast carcinoma: combination of paclitaxel and IMP321 (LAG-3Ig) enhances immune responses and antitumor activity.,” *J. Transl. Med.*, vol. 8, p. 71, Jul. 2010, doi: 10.1186/1479-5876-8-71.
[148] A. Legat *et al.*, “Vaccination with LAG-3Ig (IMP321) and Peptides Induces Specific CD4 and CD8 T-Cell Responses in Metastatic Melanoma Patients--Report of a Phase I/IIa Clinical Trial.,” *Clin. Cancer Res. Off. J. Am. Assoc. Cancer Res.*, vol. 22, no. 6, pp. 1330–1340, Mar. 2016, doi: 10.1158/1078-0432.CCR-15-1212.
[149] E. Romano *et al.*, “MART-1 peptide vaccination plus IMP321 (LAG-3Ig fusion protein) in patients receiving autologous PBMCs after lymphodepletion: results of a Phase I trial.,” *J. Transl. Med.*, vol. 12, p. 97, Apr. 2014, doi: 10.1186/1479-5876-12-97.
[150] G. Ellison, T. Klinowska, R. F. R. Westwood, E. Docter, T. French, and J. C. Fox, “Further evidence to support the melanocytic origin of MDA-MB-435.,” *Mol. Pathol. MP*, vol. 55, no. 5, pp. 294–299, Oct. 2002, doi: 10.1136/mp.55.5.294.
[151] C. Corkum, “Identification of the cellular mechanisms responsible for the generation of particular HLA-DR epitopes,” Memorial University of Newfoundland, 2018.
[152] A. Mostafa, “Mechanisms involved in the regulation of human leukocyte antigen class II expression in estrogen receptor alpha positive and estrogen receptor alpha negative breast cancer cells,” Memorial University of Newfoundland, 2014.
[153] T. Maruhashi *et al.*, “Binding of LAG-3 to stable peptide-MHC class II limits T cell function and suppresses autoimmunity and anti-cancer immunity.,” *Immunity*, vol. 55, no. 5, pp. 912-924.e8, May 2022, doi: 10.1016/j.immuni.2022.03.013.
[154] E. Morelon, V. Dodelet, P. Lavery, N. R. Cashman, and R. Loertscher, “The failure of Daudi cells to express the cellular prion protein is caused by a lack of glycosyl-phosphatidylinositol anchor formation.,” *Immunology*, vol. 102, no. 2, pp. 242–247, Feb. 2001, doi: 10.1046/j.1365-2567.2001.01166.x.
[155] E. Marcenaro *et al.*, “CD59 is physically and functionally associated with natural cytotoxicity receptors and activates human NK cell-mediated cytotoxicity.,” *Eur. J. Immunol.*, vol. 33, no. 12, pp. 3367–3376, Dec. 2003, doi: 10.1002/eji.200324425.
[156] A. Rasmussen, “Contrasting effects on HLA and PD-L1 expression through inhibition of MAPK pathway in triple negative breast cancer cells,” Memorial University of Newfoundland, 2016.

[157] H. Soliman, F. Khalil, and S. Antonia, “PD-L1 expression is increased in a subset of basal type breast cancer cells.,” *PloS One*, vol. 9, no. 2, p. e88557, 2014, doi: 10.1371/journal.pone.0088557.
[158] E. A. Mittendorf *et al.*, “PD-L1 expression in triple-negative breast cancer.,” *Cancer Immunol. Res.*, vol. 2, no. 4, pp. 361–370, Apr. 2014, doi: 10.1158/2326-6066.CIR-13-0127.
[159] P. Hemon *et al.*, “MHC class II engagement by its ligand LAG-3 (CD223) contributes to melanoma resistance to apoptosis.,” *J. Immunol. Baltim. Md 1950*, vol. 186, no. 9, pp. 5173–5183, May 2011, doi: 10.4049/jimmunol.1002050.
[160] S. Azadi, H. Aboulkheyr Es, S. Razavi Bazaz, J. P. Thiery, M. Asadnia, and M. Ebrahimi Warkiani, “Upregulation of PD-L1 expression in breast cancer cells through the formation of 3D multicellular cancer aggregates under different chemical and mechanical conditions.,” *Biochim. Biophys. Acta Mol. Cell Res.*, vol. 1866, no. 12, p. 118526, Dec. 2019, doi: 10.1016/j.bbamcr.2019.118526.
[161] S. Ilangumaran and D. C. Hoessli, “Effects of cholesterol depletion by cyclodextrin on the sphingolipid microdomains of the plasma membrane.,” *Biochem. J.*, vol. 335 (Pt 2), no. Pt 2, pp. 433–440, Oct. 1998, doi: 10.1042/bj3350433.
[162] M. Álvaro-Benito and C. Freund, “Revisiting nonclassical HLA II functions in antigen presentation: Peptide editing and its modulation.,” *HLA*, vol. 96, no. 4, pp. 415–429, Oct. 2020, doi: 10.1111/tan.14007.
[163] P. P. Nanaware, M. M. Jurewicz, J. D. Leszyk, S. A. Shaffer, and L. J. Stern, “HLA-DO Modulates the Diversity of the MHC-II Self-peptidome.,” *Mol. Cell. Proteomics MCP*, vol. 18, no. 3, pp. 490–503, Mar. 2019, doi: 10.1074/mcp.RA118.000956.
[164] R. M. Chicz and R. G. Urban, “Analysis of MHC-presented peptides: applications in autoimmunity and vaccine development.,” *Immunol. Today*, vol. 15, no. 4, pp. 155–160, Apr. 1994, doi: 10.1016/0167-5699(94)90311-5.
[165] B. J. MacLachlan *et al.*, “Molecular characterization of HLA class II binding to the LAG-3 T cell co-inhibitory receptor.,” *Eur. J. Immunol.*, vol. 51, no. 2, pp. 331–341, Feb. 2021, doi: 10.1002/eji.202048753.
[166] Q. Ming *et al.*, “LAG3 ectodomain structure reveals functional interfaces for ligand and antibody recognition.,” *Nat. Immunol.*, vol. 23, no. 7, pp. 1031–1041, Jul. 2022, doi: 10.1038/s41590-022-01238-7.
[167] N. S. Patil *et al.*, “Rheumatoid arthritis (RA)-associated HLA-DR alleles form less stable complexes with class II-associated invariant chain peptide than non-RA-associated HLA-DR alleles.,” *J. Immunol. Baltim. Md 1950*, vol. 167, no. 12, pp. 7157–7168, Dec. 2001, doi: 10.4049/jimmunol.167.12.7157.
[168] J. Menezes, W. Leibold, G. Klein, and G. Clements, “Establishment and characterization of an Epstein-Barr virus (EBC)-negative lymphoblastoid B cell line (BJA-B) from an exceptional, EBV-genome-negative African Burkitt’s lymphoma.,” *Biomed. Publiee Pour AAICIG*, vol. 22, no. 4, pp. 276–284, Jul. 1975.
[169] H. Nakagomi, R. Dolcetti, M. T. Bejarano, P. Pisa, R. Kiessling, and M. G. Masucci, “The Epstein-Barr virus latent membrane protein-1 (LMP1) induces interleukin-10 production in Burkitt lymphoma lines.,” *Int. J. Cancer*, vol. 57, no. 2, pp. 240–244, Apr. 1994, doi: 10.1002/ijc.2910570218.

[170] C. de Préval and B. Mach, “The absence of beta 2-microglobulin in Daudi cells: active gene but inactive messenger RNA.,” *Immunogenetics*, vol. 17, no. 2, pp. 133–140, 1983, doi: 10.1007/BF00364753.
[171] R. M. Chicz *et al.*, “Predominant naturally processed peptides bound to HLA-DR1 are derived from MHC-related molecules and are heterogeneous in size.,” *Nature*, vol. 358, no. 6389, pp. 764–768, Aug. 1992, doi: 10.1038/358764a0.
[172] S. B. Hake, H. M. Tobin, V. Steimle, and L. K. Denzin, “Comparison of the transcriptional regulation of classical and non-classical MHC class II genes.,” *Eur. J. Immunol.*, vol. 33, no. 9, pp. 2361–2371, Sep. 2003, doi: 10.1002/eji.200323795.
[173] J. M. God and A. Haque, “Multiple Defects Impair the HLA Class II Antigen Presentation Capacity of Burkitt Lymphoma.,” *J. Clin. Cell. Immunol.*, vol. 7, no. 4, p. e119, Aug. 2016, doi: 10.4172/2155-9899.1000e119.
[174] Y. C. Li, M. J. Park, S.-K. Ye, C.-W. Kim, and Y.-N. Kim, “Elevated levels of cholesterol-rich lipid rafts in cancer cells are correlated with apoptosis sensitivity induced by cholesterol-depleting agents.,” *Am. J. Pathol.*, vol. 168, no. 4, pp. 1107–18; quiz 1404–1405, Apr. 2006, doi: 10.2353/ajpath.2006.050959.
[175] B. J. Chen *et al.*, “PD-L1 expression is characteristic of a subset of aggressive B-cell lymphomas and virus-associated malignancies.,” *Clin. Cancer Res. Off. J. Am. Assoc. Cancer Res.*, vol. 19, no. 13, pp. 3462–3473, Jul. 2013, doi: 10.1158/1078-0432.CCR-13-0855.
[176] K. E. Fisher *et al.*, “Programmed cell death ligand 1 expression in aggressive pediatric non-Hodgkin lymphomas: frequency, genetic mechanisms, and clinical significance.,” *Haematologica*, vol. 107, no. 8, pp. 1880–1890, Aug. 2022, doi: 10.3324/haematol.2021.280342.